PETROPHYSICAL EVALUATION OF FRACTURE SYTEMS IN COAL BED METHANE (CBM) BEARING COAL SEAMS IN RELATION TO GEOLOGICAL SETTING,3 EXPLORATION BLOCKS, BOTSWANA

MINI THESIS RESEARCH PROJECT

Mvunyiswa Ondela (O)
2849782

UNIVERSITY OF THE WESTERN CAPE

Project Supervisor: Dr M Opuwari & Dr Robert Rutten

Industry Advisor: Mr. Junior Potgieter, Sasol Petroleum International (SPI)

A thesis submitted in partial fulfillment of Master's Degree (MSc) on Petroleum Geoscience in the faculty of Science, Earth Science Department. University of Western Cape, South Africa

MAY 2014

NB- original names of field and wells will be omitted in final report for confidentiality reasons and will instead be assigned names other than original names (confidential SPI & Kubu data).

DECLARATION

I **ONDELA MVUNYISWA** declare that this research paper titled *Petrophysical evaluation of fracture systems in Coal Bed Methane (CBM) bearing coal seams in relation to geological settings, 3 exploration blocks, Botswana*; is my own work. I have not permitted anyone to copy my work or any part thereof. It has not been submitted before for any degree or examination in any other university. All the sources I have used or quoted have been indicated and acknowledged as complete references.

Signed by ……………….at………………….on the day of…………………

UNIVERSITY *of the*
WESTERN CAPE

ABSTRACT

This study is focused on the Coal Bed Methane resources of Botswana with specific reference to the Central Kalahari basin where prospect license blocks forming the focus of this study are located. The aim of this study is to evaluate the fracture network in the coal seams and the fracture systems in the surrounding coal bearing sedimentary sequences and their contribution to dynamic flow. Coal bed methane sources are dual-porosity media documented on the natural fracture network, seen as micropores (matrix/natural fractures) and macropores (cleat). The coals of this region belong to the Ecca Group's Morupule Fm (Permian) (70 m), focus of this study and have been preserved in the extensive Karoo basin within the Southern Africa region. Fractures can easily be identified in Acoustic Televiewer logs (ATV) and their orientation and structural character interpreted by rose plots, tadpoles and stick dip plots. In-situ stress fields have been determined from breakout structural evaluation and maintains a general E-W dip direction and N-S strike, thus most fractures are orientated optimally with inferred in-situ stress and enhancing flow potential in pore systems. A qualitative (MID plots & M-N cross-plots) and quantitative description of the fracture system is fundamental to the petrophysical evaluation, and involves the estimation of fracture parameters (fracture porosity, resistivity fracture index and both horizontal and vertical fracture indices).
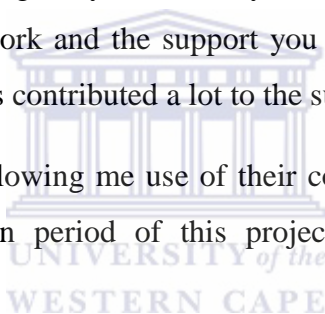
AKNOWLEDGEMENTS

CONTENTS

FIGURES

9

1   INTRODUCTION

The Ecca Group is the main focus of this study which comprises of the main coal bearing Morupule Fm. Nine exploration wells have been drilled in the three prospecting license blocks and have penetrated the coal reservoir containing coal bed methane gas. The Morupule formation forms the basis of this study as the coal bearing sequences of the Ecca Group are contained within this succession. Commercial CBM production takes place in coals of mid-rank, which usually include low to high volatile bituminous coals (Levine, 1993).

This study is focused on the Coal Bed Methane resources of Botswana with specific reference to the Central Kalahari Karoo basin (Botswana) where prospect license blocks (134/2010, 135/2010 & 136/2010) forming the focus of this study are located. The aim of this study is to evaluate the contribution to production of potential fracture network. Fractures are observed in the coal seams in the surrounding coal bearing sedimentary sequences (mudstones, carbonaceous mudstones, silts and coaly mudstones).

Coal bed Methane (CBM) is a natural gas (CH_4) that forms as a result of burial (i.e. compaction and temperature increase) related to coalification, the process whereby peat is transformed to coal through burial under high temperature conditions, either by biogenic or thermogenic processes. CBM is an unconventional gas resource involving the production of methane gas from coal seams (Garcia, 2004), the coal methane gas comprises about 90% pure CH_4 with the remaining fractions comprising of proportions of heavier gas compounds such as ethane and butane (Rice, 1997). Upon generation the methane gas is either adsorbed on the internal surface of the coal matrix or is compressed in the void spaces within the coal (Harpalani & Liu, 2013).

Coal bed methane sources are dual-porosity media documented on the natural fracture network, seen as micropores (matrix/natural fractures) and macropores (micro and macrocleat in micro meters in size). Cleat is micro-meter scale joints due to transformation of kerogen (humic material) in the coaly layers and consequent escape of methane. The organic material when becoming coalified is just blown up by escaping gas. The resulting disturbances are small joints Figure 2. The cleat network is dominated by two sets, the primary more continuous face cleats and abutting, butt cleats which appear as rungs on a ladder (Close, 1993; Levine, 1993). The butt cleats are bounded on each side by face cleats and the spacing of the cleats is usually a proportion of the coal thickness through which the cleats cut; more closely spaced cleats (mm in size) usually form in thin coals and thick coals have widely

spaced cleats (Laubach et al., 1998). Coals store significant amounts of methane gas in the low primary permeability micro fracture system and relatively small amounts in the cleat system which has high secondary permeability and therefore better flow. The primary permeability is contained within the matrix pores of the formation and secondary permeability is the result of external stresses which form vugs and caverns within the formation under the form of fractures.It is within the cleat system that coal bed methane gas is produced as coal is almost always fractured creating the secondary permeability to aid better flow of methane to the well bore during production.
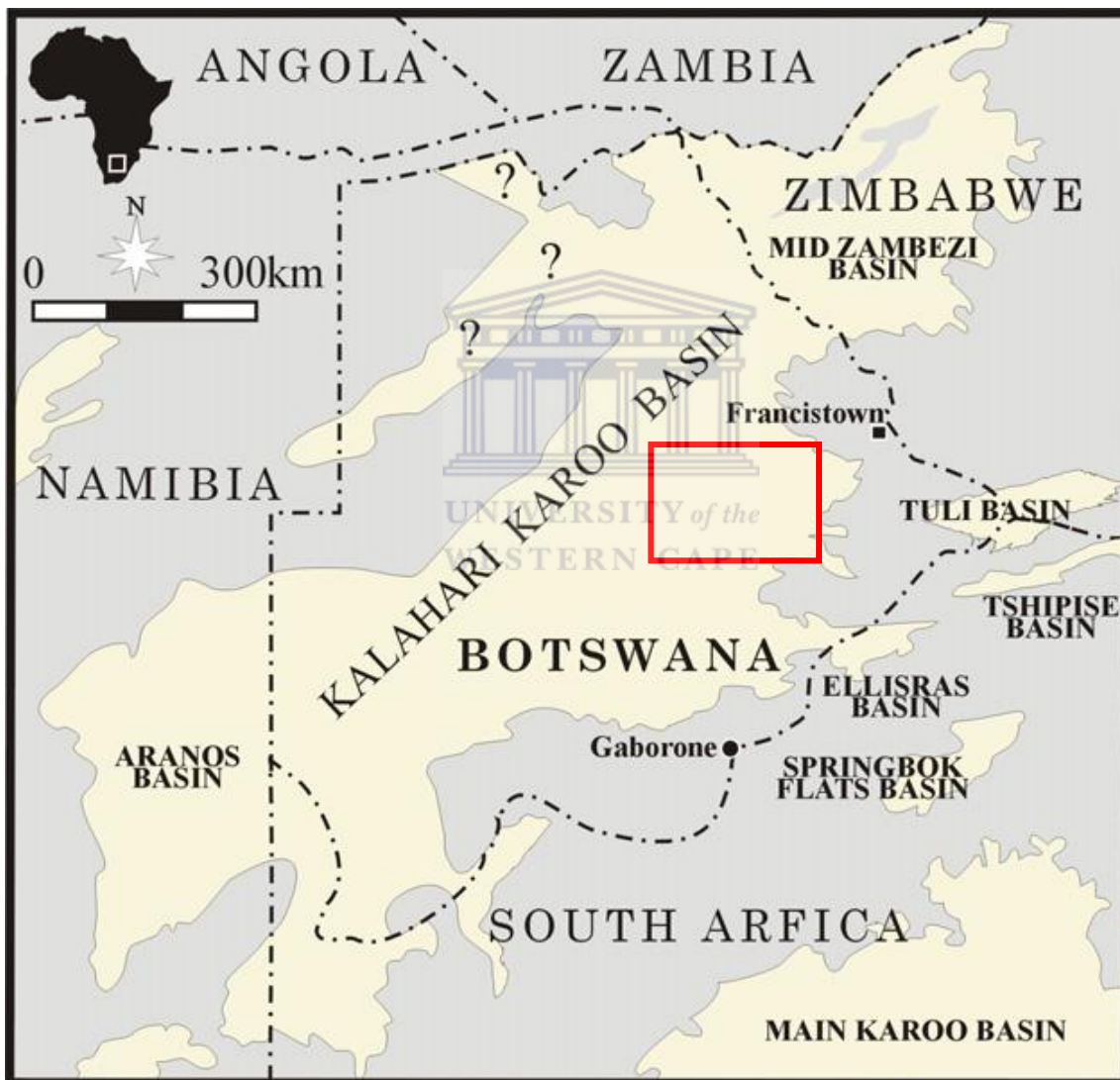
Figure 1 *Location of the study area taken from* **(Bordy, et al., 2010).**
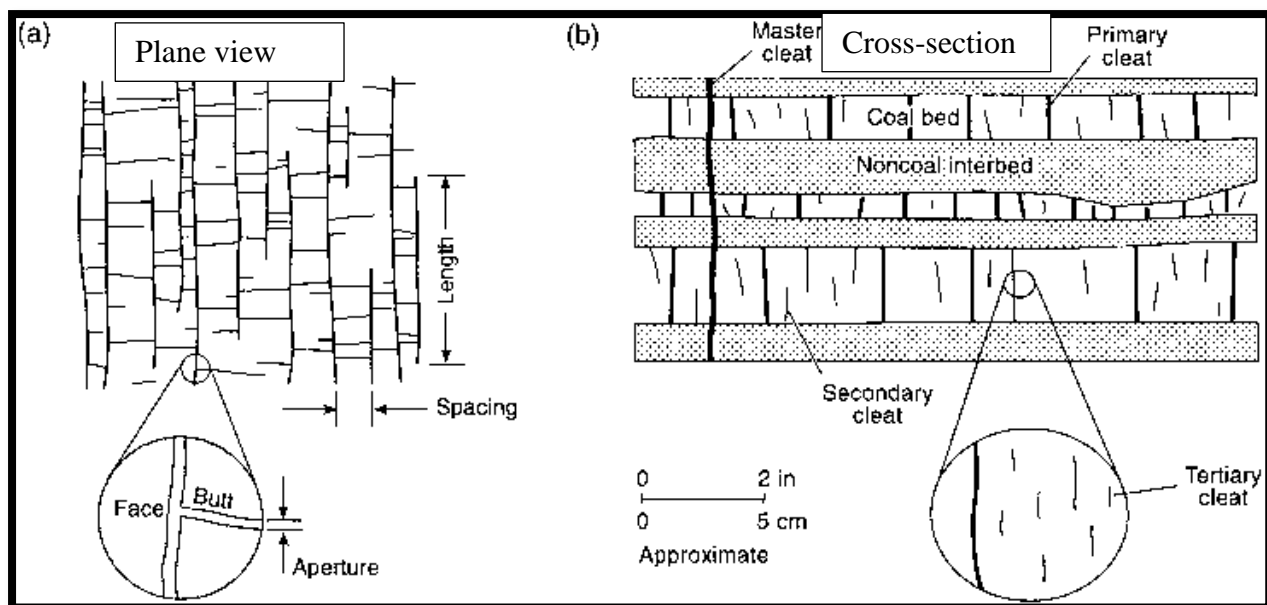
Figure 2 *A schematic representation of cleat system on coal seams* (Laubach et al. 2004)

1.1 Objectives

The research and study area include the evaluation of the current CBM development project of Botswana, with emphasis on the central province along which the prospecting license blocks and core holes are located. The studied bed are located in the South-East Central Kalahari Karoo Belt in Botswana. The beds are Permian age and belong to the Ecca Group.

The purpose of the study is to make a qualitative and quantitative fracture analysis of coal bed, with petrophysical and structural approach, this is done to assess the fracture effect on the permeability, methane gas flow and resulting production. The study will be carried out on Morupule Fm coal beds of Early Permian age. The study will involve the estimation of fracture parameters (fracture porosity index, fracture porosity, resistivity fracture index and fracture aperture) with the use of borehole-drived image logs (ATV & conventional logs), cross plots and correlations which are commonly applied to interpret fracture parameters mentioned above. This study focuses on secondary fracture porosity.

The paper aims to evaluate fractures in relation to permeability and the ultimate impact the fractures may have on recovery A detailed technical assessment (petrophysical and geological) of the PL license blocks, N-W-N region of Botswana has been carried out to define and describe the fracture systems impacting on the coal and how these fractures relate to production with collaboration of local geology. This is a particularly new development work in terms of the oil and gas industry and of course in Botswana.

13

Detecting fractures and maybe faults is the main objective of the study with the use of image logs. The study also aims to provide a distinction between open and closed fractures. Some if not most fractures have a vertical orientation with some semi-vertical attaining a near horizontal nature, these can be classified as joints and in coals as cleats. Identifying whether a fractures is open or not is critical to permeability determination for this study. Open fractures on acoustic images appear as low amplitude return and long-time of flight (Rider & Kennedy, 2011). This study will only focus on the coal intervals Z3, Z2 & Z1.

Wireline logs are very useful evaluation tools when calibrated with core measurements for estimating proximate analysis, natural fracturing and permeability in coal beds. The Petrophysical approach has been chosen for this study in order to meet the following objectives:

- Definition and description of the fracture system with use of Acoustic Televiewer and Resistivity information
- Evaluation of natural fractures and fracture networks within coal bearing sequences and their potential contribution to production.
- Understanding storage capacity of gas in coals and their resulting pore volume compressibility through core measurements.
- Determine fracture (cleat) flow potential well logs.
- Natural fracture system (if any) orientation and width; its impact on the fault system
- To obtain a field wide correlation of individual coal seams.
- Ascertain natural fractures developed and cleat structural control for gas reservoir modeling.

1.2 COAL GEOLOGY

Local Coal Origin

Predecessor of coal is peat, deposited under very shallow water level or stable water level, usually fore-deep and cratonic basins (Thomas, 2002). The Karoo coal deposits are of Late Carboniferous-Permian age and are widespread across central and southern parts of Africa and were deposited on the Gondwana supercontinent. Botswana has large black coal reserves of those Karoo coals, mainly along the eastern border of the country. Those black coals belong to the Morupule coal seams 9.5m, 4.5m & 2m thick. They are bituminous coals with high ash and sulphur contents (Thomas, 2002) and composed of inertinite and vitrinite macerals.

14

Coalification Process
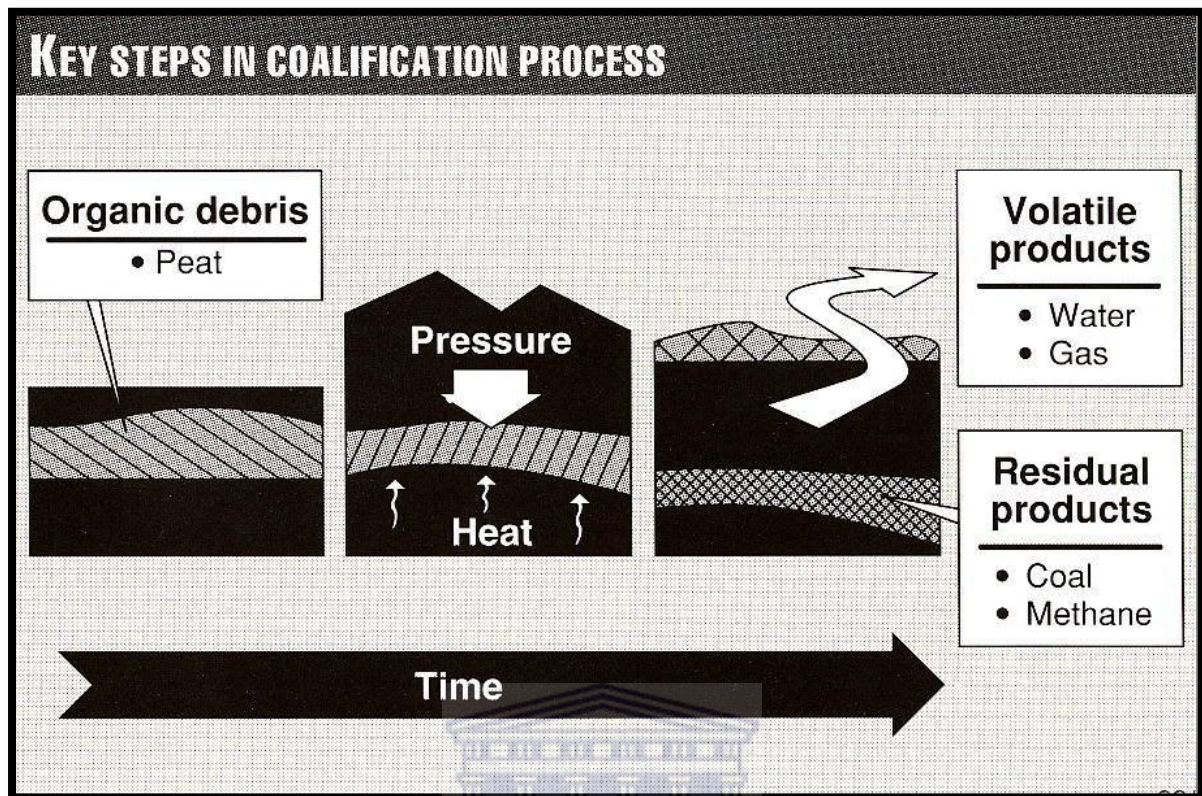
Figure 3 *Schematic representation of the coalification process and subsequent generation of methane in coal beds (Botswana Ministry, 2003).*
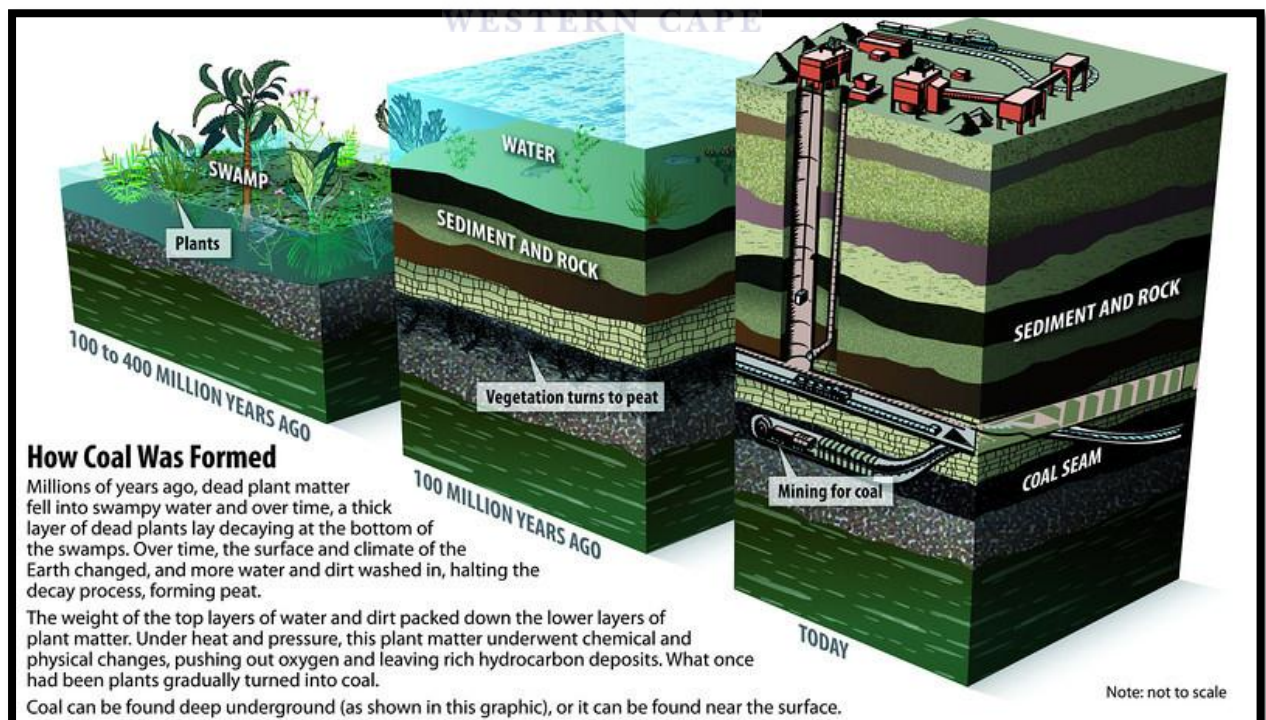
Figure 4 *A schematic representation of the process of coalification and the subsequent coal bed methane gas extraction from coal seams* *(N.E.E.D Project, 2014)*

General coal description

Coal composition is determined by the nature of initial organic and inorganic constituent accumulated (Thomas, 2002) and also by the degree to which it is diagenetically affected.

Coal by definition is a rock that contains at least 50% organic matter by weight. Coal is formed when plant material get deposited overtime in fresh or brackish water swamps (more often fresh) that are associated with coastal deltaic rivers (Survey, 2004). Botswana coals have been formed in a similar manner. During the coalification process, peat is subjected to increasing pressure and temperature due to burial resulting in the transformation from peat to coaland from sediment to sedimentary rock. These strata interbedded with the coals are sometimes referred to as "coal cycles" (Survey, 2004) or coal bearing inter-layered sedimentary sequences. During the coalification, methane gas is adsorbed into the internal structure of the coal in the micro-pores and some migrates into porous sandstones and shales of the associated sedimentary sequences (Ministry, 2003). Methane gas is generated during the transformation of peat to coal and the amount of methane gas generated is related to the rank of coal formed, where low ranked coals such as bituminous have lower gas content and higher adsorptive capacity for methane gas (Ministry, 2003) than higher ranked coals like anthracite. Conversely anthracite has a higher gas content it has a significantly lower desorption capacity and becoming an insignificant source of CBM (Levine, 1993).
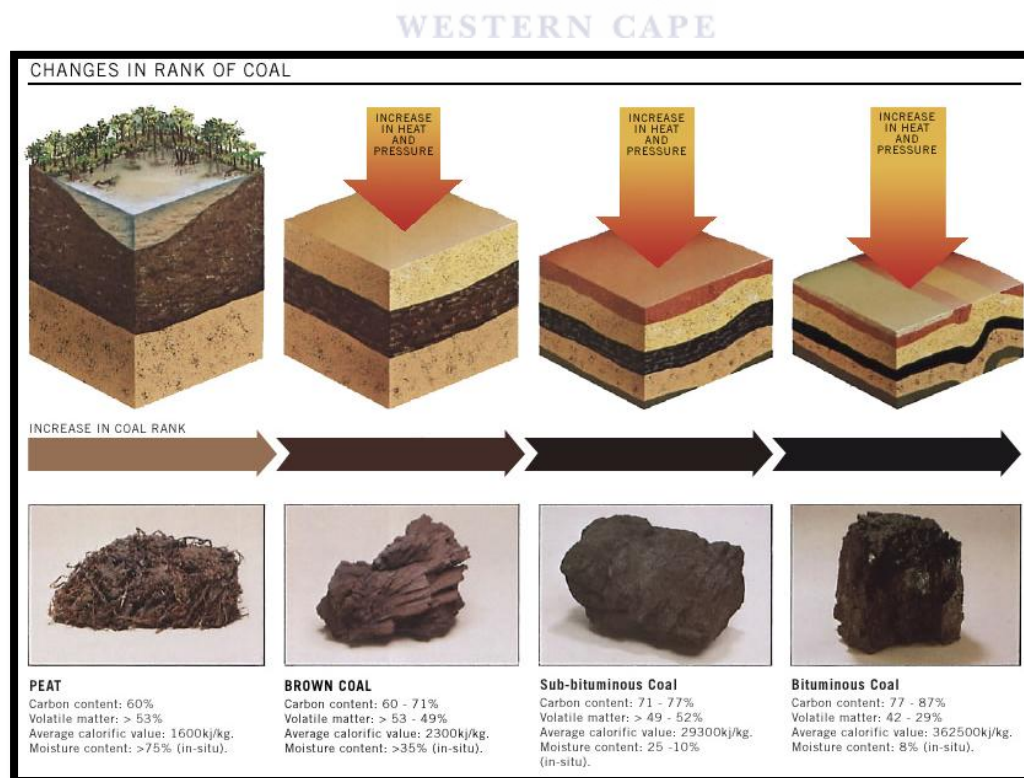
Figure 5 *Development of different coal ranks through time and burial* (**Outburst, 2013***).*

16

1.3 FRACTURE GEOLOGY

There is more than one aspect of cleat or fracture development in coal seams during coalification and later uplift, these include; dessication, devolatization and tectonic stress (Mandal, et al., 2004). Cleat-fracture development in coals is also influenced by coal rank, bed thickness, macerals and mineral composition (Mandal et al., 2004).

Most coals contain fractures along which large amounts of gas (approximately 6-12 TCF in Botswana) is desorbed and therefore a qualitative and quantitative description of the fracture system is fundamental to the petrophysical evaluation. Acoustic Televiewer (ATV) images and other wireline-log parameters are crucial to improve understanding about the fracture properties.

Fractures always play an important role in fluid flow behavior which can either be positive (contributing to fluid flow) or negative (causing seepages or barriers to flow). These fractures can greatly enhance the permeability of rocks and will change the distribution of flow in the reservoir through altered connectivity patterns. Natural fractures contribute significantly to productivity of the methane gas, however the presence and intensity of the fractures need to be evaluated in order to know the contribution to flow. For fractured reservoirs the porosity consists of induced secondary porosity in addition to the primary (original) porosity (Crain, 2013). The induced porosity (~less than 1%) system is formed after the rock is formed through tension and/or shear stresses causing fractures.

Here ATV curves are used to assess fracture aperture and intensity. The essence of the fractures is that they are expected to contribute to flow. That is because of their very high and very directional permeability within the fracture planes. Not because of their contribution to porosity because this is very little in terms of volume. Fractures occur along preferential directions, determined by the direction of regional stress which is usually parallel to the direction of nearby faults (Crain, 2013). Fractures tend to create high permeability corridors in low permeability lithologies. Sometimes (in a few cases) fractures are calcite cemented (closed fractures) thus the fracture has no permeability.

Cleats are dilatational joints formed by changing kerogen structure and subsequent escape of methane. These natural open fractures account for the majority of porosity and permeability increase in coal seams which are unconventional (low porosity) gas reservoirs. Fractures occur in all coal bed and have a great control on fluid flow and coal seam stability (Laubach, et al., 1998). Cleats are fractures and occur in a set and are generally referred to as face and

17

butt cleats Figure 6, which are perpendicular to one another and to the bedding plane. The main distinction between the two is that the face cleat (more continuous) pre-dates the butt cleat (short and truncates along the face cleat). These fractures together with their subsequent partings along bedding planes, give the coal its blocky nature (Laubach et al., 1998).
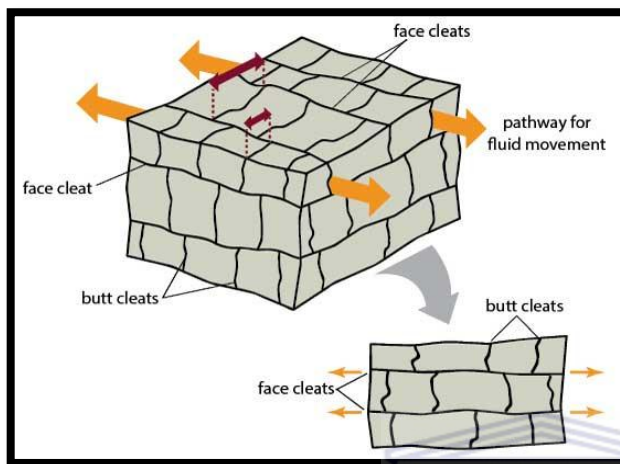
Figure 6 *A schematic representation of the cleat system (face cleat and butt cleat). The yellow arrows show flow direction of gas* **(Myers, 2010)**.

The permeability of coal seams can be influenced by variation of geological structures (fault, fracture or dyke). Coal seam permeability is generally affected by changes in a geological structure of a specific location of a fault or dyke. The degree of permeability in structures is influenced by how severe the structural variabilities are. The area of study for this specific permeability evaluation is favorable for coal-bed methane drainage as the geological structure is relatively simple and there is reservoir/coal seam continuity, however the presence of faults and dykes in the structural system makes it a complex one as the cleat system tend to be severely damaged and may lead to low permeability most especially in structurally compressed regions.

Fracture density and aperture will aid in the determination of flow potential of fractures. The main indicator of flow potential and permeability of fractures is however derived from fracture orientation relative to stress field (Rider & Kennedy, 2011). On the other hand geochemical studies suggest that it is the fracture orientation in the stress field that is most indicative of flow potential. This theory will be tested in the current study.

Fracture geometry and connectivity are of importance as they promote permeability thus isolated fractures may yield limited flow. The orientation and connectivity of cleats relative

to coal-bed permeability affects the drainage, because if face cleat is in the same direction as bed permeability the drainage will be higher than in any other direction. This connectivity is interrupted by smaller fractures terminating against the main fractures network, and sometimes by large fractures at coal-non-coal interfaces (Laubach, et al., 1998).

Cleat-fracture porosity in coal is in the order of 0.5-2.5% and though free gas exists in coal fracture systems, coal bed methane is mainly adsorbed on the large internal surface area of the impermeable coal matrix and fracture surfaces (Laubach et al., 1998). The very existence of fractures allow the non-free gas to be drained from (desorbed) from the coal matrix. Desorption of gas from the internal coal surface is followed by diffusion through the coal matrix bounded by the cleat and, finally by laminar flow through the naturally occurring fracture network, known as the cleat system (Harpalani & Liu, 2013).

2 REGIONAL GEOLOGY

2.1 GEOLOGICAL BACKGROUND

2.1.1 The Kalahari Karoo Basin and Central Karoo Sub-basin

South-central Africa Karoo basins formed during the active period of Pangea breakup which had its influence from two main tectonic regimes, the first being the southern tectonic regime which involved subduction and orogenesis along the Panthallasan margin of Gondwana and later resulting to the formation of the retroarc foreland systems seen in the main Karoo Basin of South Africa and neighboring countries, the second tectonic regime was the influence of the northern and Tethyan margins dominated by extension and transtensional stresses which propagated southwards (Catunean et al., 2005). The extensive basins of Botswana have developed on a stable Precambrian infrastructure with a thin condensed preservation of the Karoo sequences.

The Kalahari Karoo Basin is subdivided into seven sub-basins based on their geological setting and facies distribution according to (Smith 1984). These sub-basins are: (1) western, (2) southeast, (3) southern and (4) northern belts of the Central Kalahari Sub-basin together with (5) southwest Botswana; (6) Northeast Botswana and (7) Northwest Botswana. The study will only focus on the southeastern belt of the Central Kalahari Karoo sub-basin where the study area is located and the Morupule coal seams are seen.

2.1.2 STRATIGRAPHY OF THE CENTRAL KALAHARI KAROO SUB-BASIN

The stratigraphy of the Central Kalahari Karoo sub-basin comprise of five lithological units making up all the geological sequences of the entire basin. The groups and formations seen along each locality belong to the Dwyka, Ecca, Beaufort, Lebung and the Stormberg Lava Groups. A general stratigraphical outline of each will be given herein and further description as per each sub-basin in the Central Kalahari Karoo with more emphasis on the South-Eastern belt.
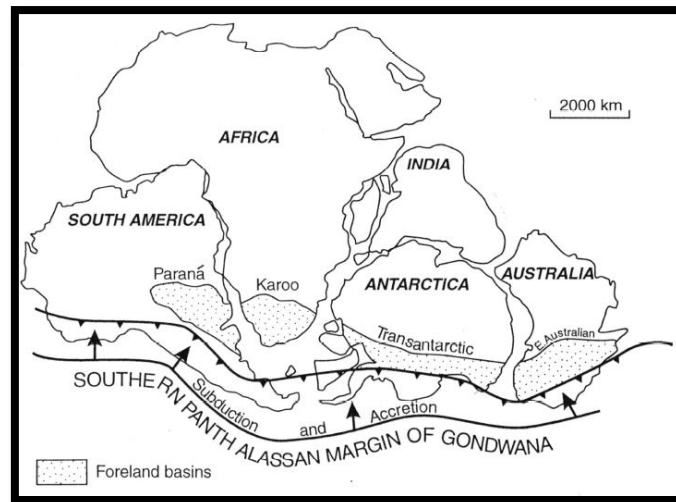
Figure 7 *Late Gondwana framework showing the areas affected by accretion and formation of the foreland basins* **(Segwabe, 2008).**
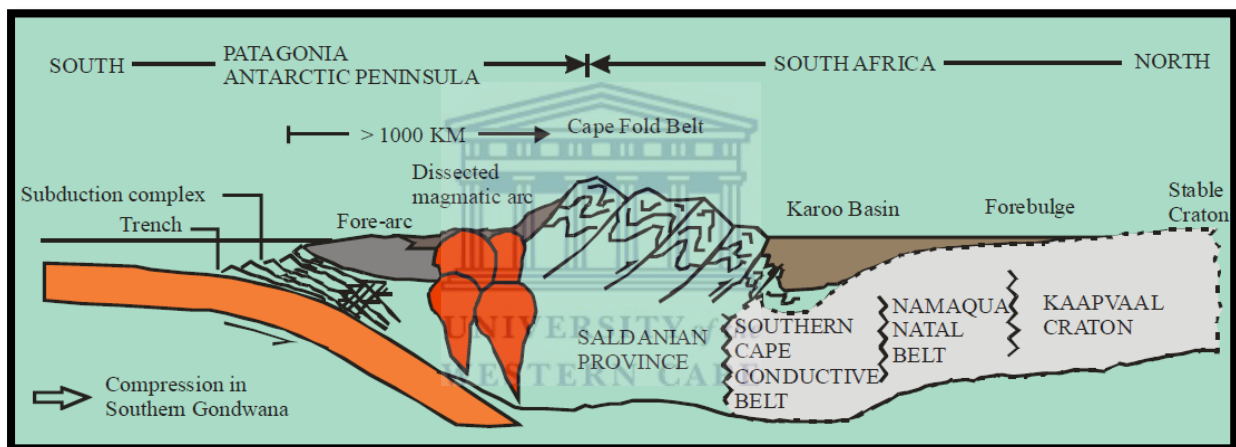
Figure 8 Formation of the retroarc foreland basin of the Karoo Supergroup during Pangea breakup, seen in the Main Karoo Basin of South Africa **(Segwabe, 2008)**

 The Karoo sequence rests uncoformably on the Precambrian basement (Bennet, 1989). This Kalahari Karoo basin has been mapped as a shallow interior sag basin owing to its centrally located nature, it is also described by seismic and aeromagnetic data as a rift basin (Modie, 2007) . Some hidden fault trends along the northeast side of the basin thus forming what may appear as half graben structures, the hidden fault is interpreted as a normal fault with a southeast throw (Kingston, 1988) although many other authors have decribed these series of faults to be strike-slip transtension faults. The half graben structures thus relate to trantensional (extension related to strike-slip tectonics).

The Kalahari Karoo basin of Botswana covers an approximate area of 70% of that country and is filled by Carboniferous to Early Jurassic beds (Bordy et al., 2010). It is elongated in

the northeastern direction attaining a maximum area of 217 square kilometers (Kingston, 1988). Kalahari Karoo Basin documents the thickest sequences along the south-west (thickening direction) with an average of 1500m and decreases to the north to about ~1000m, with a general south-south-west thickening sequence (Bordy et al., 2010).

The basement of the basin comprise s Archean to Neoproterozoic rocks (Kampunzu et al., 2000)The Karoo sediments which dominate the central region of the country are mainly of continental-fluvial origin and to the east of the country are represented by thick basaltic lavas which overlie the Precambrian rocks. Northern Botswana comprise of a series of deep, underlying fault lines which run beneath the sands. Sedimentation in the Kalahari Karoo Basin occurred along fault bound graben structures (Modie, 2007).These faults appear to be the southernmost extensions of the same system of parallel fault lines forming the East Africa Rift Valley (Mclntire, 2010). In Botswana these fault lines are observed to run parallel to each other trending in a northeast to southwest direction

The Kalahari beds regionally cover the underlying Karoo sequence (Smith,1984). The stratigraphy of the Central Kalahari Karoo sub-basin depicts a transition from glacial period through fluvio-deltaic and swampy periods and finally turning arid prior to the continental basaltic lava extrusions (Modie, 2007). It sudivided into the lower, Dwyka, Ecca & Beaufort Groups and overlying upper Lebung clastics and Stormberg Lava Groups with their corresponding formations (Smith,1984). A regional unconformity informally divides the Kalahari Karoo Basin stratigraphy into upper and lower units above and below the unconformity respectively (Bordy et al., 2010). Cessation of the Karoo sedimentation was soon followed by theoleitic flood basaltic lava outpouring during Early Jurassic (Advanced Resources International, Inc, 2003) thus forming the blanket of Stormberg Lava Group seen across most localities of the basin. Faults and fractures resulted in enormous outpouring of the basalts.

Depositional Environments & Lava Emplacement

The Dwyka Group is the lowest lying and comprise of a series of glacial deposits such as diamictites, varvites and sandstones, these beds are overlain by fluvio-deltaic Ecca Group sucession comprising predominantly of the coal-bearing successsions of carbonaceous sequences of mudstone and arkosics sandtones of the entire Botswana region. Above the deltaics there is a sequence of fluvio lacustrine Beaufort Group overlain by aeolian and fluvial dominated clastic deposits of the Lower Lebung Group which is dominated by

mudstones and sandstones. Unconformably overlying this group it is the Upper section of the Stormberg Lava Group of continental flood basalts and subvolcanic complexes (Bordy et al., 2010).

AGE	STRATIGRAPHY			LITHOLOGY	DEPOSITIONAL ENVIRONMENT
Jurassic		STORMBERG LAVA GROUP		Basalt > amygdaloidal	Continental flood basalts >extensional tectonics related to on-set of Gondwana break-up.
Triassic	SUPERGROUP	LEBUNG GROUP		Red beds > sandstone	Arid continental palaeo-climate >Aeolian >Fluvial >Lacustrine
		BEAUFORT		> siltstone, mudstone > sandstone, rare c/glomerate	
	KAROO			Siltstone, mudstone, limestone	Transitional >Lacustrine
Permian		ECCA GROUP		Sandstone, siltstone, carbonaceous mudstone, and coal	De-glaciation, and amelioration of the palaeo-climate. >Fluvio-deltaic >Swamps >Lacustrine/marginal marine
				Mudstone	
Carboniferous		DWYKA GROUP		Mudstone, varvites, siltstone, sandstone, and tillites	Glacial palaeo-climate >Subglacial >Glacio-fluvial >Glacio-lacustrine

Figure 9 A general lithostratigraphy and palaeo-environments of the Karoo Supergroup, Kalahari Karoo Basin, Botswana. (Modie, 2007). The coal zones are contained within Ecca Group, modified after (Modie, 2007).
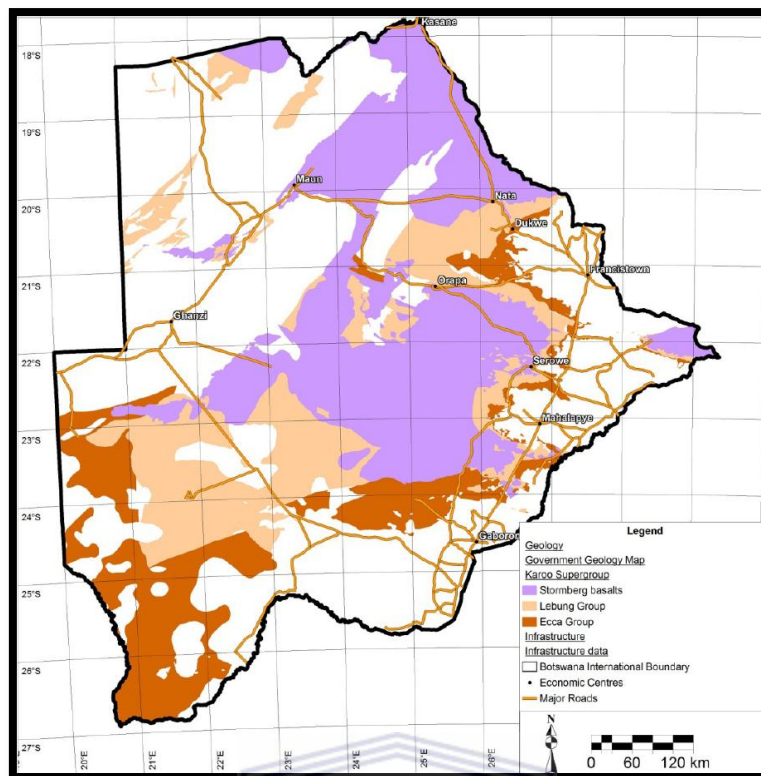
Figure 10 *Index map of the Karoo Supergroup showing major exposures of rock sequences as explained in legend* **(Potgieter & Andersen, 2012).**

The Ecca Group (Figure 10) is described as a post glacial deposit which is characterised by complexes of fluvial and delta plain systems with lacustrine and swampy conditions, wherein siltstone, mudstone, carbonaceous mudstone and coal beds have accumulated (Modie, 2007; Smith, 1984).

The sediments of Beaufort Group were subjected to aridity conditions during the migration of Gondwana from polar regions, that led to the deposition of the lacustrine Thlabala formation of this group (Modie, 2007; Smith, 1984). Modie (2007) described the Thlabala Formation lithology as monotonous, non-carbonaceous, silty and calcareous nodules and silty limestones.

The Lebung Group Figure 9 represents the end of the Karoo sedimentation. This group is predominatly characterized by progressive arid conditions passing from lacustrine to fluvial and finally to aeolian systems. Formations within this group are the Mosolotsane and Ntane Fm with red beds (Figure 9). The Mosolotsane formation forms base of the Lebung Group. It is conformably succeeded by the Ntane Fm composed by thick sequences of massive and bedded sandstones (Modie, 2007).

24

Sedimentation in the Kalahari Karoo basin ended in the Early Jurassic with widespread continental flood basalt sheets of the Stormberg Lava Group, due to the extension tectonics. The flood basalts are described to represent major regional magnetic event that occurred between 185-177 My (Modie, 2007).

.

2.2   CENTRAL KALAHARI KAROO BASIN
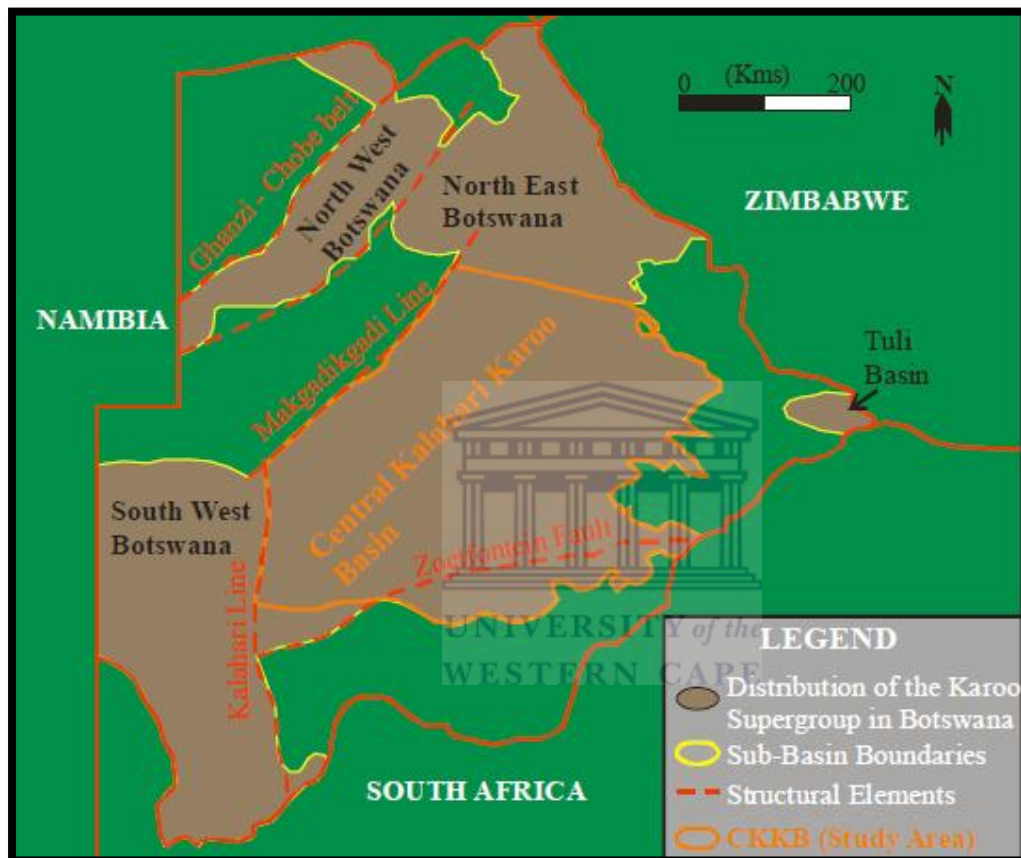
Figure 11 *Structural features and sub-basins (according to* **Smith, 1984) of the Kalahari Karoo basin (Taken from Segwabe, 2008).**

2.2.1   GEOLOGICAL BACKGROUND

Pre-Karoo formations border the central sub-basin along the east and northwest regions, south of the Zoetfontein fault (Figure 11) is the limit of the Karoo sequence in the south-eastern Central Kalahari sub-basin and the northern region of the sub-basin the Karoo strata is confined by crest of the basement high through the Makgalakgadi Pans (Smith, 1984).

Within the central Kalahari sub-basin more emphasis will be given to the south-eastern belt. Smith 1984 has sudivided the Central sub-basin into four regions or belts based on their different stratigraphy (Figure 12).

Zoestfontein fault is described by Modie (2007) as a reactivation of older tectonic features between the Archean Kaapvaal Craton and Limpopo Belt and it also shows the influence of the Karoo loading by sedimentation, maintaining a growth fault geometry and nature. The fault is well documented in the southern localities of the central sub-basin.

The coal bearing Karoo strata in the Central Kalahari Karoo Basin are however confined to the Ecca Group. The Botswana Ecca Group coals are comparable with the large South African coals belonging to the same lithostratigraphic succession. For the scope of this work focus will be on the southeastern belt of the Central Kalahari Karoo sub-basin and emphasis will be primarily on the Morupule Formation of the Ecca Group, due to time constraints and lack of data.

2.2.2 TECTONIC SETTING

The Central Kalahari Karoo Basin is described as a north-westerly plunging synform, with the flanking areas of crystalline basement forming the complementary anticlines (Segwabe, 2008). The tectonic regime of the entire Karoo basin is due to compression and accretion (Catuneanu, et al., 2005). The basins and sub-basins of the Karoo basin were subjected to extension tectonics that eventually gave way to the extrusion of Stormberg Lava rise of upper mantle and thinning of continental crust. The faults seen in this region have been inferred to post-date the Karoo period (Segwabe, 2008). Hence: first thermal crustal thinning and no faulting (continental sag + sedimentation occured, then extrusions and then faulting. Most of the faults are described to be the main controllers of the observed graben-like structures of the central block.
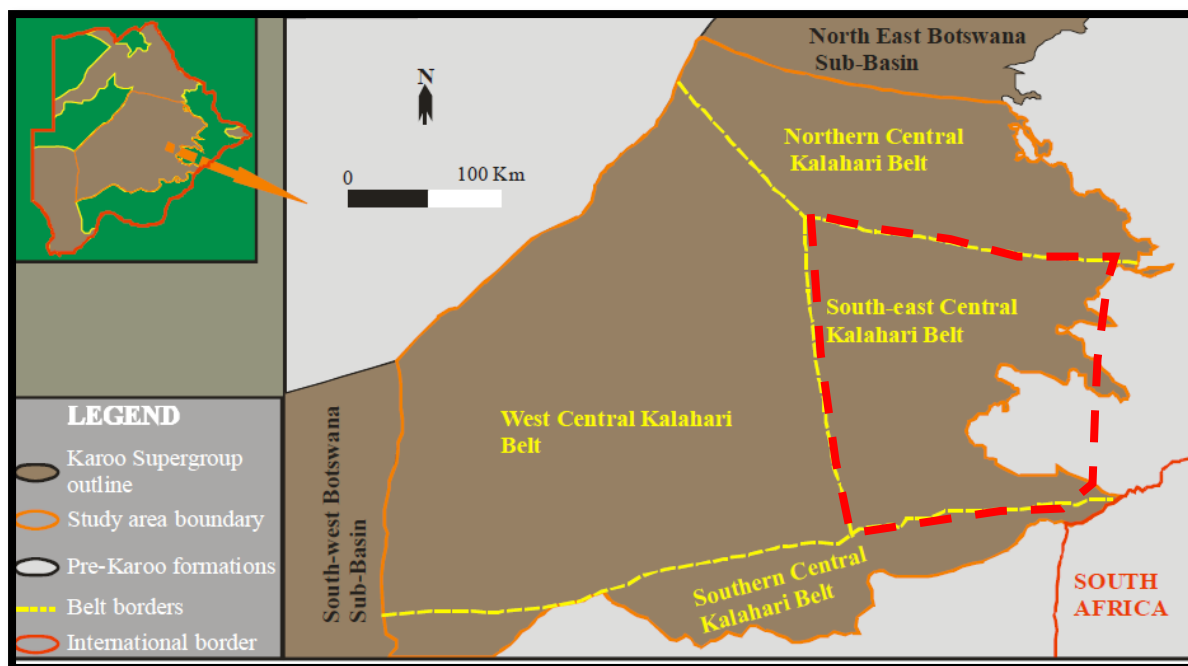
Figure 12 *The sub-divisions (Belts) of the Central Kalahari Karoo sub-basin, top right corner of image is the index map of Botswana* (Segwabe, 2008)*, Study area is denoted by the red dotted box.*

2.3 LOCAL GEOLOGY

2.3.1 Southeastern Belt

2.3.1.1 Geological Setting

The southeastern basin of the Central Kalahari Basin lies above the Archean Limpopo Mobile Belt (LMB) basement succession. A series of shear faults have been observed along the LMB trending ENE-WSW and, dated 2700 Ma. They have an impact on the Karoo Super-Group and the Waterberg Super-Group (Smith, 1984). The SE Central Kalahari Belt is bounded by both Zoetfontein and Letlhakane faults, south and north of the belt respectively. Due to the activity of LMB tectonism central zones of troughs and ridges developed along the Archean basement.

The Makoro trough formed before Karoo sedimentation, is of great importance in the region because it holds the thickest succesions of the Morupule Fm. Smith, 1984 suggested the thickness may be the result of syn-sedimentary WNW-ESE trending faults with of throws ranging 15-20m. North of the Makoro trough there are some smaller graben and horst structures which may have affected the Karoo deposition, and also associated with some post-Karoo reactivation of the WNW-ESE trending and of the minor NE-SW faults (Smith, 1984).

2.3.1.2 STRATIGRAPHY (green box delineates the area of interest)

Lithostratigraphy of the Central Kalahari Basin of Botswana

Age	Groups	Western Belt	Southern Belt	South-Eastern Belt	NE & Northern Belt
Jurassic	STORMBERG	Stormberg Lava Goup (Undivided)			
L. Triassic-E. Jurassic	LEBUNG	Ntane Sandstone Fm			
		Mosolotsane Fm			Ngwasha Fm
					Pandamatenga Fm
				Dolerite dykes &sills	
Triassic	BEAUFORT	Kwetla Fm		Tlhabala Fm	
Permian	ECCA	Boritse Fm	Korotlo Fm	Serowe Fm	Tlapana Fm
			Mmamabula Fm	Morupule Fm	
		Kweneng Fm	Mosomane Fm	Kamotaka Fm	Mea Arkose Fm
		Bori Fm	Bori Fm	Makoro Fm	Tswane Fm
Carboniferous	DWYKA	Dukwi Formation			

2.3.1.2.1 DWYKA GROUP

The Dwyka Group rests unconformity over the pre-Karoo sequences of the Waterberg Supergroup along the SE sub-basin. The glacial deposits of the SE Central basin have been grouped into the Dukwi Formation. The Dukwi Fm apart from comprising of glacial deposits also contains an intercalation of sediments found above the basal unconformity, the sediments include varved siltstones and mudstones which may/may not have dropstones (Smith, 1984), tillite sediments make up the basal succession of this group (Advanced Resources International, Inc, 2003).

2.3.1.2.2 Dukwi Formation

Comprise of the thickest succession very far in the SE Central basin, information on the thicknesses acquired from borehole data. The Dukwi Fm (Late Carboniferous) is divided into Members which have high facies variation throughout the formation (tillite, varvites and sandstones). The base of formation is dominated by tillite deposits, Smith (1984) interpreted these as tillites on the basis of their association with varved deposits

A sequence of varved mudstone division follows the sandstone and attains a thickness of ~6m, also observed are cyclic laminations of siltstone and mudstone which may or may not include of scattered dropstones, these deposits are collectively called varvites.

Smith (1984), has divided the glacial deposits of the Dukwi Fm to Members or divisions and the facies interpreted to be proximal facies with deposition in a terrestrial environment. The patchy distribution of the tillite deposits in some localities may be due to deposition in a high basement topography. Smith 1984 also states that the implication of lack of till deposits in some regions may suggest that no till was deposited below the ice sheets as a consequence of erosion or debris transportation of the sheet elsewhere.

2.3.1.2.3 ECCA GROUP

. The Ecca Group (Permian) comprise of the Karoo strata above the glaciogenic deposits and below the non-carbonaceous silty mudstones of the Thlabala Fm. In the Central Kalahari Karoo sub-basin the Ecca strata most especially the lower Ecca deposits are a continuation of the Dwyka Group with strong thickness variations This is attributed to deposition in glacial lakes that expanded through erosion expanded to what is now the Central Kalahari sub-basin (Advanced Resources International, Inc, 2003). The glacio-lacustrine origin of the Ecca Group deposits has led to the relatively high prospectivity of this group in terms of coal generation.

2.3.1.2.3.1 Makoro Formation

The Makoro Formation forms the basal Ecca strata in the South-East belt. The Makoro Fm strata are seen and restricted to the deeper parts of the region including the Makoro trough. This formation may be described as the lower Ecca which overlays contain small amounts of the preceding glacial deposits; however the sediments are sandier sediments (Advanced Resources International, 2003). Based on relative abundance of facies the formation is divided to two members outlined below on the basis of facies distribution

a) Mantshididi Member

Borehole data (well logs) acquired from certain localities suggest a thickness of 53m made up of all the mudstones conformably overlying the Dukwi formation. The sedimentary rock types making up the Mantshididi member are siltstones, sandstones and mudstone intercalation. Although this member is mainly clastic, some carbonate cemented zones have been reported.

b) Limoni Member

The Limoni Member is approximately 56m in thick and compose interbedded sandstones and mudstones, occasionally bioturbated, conformably overlying the above member. The strata were interpreted as distal turbidites in a deltaic environment (Smith, 1984).

The presence of the cemented carbonates (exclusively cemented by calcite or dolomite) represents a quiet depositional setting as a result of precipitation from biogenic sources such as phytoplankton. The argillaceous member may be described as pro-delta mud and the observed subsequent influxes of fine grained clastic sediments as distal turbidites. The alternation of sandstone and rippled siltstones suggest an increase in bottom current activity with low energy levels.

2.3.1.2.3.2 Kamotaka Formation

The Kamataka Fm is represented by a Feldspathic sandstone unconformably overlying the Makoro Fm in the homonious trough. Komstsks Fm deposits prograded over the basement of the sub-basins as it is noticeable towards the margins of the sub-basin, where Kamotaka Fm unconformably overlies the pre-karoo basement through a basal conglomerate (Smith, 1984; Advanced Resources International, 2003) .The Komotaka Fm pinches out against the higher basement ridges (Smith, 1984). The Kamotaka Fm is widespread throughout the basin with facies indicating fluvial dominated, proximal deposits which may have formed as a delta overlying the Mokoro Fm laterally migrating facies with rip-up clasts and good sorting were seen. Peat and overbank were preserved on floodplains or delta plains before the deposition of the Morupule. Some sandstone sequences are derived from reduced environment settings which may be an indication of waterlogged sediments of cool humid environments or climate (Smith, 1984).

2.3.1.2.3.3 MORUPULE FORMATION

The Morupule Formation hosts the coal beds studied in this thesis. The Morupule strata appearalong most of the Central Kalahari sub-basins (Smith, 1984) with the thickest seams are seen along the eastern limit and gradually thinnig along the northern and western flanks (Callaghan, 2013). The Morupule Formation overlies the carbonaceous mudstone layer of the Kamotaka Fm. The marker bed seen at the top of Morupule Fm consist of the non-carbonaceous siltstone of the Serowe Fm (Smith, 1984). The Morupule Fmwas also subdivided into members and sub-members (Smith, 1984) according to the coal seam features.

a. F1 Member

This member is the lower one of the Morupule Formation it is composed of interbeddedcoal, carbonaceous mudstones and calcareous nodules, up to 19.5m thick that occur between ~ 285-304m in some wells. The coals of F1 Member are relatively thick and are separated into two different seams by interbedded carbonaceous (Smith, 1984).

➢ F1a Seam

This is the main Morupule coal seam and at well C165 appears at a depth of 298.3-304.7m. Texturally the coal seam grades from a dull coal with some silty mudstone stringers thickening to a few centimeters. This seam is inertinite rich with some sporadic pyrite nodules or disseminated pyrite. At the top and base of this seam is an occurrence of a vitrinous coal band a few meters thick. Within the bands thin carbonate coatings may occur on the cleats the brighter bands. Some light brown irregularly developed limestone bands about 13cm thick, can be observed they have been interpreted by Smith 1984 as channel fill deposits owe to their sharp bases. These may be siderites precipitated in reducing environment.

➢ F1b Sub-member

This sub-member comprise of a carbonaceous mudstone sequence approximately 5m thick and is observed at depths of 293-298m above the F1a seam. Colour variation grades from black carbonaceous mudstone with dull coals and lenticles of brighter coal (Smith, 1984).

➢ F1c & F1d Sub-members

These sub-members overlay the F1b sub-member and comprise of dull heavy coal seams with some thin coaly mudstone beds separating one from the other. The coaly mudstone band found within this facies is seen to the top of the F1 member. F1c and F1d sub-members are not as well developed as the lower sub-member and the overlying F2 Member (Smith, 1984).

b. F2 Member

This member is made up of carbonaceous mudstones with interbedded thin heavy dull coals containing bright coal stringers. It occurs at a deph of 254.60-285.14m, attaining a

maximum thickness of ~30.5m. Thin (centimeter thick) veined and shaly limestone bands just below the top of F1 member can be observed Smith, (1984) has decribed the coaly bed as a lens with gradational boundaries, which can evidence the transportationof the carbonaceous material and its mixing with the argillaceous sediments. The sandstone wedges in the Morupule coalfield shows varying vertical and lateral extensions widening and thinning towards the top of F2 Member where sandstone wedges are confined (Smith, 1984).

c. F3 Member

It is the uppermost member of the Morupule Formation occurring at depth of 239.98-254.60m and attaining a maximum thickness of ~14.6m, also subdivided into sub-members. At the base of F3 member is the Lotsane seam sub-member F3a appears, with mixed or bright coal, 2.65m thick. Outside the Morupule Coalfield this member becomes more variable in both thickness and quality such that intercalations of the thin coal seams and carbonaceous mud may be observed. At depth of 239.98-251.95m in well C165 there is a 12m thick carbonaceous mudstone interbedded with some bright coal or siltstone stringers (Smith, 1984).

2.3.1.2.3.4 Serowe Formation

This formation is very distinctive at the base and thus can be seen along the major parts of the southeastern belt comprising more of siltstone and mudstone members. The argillaceous units are slightly carbonaceous with some stringers of rare limestones and relatively thin coal sequences ~0.2-2.5m thick (Smith, 1984; Advanced Resources International, 2003). The upper section of this unit observed by Smith (1984) contains channel fill deposits. Smith, (1984) has analysed the channel system and they mainly occur in thickened sequences with non-erosional bases. These channel sytems have lucustrine infills which may be the result of subsidence. The Serowe formation has a relatively stable and low energy environment, with the coals deposited in a flat surface of a tectonically stable trough of slow subsidence (Smith, 1984). Peat always grow where there is a low-relief environment with very stable shallow water conditions.

2.3.1.2.4 Beaufort Group

This group is generally defined by deposits of lacustrine nature comprising of silty mudstones overlying the coal sequence of Serowe formation below. These lithologies according to Smith can be correlated to sandstone members of other parts of the Thlabala formation across the

southern parts of the East Central sub-basin. The depositional history of the Thlabala formation has been discussed and interpreted as an unristricted wide lake containing some arenaceous sediments. Some calcite is present within the formation and may be an indication of chemical precipitation or biogenic origin for the carbonates combined with signs of bioturbation in the region. A large unconformity exists in this formation and is preserved at different levels in each interval along the formation, this is caused by the different levels of erosion across the formation (Smith, 1984).

2.3.1.2.5 Lebung Group

An unconformity exists at the base of the Group and top of Tlhabala formation below. The Lebung Group can be defined as a red terrestrial rock sequence which has both a vertical and horizontal sequence variation and theses variations are inclusive of sub-basinal margin disconformities (Smith, 1984). The Lebung Group has two formational subdivisions, the Lower Mosolotsane Formation (Fm) and the Ntane sandstone Formation. The Mosolotsane formation contains of clastic sediments with eaolian characteristics and are overlain by the sandstone member of the Ntane Formation. The environment of deposition of the Mosolotsane Fm is of fluviatile terrestrial conditions with some evidence of renewed uplift seen from influx of coarse clastic sediments after a period of erosion (Smith, 1984). Red siltstones and mudstones may be due to deposition in a distal flood plain in shallow water or flash floods (Smith, 1984). The red colour of the beds is an indication of a period of semi-arid conditions. The Ntane Fm rests on the Mosolotsane Fm and in some localities where the Msolotsane Fm has been eroded away the Ntane sediments rests directly on the member below. The Ntane Fm depositional environment appears to be arid or desert environment which is dominated by eaolian sandstones. Sedimentary features such as cross-bedding on massive sandstone layers indicate ancient dunes

2.3.1.2.6 Stormberg Lava Group

The Stormberg Group comprise of an undifferentiated volcanic suite. The base of the Lava Group appears sharp and is unconformable on the Ntane Sadstone. There are six lava flows identified with the minimum thickness of flow 17.27m (Smith, 1984). The nature of the basaltic lava is mainly of tholeiitic type with intersertal texture (Smith, 1984), fractures and joint sets from deeper lithologies have allowed for the movement of the basalts forming dolerites which have greatly impacted on the coals of the Morupule and Serowe respectively.

3 DATA & METHODOLOGY

Most coal seams possess a dual fracture system which may contain large reserves of gas adsorbed to the cleat network system and which is responsible for desorption during production, therefore a qualitative and quantitative study of the fracture system is fundamental to the petrophysical evaluation. The Acoustic Televiewer (ATV) log is crucial to this study and helps improve the understanding of coal fracture properties and is (including the petrophysical attributes)

This study will involve the estimation of fracture parameters with the use of well based image logs (ATV), according to the succession of steps to interpret Fracture systems developed by Yan et al. (2009). The evaluation of fractures will help in with permeability enhancement that will lead to a better gas flow.

3.1 Fracture Identification & Interpretation

Acoustic Televiewer (ATV) image data were analyzed for nine wells across the three license blocks in the study area, wells C1-9 and only wells that are indicative of fractures will be displayed herein. Instead of acquiring expensive seismic data, the ATV tool was used to properly define lithologic changes with depth as well as any feature intersecting the wellbore. For the purpose of this study we will analyze the microscopic fractures detected by the tool. Some of the features detected may be bedding and lamination which are very noticeablein cores (Figure 31) and also on the interpreted ATV log where they appear as continuous sinusoids with low dip angle. The tool detects the features as a result of a contrast in acoustic impedance of the specific features with the coal or clastic host rocks. Though the tool is capable of identifying such features from the other it is usually very difficult to filter specific ones against each other, such as bedding from flow banding or foliations. For this reason the dip and dip azimuth plots are used to better understand the features and their respective orientations.

On the ATV log planar features intersecting the borehole appear as sinusoids on an unwrapped 360 degree image view. The sinusoids indicating fractures tend to be often discontinuous. Each sinusoid can be represented by a tadpole plot and the dip and dip direction of each can be determined at each specific depth. Stick plots where dip was plotted as lines, can be used to identify high angled features that represent fractures at angles between 60 degrees and 80 degrees. The low angled features would represent of bedding.

3.1.1 Azimuth rose plot

This is circular histogram of azimuth data and are plotted as frequency rose diagram. The rose diagram is a useful indication of structural strikes. These have been plotted at 50m intervals across the zones of interest. The orientation of the main features and their stress fields will be interpreted based on this plot calibrated with other parameters such as fractures on core photographs, resistivity logs and ATV logs.

3.1.2 Lithostratigraphic Correlations

Interactive Petrophysics (IP) was used to model coal and formation correlation. Two types of well logs have been used to describe the formation properties within this study. Gamma Ray and Density logs have been displayed in the above well log correlation for the Serowe-Morupule coal seams, these have been chosen on the basis of their ability to detect responses of lithologies and distinguish coal from other siliciclastic rocks. Gamma ray log is applied to record individual shaliness for Uranium, Thorium and Potassium bearing minerals within the formation. The response of these radio-active elements records the radiation emitted by shales, sands or carbonaceous mudstones.

Coal Identification on logs:

- Bulk-density measurements less than 1.75 g/cc.
- Gamma ray measurements less than 60 API, used cut-off value of 40 API.
- Neutron porosity measurements greater than 50%.
- Sonic transit time greater than 80 μs/ft.> 240us/m (faster in coals)
- Resistivity greater than 50 Ωm.m.

3.1.3 Step 1: QUALITATIVE IDENTIFICATION OF FRACTURES

- Fracture response on logs: There is a set of common petrophysical logs that can be analyzed qualitatively to indicate the presence of fractures.
- MID cross-plot (Figure 14): gives a relationship of apparent-matrix density (g/cc) vs apparent-matrix transit time (μs/ft) in a fractured reservoir, data points depicting fractured zones plot to the left of the graph.
- M-N correlation (Figure 13 & Figure 15): M and N of the petrophysical properties are derived from a series of porosity logs (such as DEN, NPHI and DT), and the presence of fractures can be identified based on a cross-plot of M-N plotting near the top of the graph.
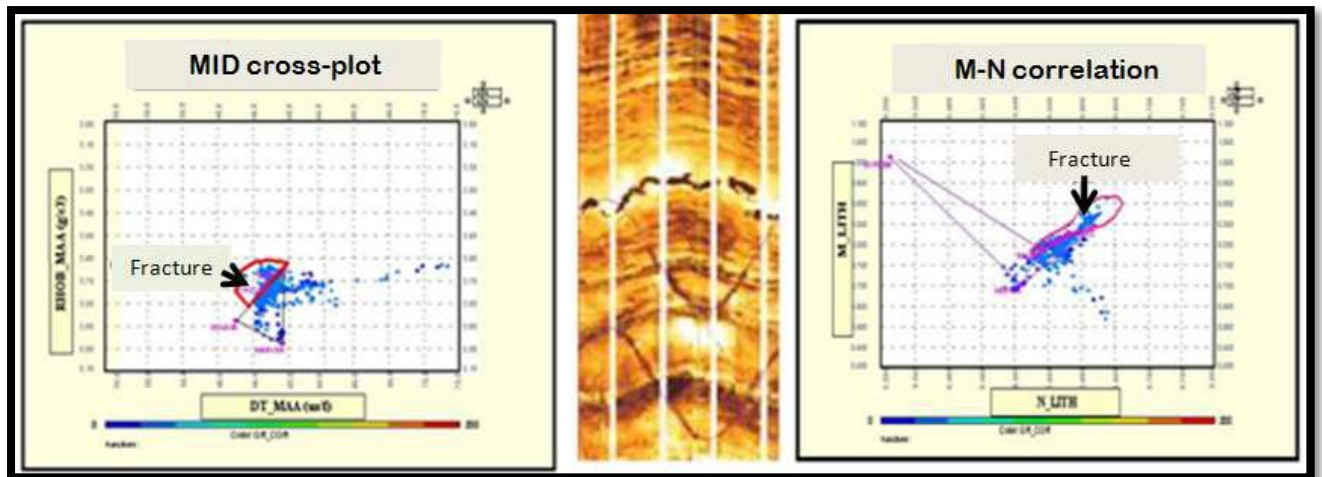
Figure 13 *An example of fracture identification, left Image shows an MID cross-plot, right is the M-N correlation, Fracture identification* (Yan, et al., 2009).
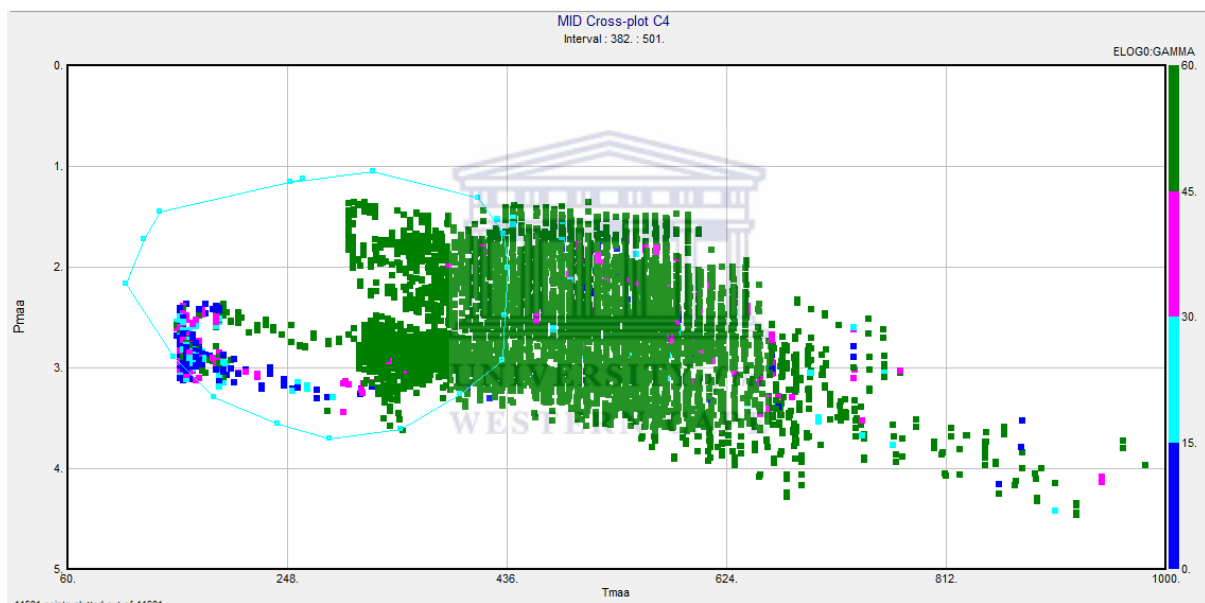
Figure 14 *Plotted MID cross-plot of calculated apparent-matrix density and apparent-matrix transit time, the colour bars depict GR points. Note the low GR points plot to the left evidencing fractured intervals, possibly in coal.*
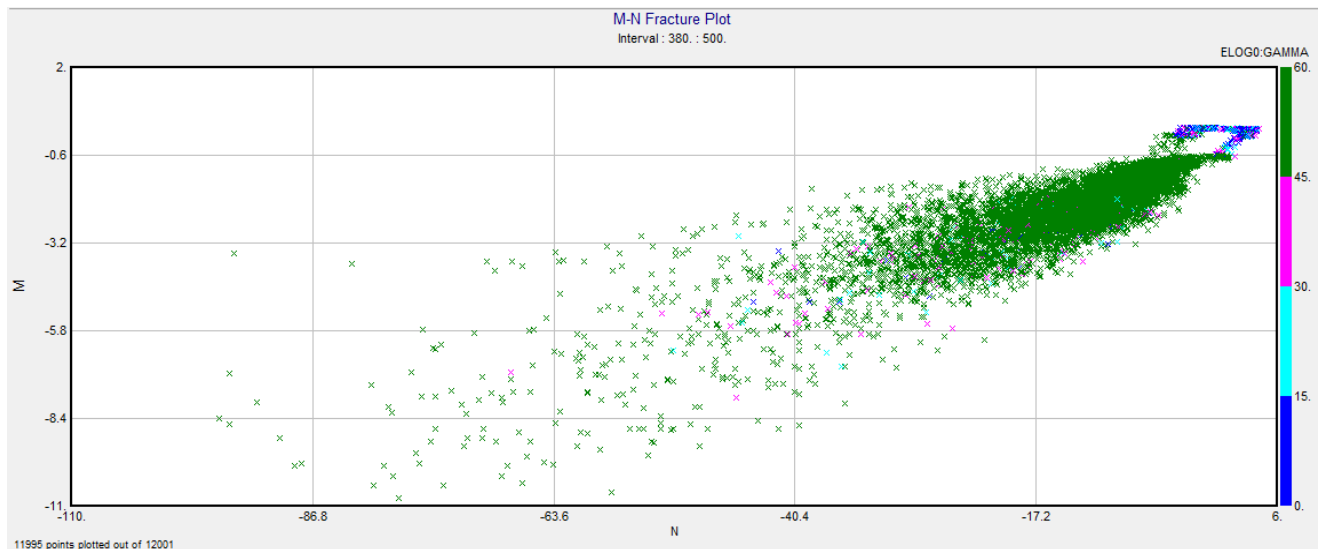
Figure 15 *Plotted M-N cross-plot calculated using density, neutron and sonic logs, colour bars depict GR points. Note the low GR points plot to the left evidencing of fractured intervals, possibly coal*

3.1.4   Step 2: QUANTITATIVE ANALYSIS OF FRACTURES

- **Porosity fracture index**: If a fractured formation can be considered as a dual porosity system then the effective porosity consists of both matrix porosity and a secondary fracture porosity. The effective porosity, obtained from the sonic log, is sensitive to the inter-granular porosity. Conversely, the porosity calculated using the neutron and density logs includes the fracture porosity (Yan et al., 2009).

- **Resistivity fracture index**: The resistivity fracture index predicts fracture information quantitatively based on mud filtrate invasion principles. It is calculated based on the deep and shallow resistivity logs in fractured zones for different hydrocarbon and water zones (Yan et al., 2009).

- **Fracture aperture**: The estimation of fracture aperture assumed that fractures were randomly distributed. Both horizontal and vertical fracture aperture are estimated using dual resistivity laterologs (LLD, LLS) and mud filtrate resistivity (R mf) (Yan et al., 2009).

These methods of analysis do work but the obtained values need to be checked for reliability. If a specific interval has been depicted to have high porosity fracture index (that is high fracture frequency) then a higher Fracture porosity should be expected. With regards to resistivity index which is obtained based on mud filtrate invasion it may indicate fracture presence where there is an increase in the resistivity fracture index curve, then a fracture aperture is estimated for both horizontal and vertical fractures. Particularly in this study the horizontal fractures seem to be better developed. This will be elaborated in the next few

sections. The methodology was developed in tight carbonate reservoirs, therefore it is possible the same methodology be applied to coals, as they have tight matrix and are naturally fractured.

All the boreholes in this report were drilled on gauge (where the hole diameter is the same size as the drill bit, where in a few sections of the hole is not the case may represent washed out zones.

4 Tool Suit Information & Description: Wireline Logging

4.1 Caliper tool

A three arm caliper used to measure the dip meter of the borehole and can be used in both open and cased holes (Potgieter, 2013). The tool measures the borehole size and shape, acoustic calipers use acoustic signals to derive a very detailed orientation of the borehole size and shape that can be displayed as 3-D images (Rider & Kennedy, 2011). The tool works by transmitting ultrasound source (transducer) within the tool to signal off the borehole wall as it rotates (Rider & Kennedy, 2011). The tool thus records the travel time from the transducer to borehole well and back to calculate the borehole size.

4.1.1 Caliper Log

Caliper logs are usually the first set of logs run in a borehole to measure the diameter of the hole or casing and quality control and or to correct inaccuracies for other suit of logs to be run. The caliper log is usually plotted as a dashed line or as in this report as mirror with scales 6 to 16 inches. The logs record the formation response of the formation to drilling, the caliper is often measured considering the drill bit diameter used. The logs also give information on fracture identification, lithologic changes, well construction and can be run in any borehole or under any conceivable borehole condition.

4.2 Acoustic Imager tool

Image logs are a computer created borehole images based on geophysical and electrical measurements such as acoustic conductivity and electrical reflectivity or formation density, the images are viewed as false colour images (Rider & Kennedy, 2011). The logs unlike standard logs, it sample every 2.5mm as opposed to the usual 15cm. The log is mainly used post-drilling to interpret smaller features such as fractures, bedding plane and sometimes borehole geometry.

The acoustic televiewer (ATV) uses a rotating transducer which emits repeated ultrasound pulses to and from the borehole wall, sweeping the full circumference of the borehole at least a few times a second (Rider & Kennedy, 2011). The Acoustic Televiewer takes an oriented image of the borehole with the use of high-resolution sound waves, which is then displayed in both amplitude and travel time (Potgieter, 2013). The data is thus presented in an unwrapped borehole format (Figure 16) orientated to north and unrolled to a flat strip (Rider & Kennedy, 2011). The tool needs to be centralized and therefore for the current study a three-arm caliper is usually run together with the ATV tool to achieve reliable orientation.
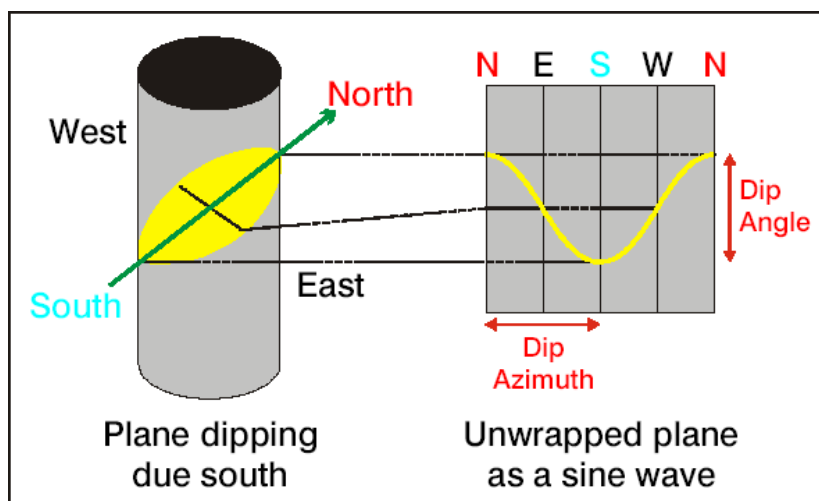
4.2.1 Acoustic Image Log

The data is by standard presented in the un-wrapped log format, where real vertical features remain vertical and horizontal remain as such, but real dipping surfaces on a log view will appear as sine wave (sinusoid) on the log (Rider & Kennedy, 2011). (Figure 16) if the dip is very steep, the amplitude of the sine wave will be also large and with the dip value measured from the sine wave. The crest of the of the curve is the highest point of the surface or fracture as it intersects the borehole and the trough is the lowest point as it leaves (Rider & Kennedy, 2011). Heated colour scales are generally used to visualize the image logs using a series of brown-black-orange-yellow-white, where light colours are evidence higher acoustic impedance high densities (Rider & Kennedy, 2011).

Coal tend to appear white due to their highly resistive nature and shale will have darker colours with lower acoustic impedance and lower density. Fractures reduce the reflected amplitudes and often appear as dark sinusoidal traces on logs. In terms of surface reflections a smooth surface reflects better than a rough surface and a hard surface better than a soft one (Rider & Kennedy, 2011). In water based mud, open fractures tend to be more conductive relative to the background matrix (dark on the image). Mineralized fractures will generally be resistive with high acoustic impedance.

4.2.2 Tadpole Plot

Tadpole plots are generally used in processed logs that show dip and dip direction of bedding planes and structural features. The tadpole plot displays a grid where the vertical scale is depth and the horizontal scale represents dip from 0^0-90^0. The Fracture dip on the log is represented by a circle (tadpole head) and the azimuth of the dip direction shown by an

orientated segment (tadpole tail) considering the north as a vertical line (Rider & Kennedy, 2011). The tadpoles plotted for this data set are of low quality (low correlation factor) this is seen by the non-solid nature of the tadpole heads.

4.2.3   Stick Plot

Stick plots are generally dips plotted as lines and are presented herein in two sections 90^0 and 0^0 view angles. The sticks show apparent dip in a direction indicated by how plot (Figure 17).
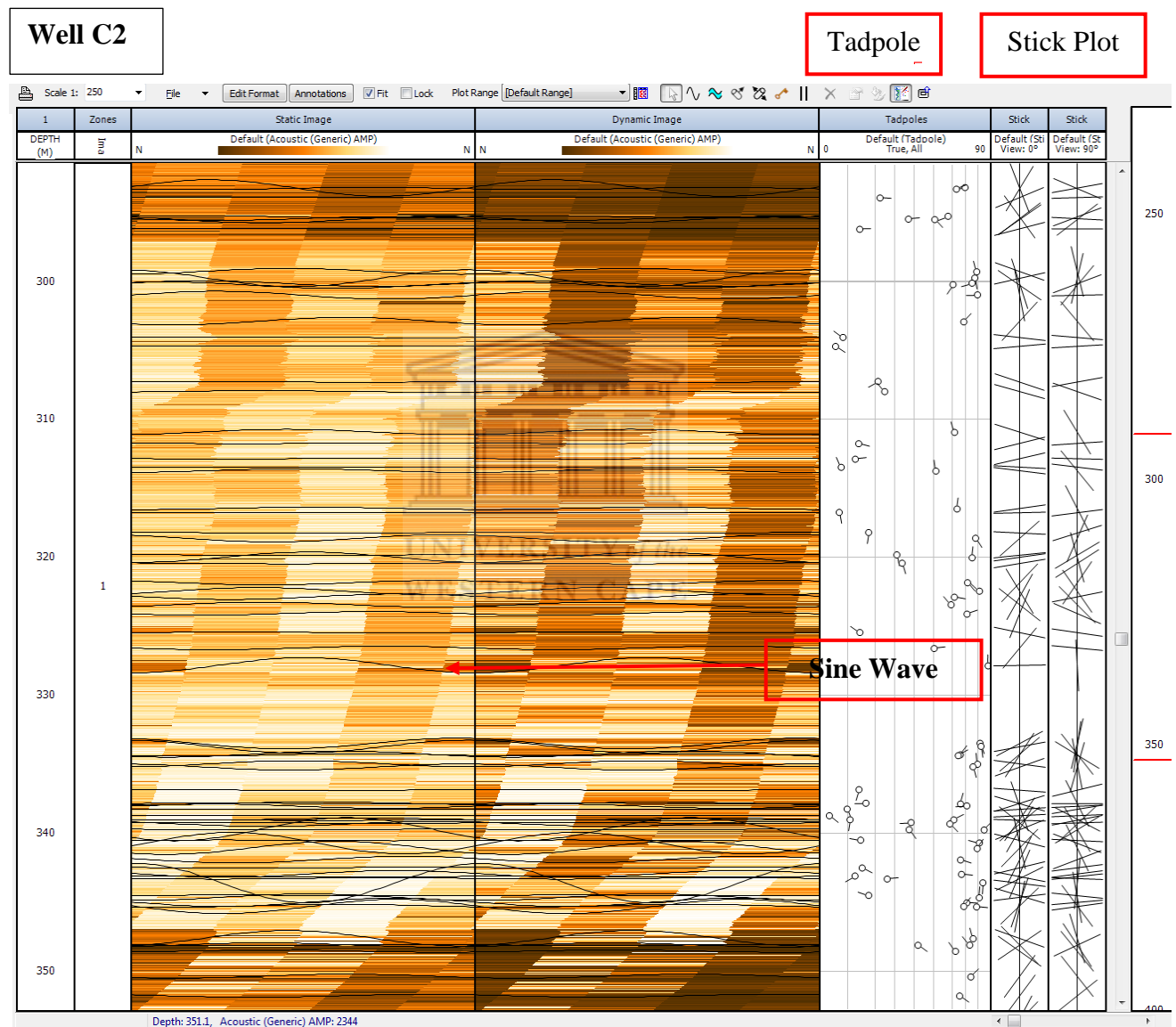
Figure 17 *Image log plot C2 well displaying picked sine wave alongside tadpole plot and stick plots dip azimuth*

4.3   Porosity Tools

The compensated density logging tool uses the two focused density detectors to compute borehole compensated while logging (Potgieter, 2013). The tool emits a gamma ray source in this case Cesium (^{137}Cs) into the formation, which electrons are responsible for scattering of

gamma-rays depending on their atomic weight (Rider & Kennedy, 2011). Formation density can therefore be calculated from an analysis of the near and far detector counting rates. Density tool is an excellent tool for coal-bed evaluation. This tool is normally run in combination with the compensated neutron. The compensated neutron has high gamma ray energy and detects the hydrogen index of the formation.

The density log is normally plotted on a linear scale of bulk density in units of g/cm^3 (Rider & Kennedy, 2011); generally the standard scale is 1.95-2.95 g/cm^3. The range of bulk density measurements for coal is between 1.2 g/cm^3 and 1.75 g/cm^3 which was the cut-off chosen for the Morupule Fm coals. For identification of coal thicknesses using density logs it must be considered the borehole conditions and the presence of washouts if any to avoid overestimation of coal thicknesses. The compensated Neutron log in combination with the density log can be used as coal identifiers. Coal has high hydrogen index values, so the compensated neutron log in coals records very high apparent porosity (Halliburton, 2008).

Well C1
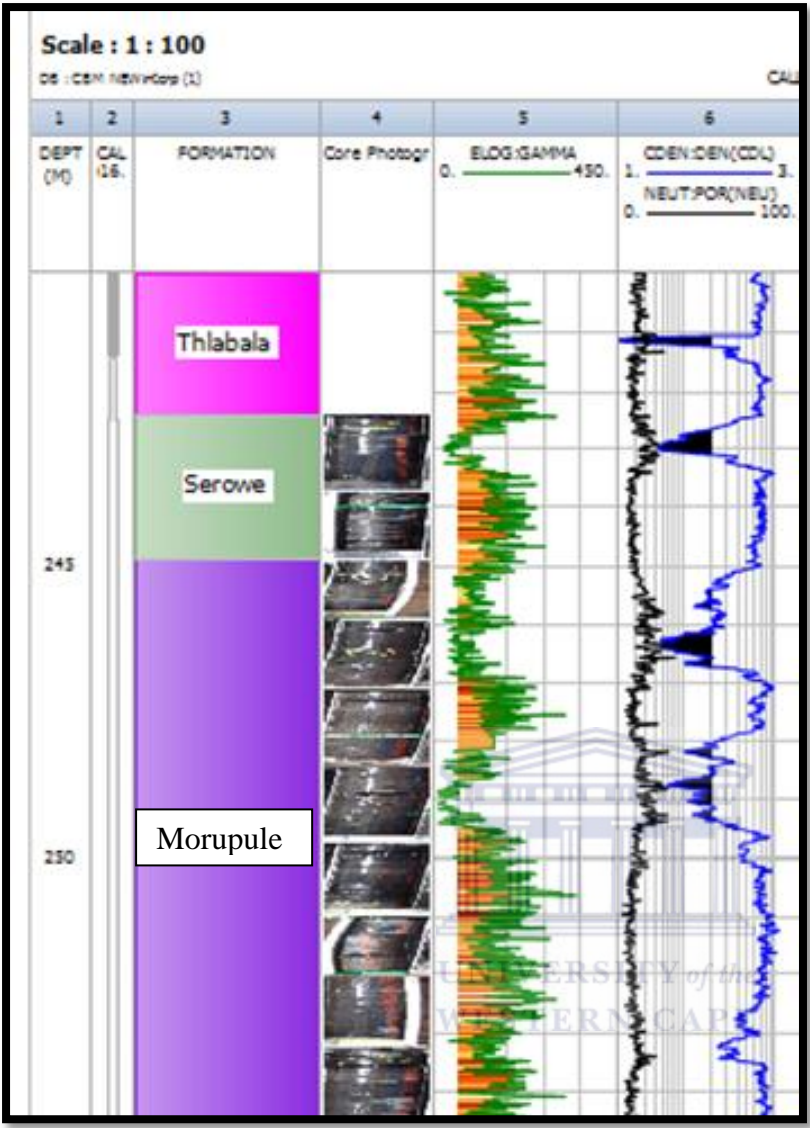
Figure 18 *Well log representation of well C1 depicting litholologic formations and core photographs taken from those intervals, the scale of core photos with the log depth is not one-to-one thus the resolution of the core, also the density log displays the coal zones with the black shading.*

4.4 Gamma Ray Log (GR)

The tool measures the bulk gamma radiation emitted from the radioactive minerals near the wellbore. The gamma ray tool derives radiation from thorium, uranium and potassium which are the bulk radioactive minerals in clays. Coals have very low GR readings due to low clay concentration (Halliburton, 2008) (Figure 19). The gamma ray log can usually be used to detect shale partings in a coal bed (Wood, et al., 1980) The Gamma ray logs can be used together with density logs for coal-bed evaluation to resolve uncertainties of rock identification.
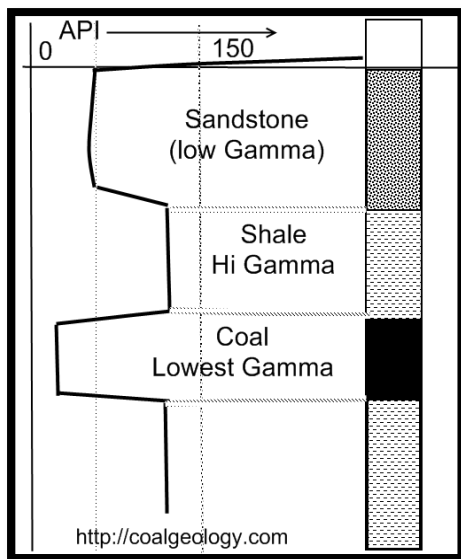
Figure 19 *GR log response to different lithologies, note very low GR value in the coal bearing zones* **(Geology, 2013).**

4.5   Resistivity Log

Three resistivity measurements were recorded, the single point resistance 16 inch, normal resistance 64 inch apart and the normal resistivity 48 inch and were used in the log analysis of this current data set. Resistivity is the most commonly used induction based tool in Coal-bed Methane (CBM) deposits. Coal exhibits rather high resistivity measurements though cleats I the coal seams tend to reduce the resistivity. Permeable coals typicallyshow an invasion profile while a tight coal shows very high resistivity with no invasion. For this study resistivity logs were used not only as calibration for lithology indicators but also for fracture zone identification.
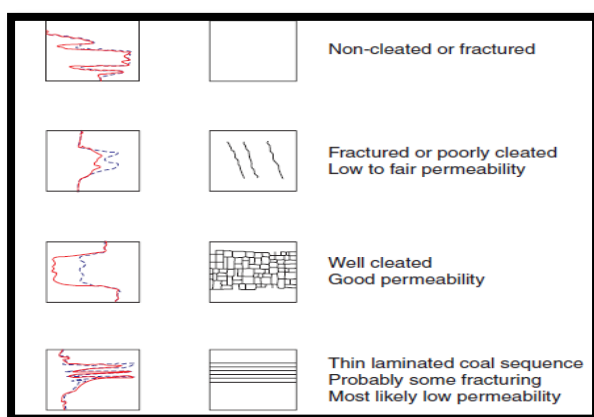
Figure 20 *Short spaced resistivity signatures for fracture identification* **(Halliburton, 2008).**

5 PRESENTATION OF RESULTS AND INTERPRETATIONS

Presentation of interpreted well log correlations, core photographs, well and image logs and cross plots.

5.1 Lithostratigraphic Correlation

The correlation is done for the wells C1-C9 using well top depth and bottom depth to delineate the actual thickness and the distribution across the three prospect license blocks.
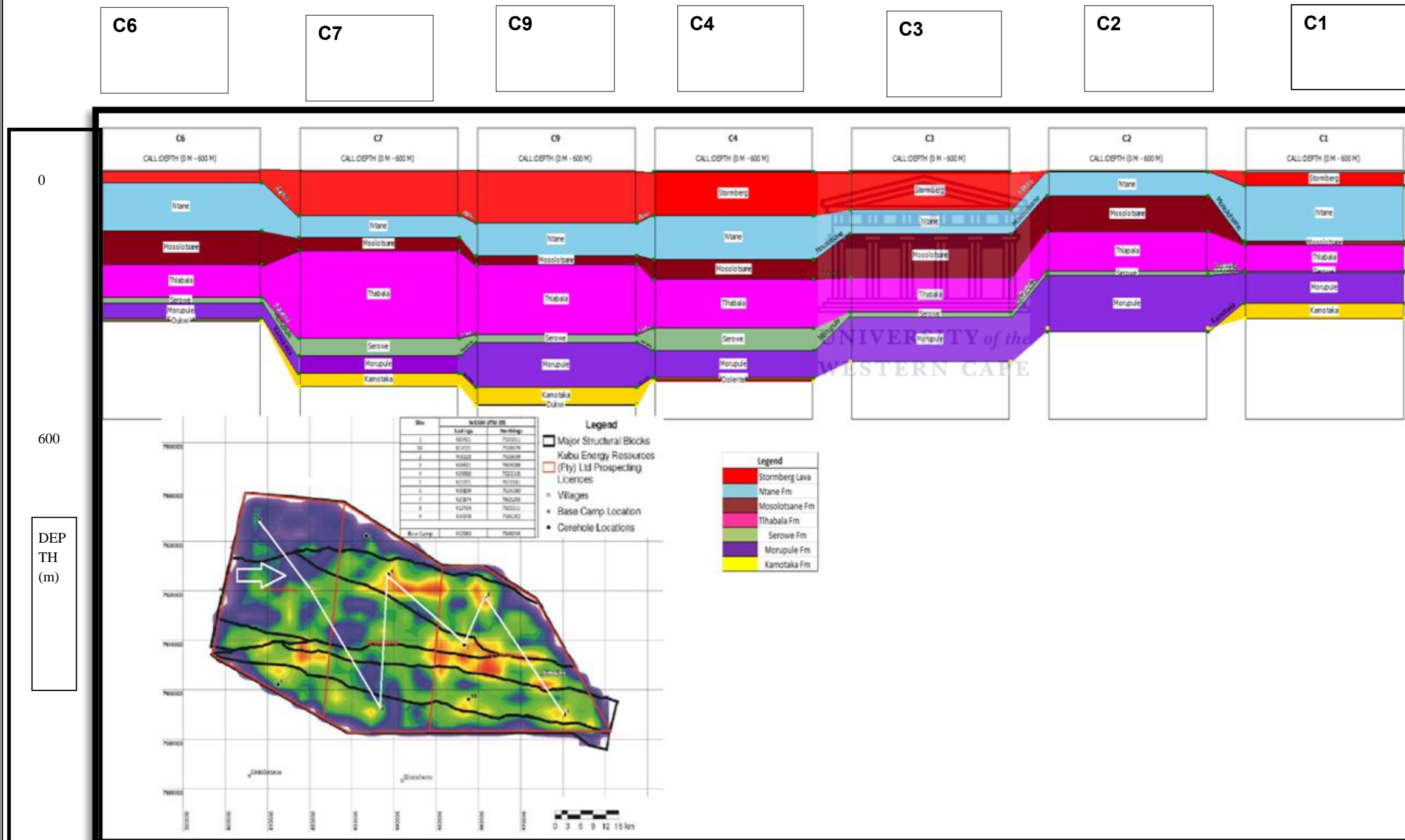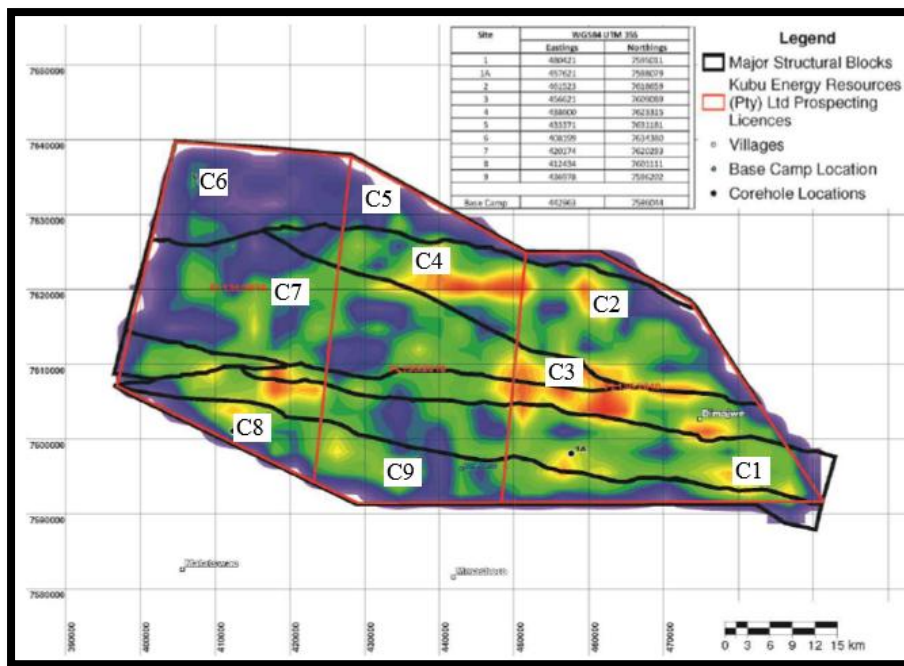
Figure 21 A field map of the three license blocks delineated by the red polygons containing the nine drilled wells C1-C9, Botswana **(Potgieter, 2013)**

The constructed well lithostratigraphic correlation depicts the general distribution of the Ecca Group formations. The Morupule formation (purple) represents the reservoir & source for methane gas comprising of the main coal seams across Botswana. The Morupule formation generally thickens to the east with the thickest packages observed in wells C2, C3, C9 & C4 respectively. Morupule and Serowe (green) coal seam thicknesses range from 9.5, 4.5 and 2m.

Dolerite dykes intrude these formations, and they had a large impact on the coals of these localities. These dolerites may have accelerated coalification and intensely matured the coals, but also caused fractures and hydrothermal fractures and hydrothermal mineralization.

Wells C1 and C6 at the fringes of the blocks were the only wells that did not penetrate dolerite intrusion. The zones affected by the dolerite intrusion could also be thermally matured or slightly over mature depending on the timing of the dolerite.

Major structural blocks segment the study area with at least two wells drilled in each block to test the potential yield of each. However the orientation and stress field may contribute to the gas permeability and gas flow only if these align with the fracture systems.

The overall distribution of the formations is uniform, the beds are laterally continuous and extensive and dip about 4^0 angle. An intercalation of shales, sandstones and carbonaceous

46

mudstones separates the coal seam intervals, which are also underlain and overlain by more siliciclastic sediments. Looking at the general geometry of the formations in the basin appears to take shape of a graben structure but this is not entirely documented by this correlation panel, further sedimentological and structural interpretation is needed. The segments of the correlation transversal to the faults can be reconstructed to a graben or lowlands and high blocks.

5.2 Presentation of Coal Zone Intervals

Table 1 Presentation of the selected coal intervals for correlation and their thicknesses

Hole ID	UMH FROM	UMH TO	UMH Thick	Z3 From	Z3 to	Z3 thick	Z2 From	Z2 to	Z2 thick	Z1 From	Z1 to	Z1 thick
C6	310,81	310,83	0,02	319,41	334,62	15,21	336,72	344,7	7,98	350,17	356,91	6,74
C7	404,06	404,89	0,83	415,37	446,83	31,46	451,5	476,2	24,7	477,39	487,94	10,55
C8	373,77	374,66	0,89	384,93	407,44	22,51						
C4	381,25	382,22	0,97	438,24	448,83	10,59	450,95	476,7	25,75	479,36	500,04	20,68
C5	247,56	248,61	1,05	285,11	310,6	25,49	318,05	336,89	18,84	338,02	342,16	4,14
C9	397,4	398,63	1,23	406,51	448,48	41,97	505,3	514,93	9,63	516,64	523,2	6,56
C1	241,07	249,36	8,29	255,42	283,05	27,63	286,12	312,72	26,6	325,59	337,04	11,45
C2	241,35	244,95	3,6	251,97	289,09	37,12	351,96	385,93	33,97	387,21	389,66	2,45
C3	341,35	342,56	1,21	348,79	388,86	40,07	392,05	412,05	20	413,65	430,54	16,89

The (Table 1) indicates the coal zones of interest that also are the main zones where the fracture study will concentrate on. These zones mainly fall along the Morupule Formation and some intervals correlate to the Serowe Fm, although these form part of the coal intervals they are very thin if individual coal lenses are to be considered. Coal seams of **Z1** belong to the Kamotaka sandstone member, with a total thickness of 79.46m; **Z2** comprise of the lower Morupule coal seam and a total coal thickness of 167.47m; **Z3** coal seams from the main Morupule formation shows a total thickness of 252m and forms the largest coal interval and thickest coal seams recorded across the nine wells. Upper Marker Horizon (**UMH)** seam interval comprises of thin zones of the Serowe Fm coal seam and the upper Morupule Fm coal seams totaling a coal seam thickness of 18.09m and is the thinnest layer and forms the marker bed for the field-wide coal seam correlation.

A correlation of the studied coal seams using UMH as the marker bed was done in IP (Interactive Petrophysics) to understand further the thickness variation and distribution of the three selected intervals (

Figure 22). It can be easily noted that the Z3 interval is the most developed of the coal seams and lies within the main producing Morupule Formation, while Z2 interval isless developed

and is also within the Morupule formation. Finally Z1 comprises of the Kamotaka Member seams and some basal Morupule Fm coal seams.
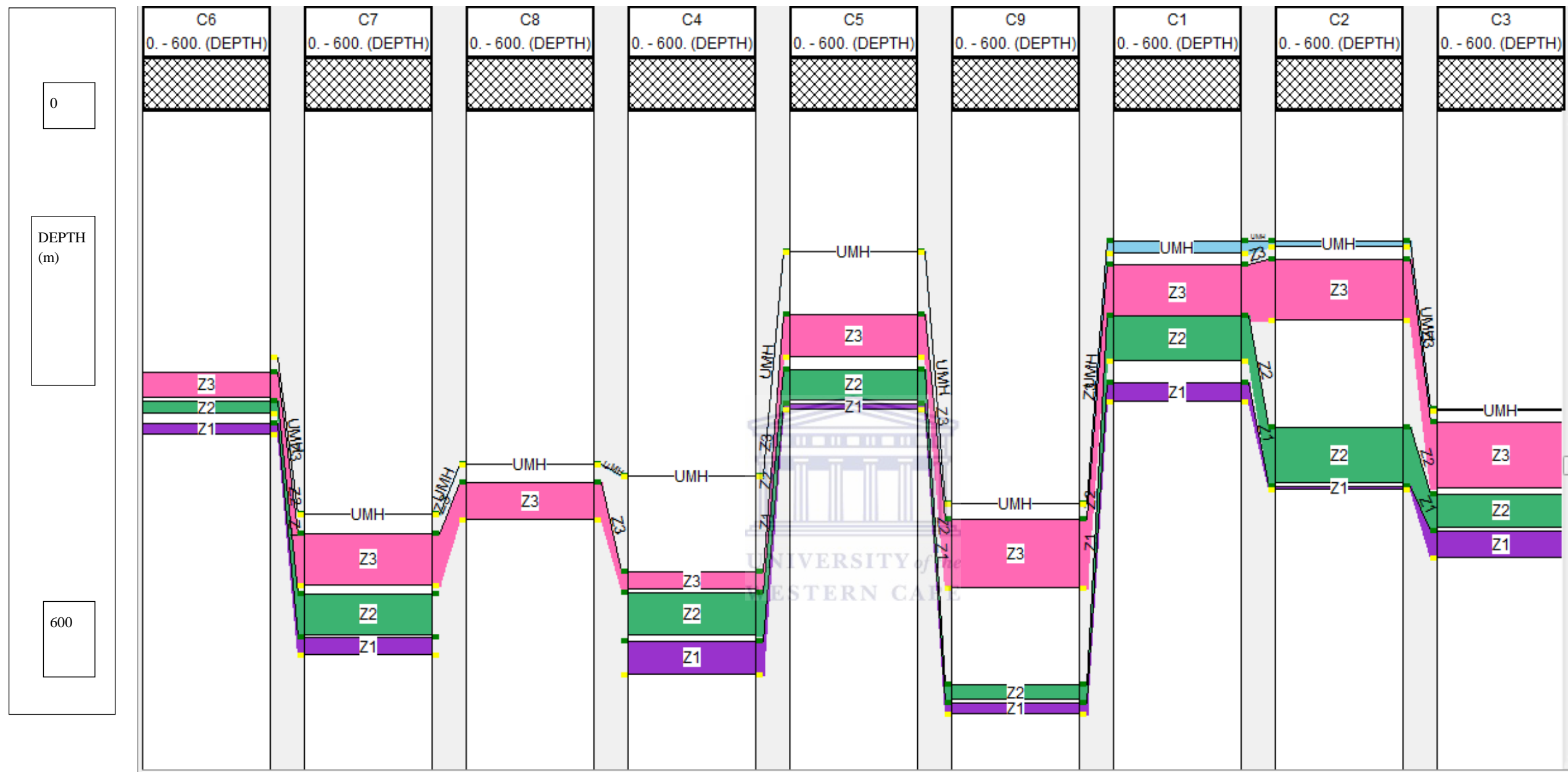
Figure 22 *Coal interval correlation (IP) based on the zones outlined on (Table 1). Z3 coal seam is the most developed coal interval and it is correlatable across all nine wells in the study area, Note the absence of Z2 in well C8 is due to dolerite intrusion.*

5.2.1   Coal zone Correlation (Petrel)

The main purpose of the gamma ray log is to have control on the type of lithology correlated and coal have a generally low GR count but in the case of some well with a dolerite intrusion such as well C8 which also have very low GR count, GR is displayed on track one of the well log section (Figure *23*).

This is why the density log is added to be used as a calibration log in order to be precise about the lithological correlation. The density contrast between a dolerite and coal lithology is significantly large, as seen on wells C8, C4, C5, C9, C2, and C3 respectively. For coaly intervals to be considered as true coals the 1) GR log signature must be lower than 60 API and in this thesis a GR cut-off of 45API has been used to distinguish the coals,and 2) The density log must be lower than 1.75 g/cc and if only the density is spiked with still low GR count then the lithology is not regarded as a coal but as a dolerite (density >3g/cc) though other parameters must be investigated to reach these conclusions.

The wells are displayed as they are located on the field in order to visualize lateral lithostratigraphic variations and areal distribution of coal intervals. Thus well C6- C8 the westernmost well in the field, C4, C5&C9 center most and C1-C3 the easternmost well in the field (Figure *23*). Four correlation panels were interpreted for the four coal zones UMH, Z3, Z2 and Z1 along with their respective fracture zones.
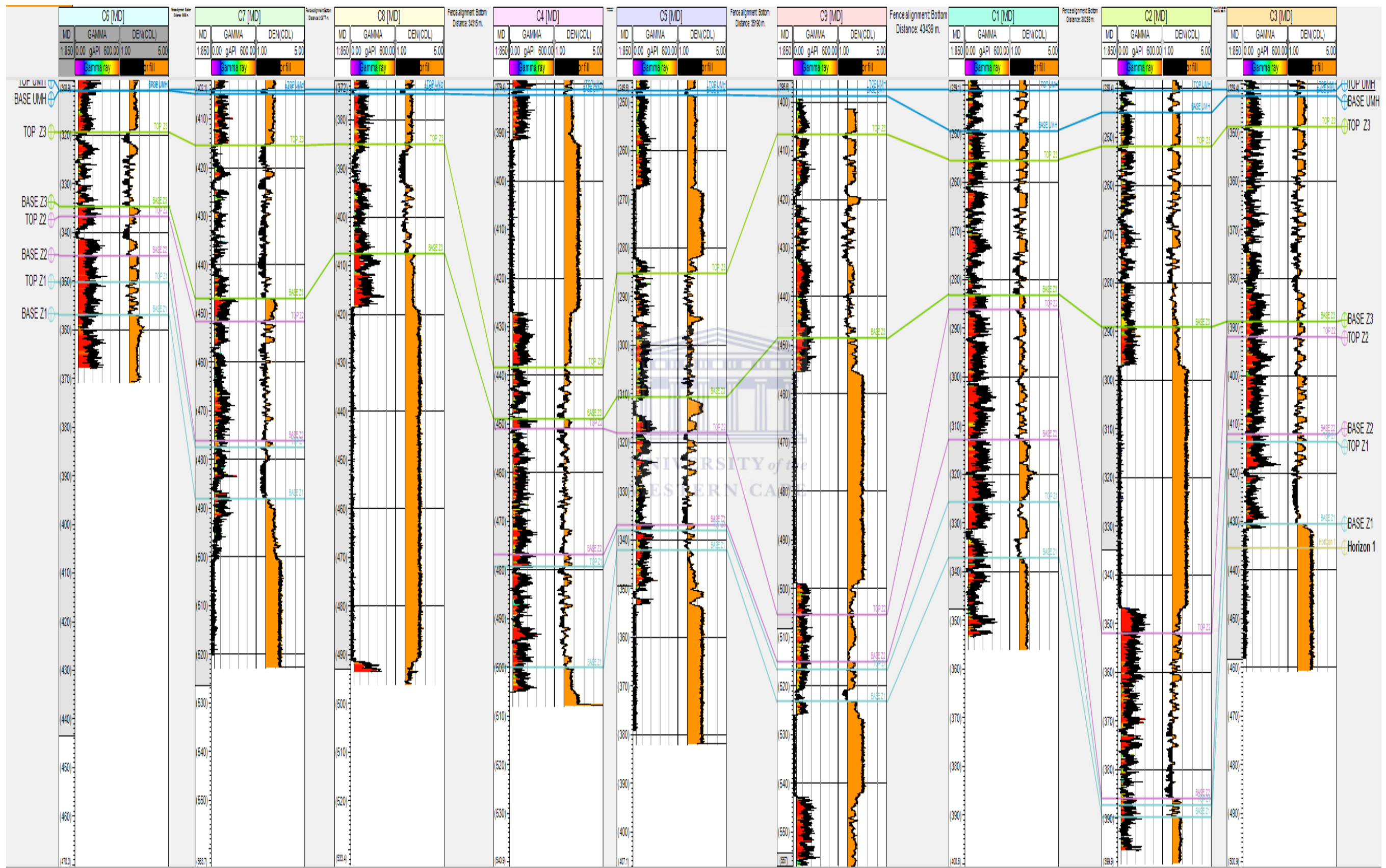
Figure 23 A coal correlation of the three main coal zones UMH, Z1, Z2 & Z3 to the top of UMH. The gamma ray log on track 1 is a lithology and density log on track 2 delineates the coal intervals in black and other lithology in brown.

5.3 QUALITATIVE ANALYSIS OF FRACTURES

5.3.1 Core Data

5.3.1.1 (Upper Marker Horizon) UMH Coal Seam

Well C5

Top 2542 m

Base 249 m

Figure 24 Normal light core image taken when un-slabbed core was wet. UMH 1 core from well C1.Abundant calcite micro-cleats in brittle core zones.

Base 2604 m

Well
C3

Top 245 m
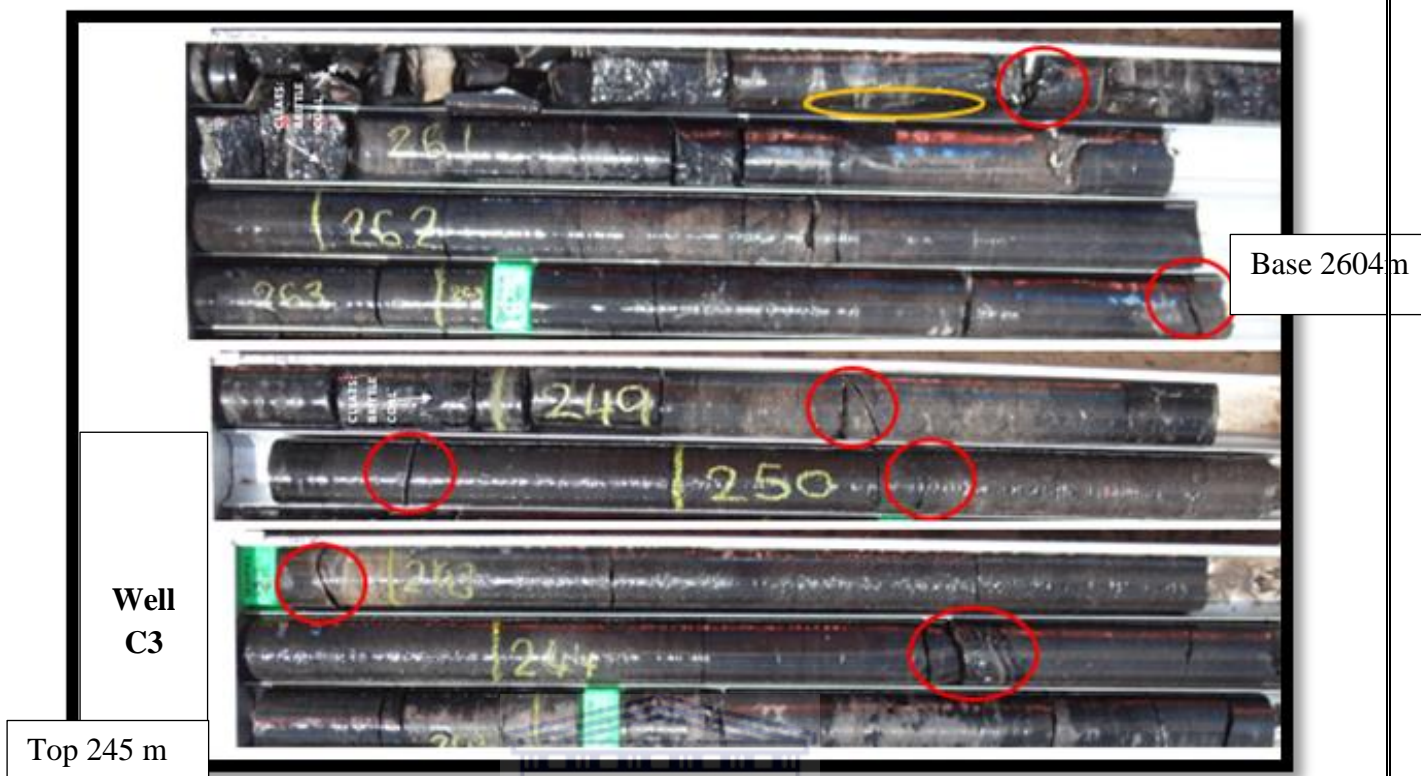
Figure 25 *UMH from well C3- dull coal with frequent bright interlaminations with mudstones, dull & lustrous with abundant calcite micro-cleats shown by the brittle zones. The red box shows artificial stress release due to coring and high angles fracture in orange.*

UMH coals are dull and lustrous with abundant calcite veins filling micro-cleats on well C1 at 242.40-242.89m and carbonaceous micro-veins just 2m below that depth and these features are continuously seen throughout the sequence on this well and along the wells C2 and C3. There is a distinct interlamination of coal and massive interbedded mudstones which are homogenous and contain mud-clasts. The coals of this zone tend to be thin along well C2. This core interval both inclined (red circles) and almost vertical fractures (orange circles) can be observed (Figure 25). These two fracture orientations are seen throughout the fractured intervals and are the main dominating trends.

The more horizontal structures are due to stress release and may be related to low angle bedding or formed during core handling (Figure 26) by flexure of the core barrel when it is laid on the surface after the coring process.

The coals locally depict hair like fractures (Figure 26) which could either be tectonic or mechanical resulting of the coring process, like the petal-centerline fractures which are drilling induced fractures (explained below).

53
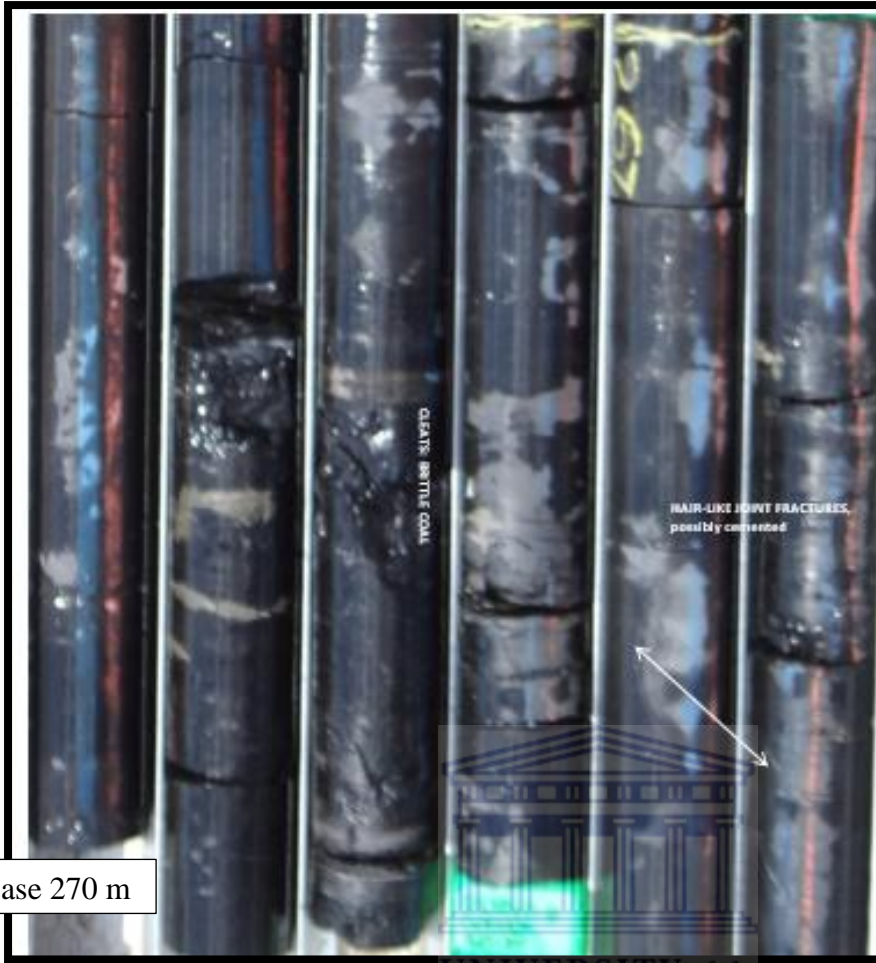
Well C1

Top 266 m

Stress release structures

Base 270 m

Figure 26 *Core interval from well C1 at depth (+267m) showing hair-like fractures and a cleated zone seen through the brittle coal where cleats may be indicated. The white arrows outline the hair-like fractures observed along the core.*

5.3.1.2 Z3 Coal Seam
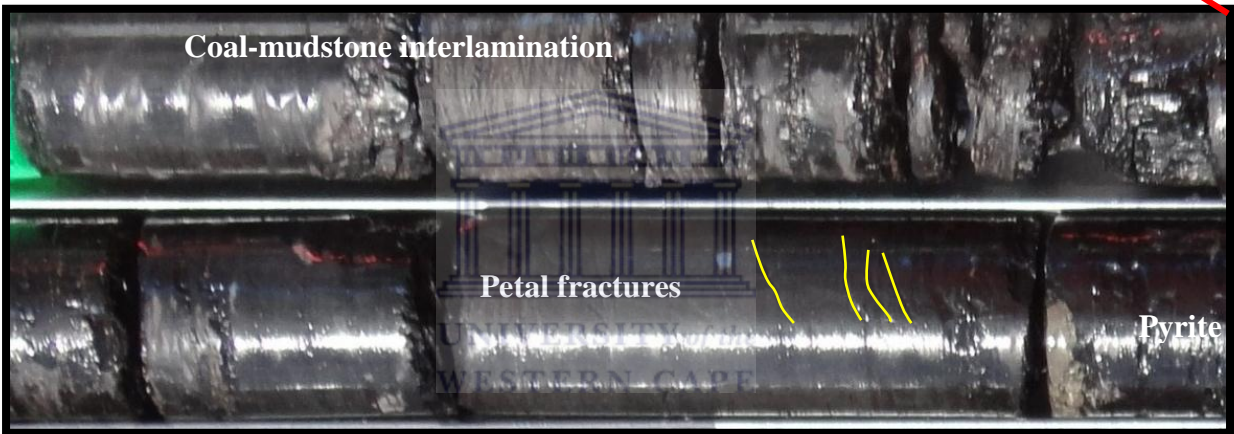
Figure 27 *Well C1 core showing petal fractures which are not related to a centerline fracture at depth 277m, caused by the drilling process.*

Petal Fractures

Petal fractures are curved fractures that begin on the edge of the well and curv parallel to the centerline fracture if one has developed in this case these are petal fractures still young fractures with no observable centerline fracture in the centre of the core, appearing isolated from the centerline fracture (Figure 27).

Well C5

Top 278m
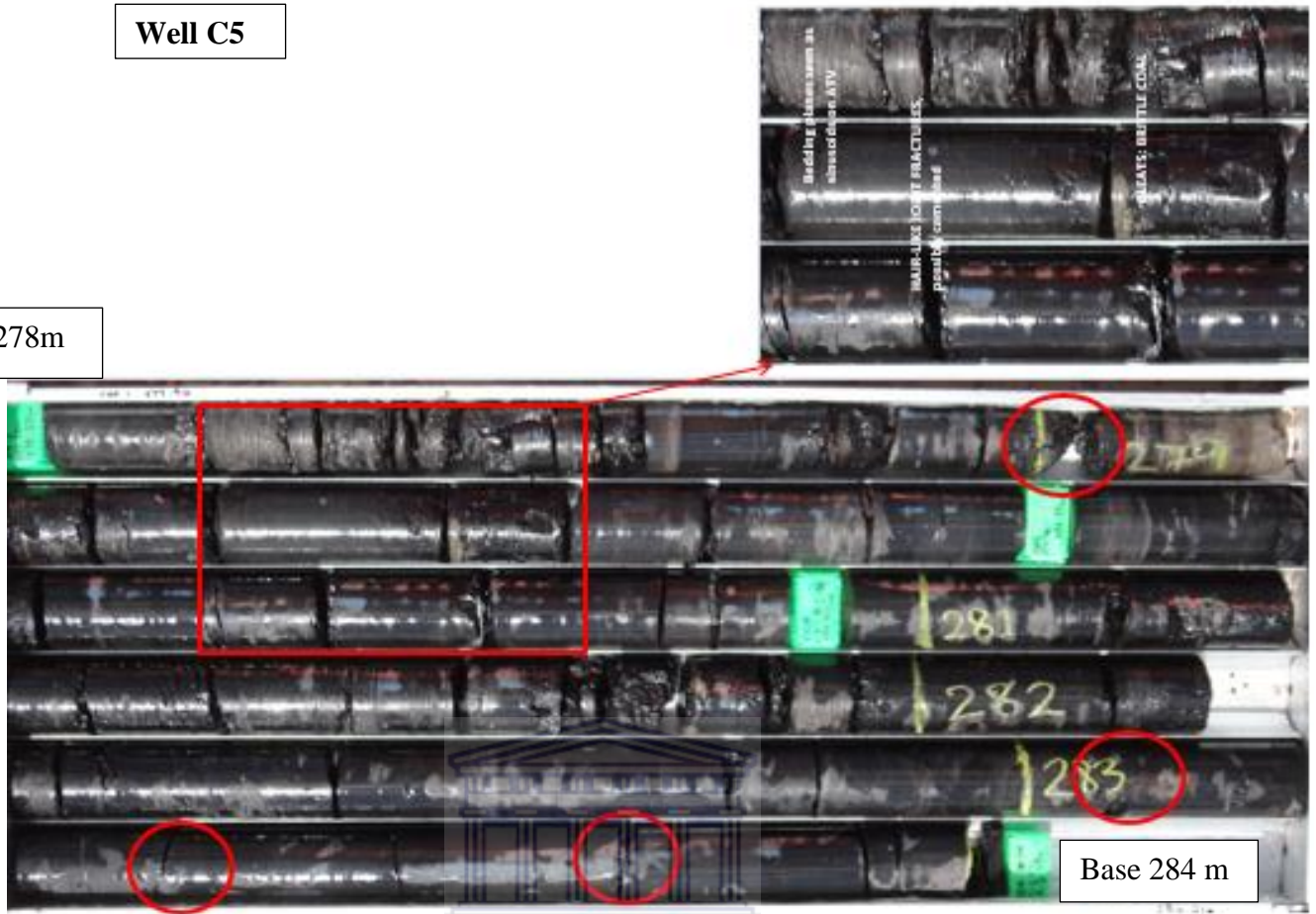
Base 284 m

Figure 28 *Core from well C1 showing low angled fractures, petal-centerline fractures and brittle coal wherein cleats may likely be observed.*

The Z3 coal seam has abundant pyrite with rare calcite micro cleats, the coals are bright coloured and interlaminated. Rare coal stringers are seen through the massive homogenous mudstones, angular calcite veins are 258.25-258.41 m on well C2, and also calcite micro-cleats throughout the seam are also observed. The lithology is coal-mudstone-coaly mudstone-siltstone-carbonaceous from top to base of the succession.

Cleats

Micro-cleats have been reported before. In core they may be seen in regions of brittle coals where the coal has been shattered into partly lose material. The chemical composition in these zones may be different containing more organic matter. The denser system of cleating in those zones may yield better permeability.

Well C2

Top 278.5 m

Base 284.5 m
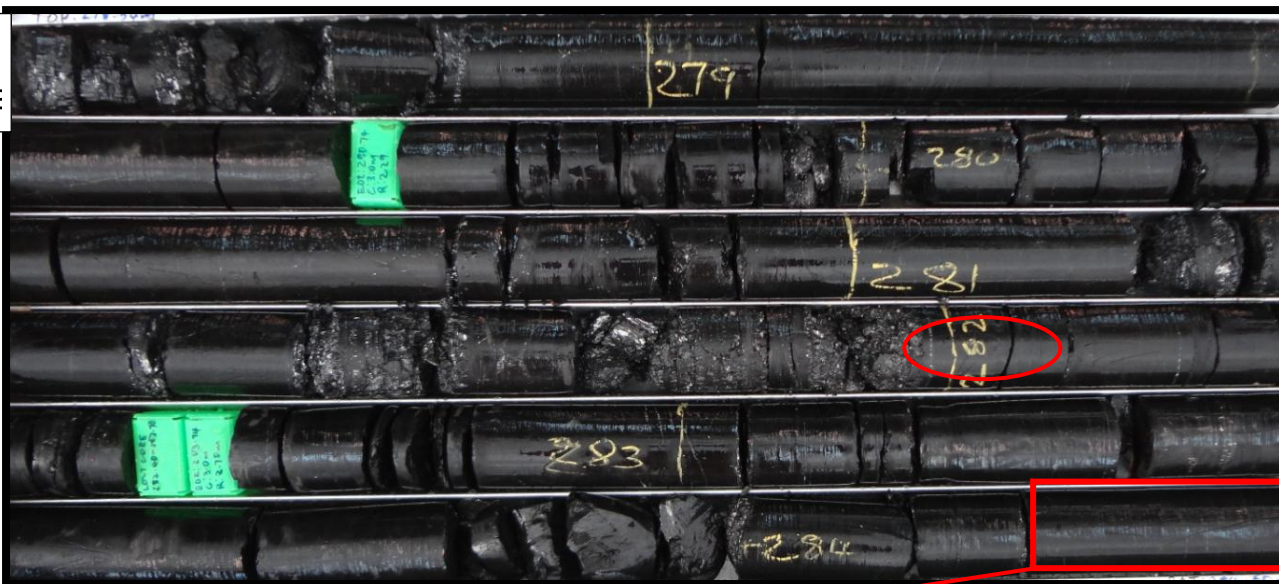
Petal-Centerline fractures

Figure 29 Well C2 showing Petal-centerline fractures (hair-like fractures) along the main coal interval at depth of 284m

Petal-Centerline Fractures (Hair-like fractures)

The core in (Figure 29) above has abundant hair-like fractures which mostly fan out when the image is turned to its side. These fractures start on the side of the core and comes to the center of the core where they diverge. They are referred to as Petal-centerline-fractures and are typically induced during the drilling process. The Petal-centerline fractures are curved fractures which begin on the edge of the wellbore and curve parallel to the center of the core (Lacazette, 2000). The morphology of these fractures suggest that they are produced under pure tensional stress regime. These fractures form ahead of the drill bit as a result of coring and normal drilling operations (Lacazette, 2000). These are therefore referred to as induced borehole fractures.

5.3.1.3 Z2 Coal Seam

Well C1

Top
295.1 m

Base 200.03m

Figure 30 *Well C1 coals dominated by coaly mudstones of homogenous and massive nature.*

The coals in well C1 tend to be dense, dull, sideritic with scarce bright laminations. The mudstones grade into carbonaceous mudstones towards the base. The siderite nodules interlock into veins at 297.64-298m. The overall dominant lithology consists of mudstones and carbonaceous mudstones with coal stringers without cleats. Well C2 however intersected some calcite cleats with some frequent lamination in the coals.
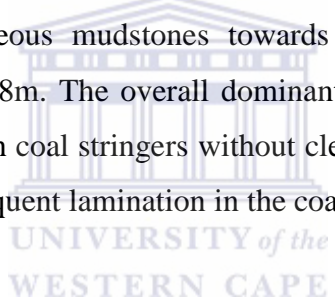
Well C2

Top
382.
4 m

Base 386.43m

Figure 31 *Carbonaceous mudstones with coal stringers from well C2. Note also the distinct bedding lamination along the red arrow position.*

5.3.1.4   Z1 Coal Seam

Well C3

Base 427.3 m

Figure 32 Coal interval Z1 as observed on well C3 with high angled fractures orange circle and low angled fractures red circle at depths of 421.55-422.82m. The sub-horizontal cracks are stress release structures.

In well C1 comprise of coaly mudstone interbedded with mudstones, all belonging to the Kamotaka Fm. Well C2 records the sandstone member of this formation with bright lustrous coal laminations seen in mudstone intervals. The coals are non-bright, dull and slightly lustrous. Calcite joints have been reported at depth of (421.55-422.82m) on well C3 and also fractured intervals are recorded one meter below this depth. Irregular calcite veins in coal continue downwards, grading to micro-cleats. A thick dolerite intrusion is observed in depths 430.13-459.97m of this coal zone.

5.3.2 Fractures on ATV Image Logs

Well C5 shows more bedding than fractures, like at the top of (Figure 33) where it shows gentle dipping sinusoids stacked one on top of the other, these dip at an angle of +/- 20^0 at a depth of 240-255m. Just below this depth is a sinusoid at a very high dipping angle (~78^0) representing a continuous dipping fracture with depth from +350m, the orientation of these features is also seen on stick plot. At the same well at a depth of +-360m 60^0 angled fractures are again detected with limited bedding in those zones. Fracture density in some zones like UMH coal zone makes it difficult to resolve the individual fracture orientation, but series of fractures can be identified on stick plots because they show a similar orientation implying a similar generation and therefore can be interpreted as a single unit.

Well C1 (277-288m)
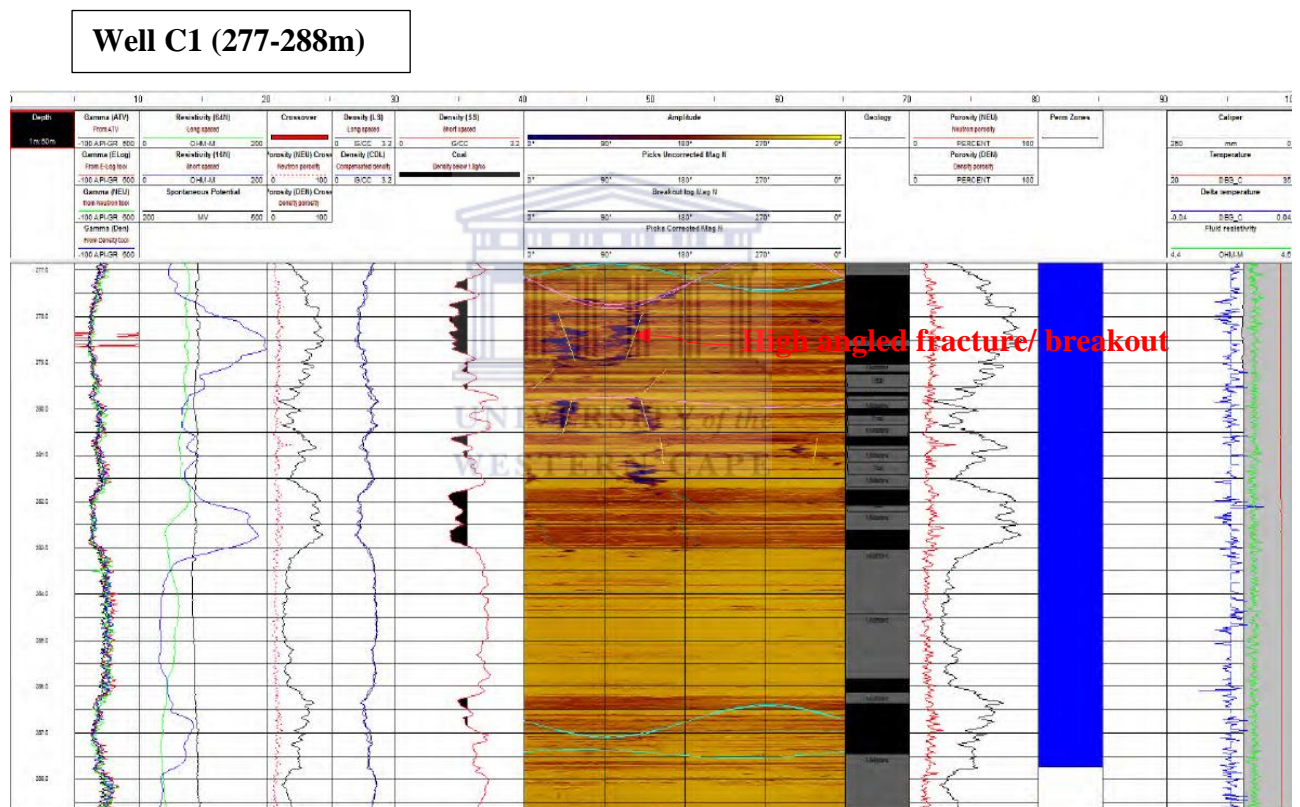
Figure 33 *Suite of logs well C1 showing from left to right, gamma ray log, resistivity, porosity, long spaced density log, short spaced density log with coal shading, ATV log with fracture indication as sticks and sinusoids, lithology, porosity and temperature logs.*

Structural features

Figure 33 depicts a suite of well logs generally used for lithology identification and its response using different logging tools. From the first track on the left, the gamma ray log shows the variation of response of certain lithologies, in this case the low GR evidence coaly intervals and very low GR indicates dolerite. In the following tracks to the right, the

resistivity log, density log with coal shading in black, the ATV image log with some features to be discussed, the lithology track, the porosity log and caliper are also displayed.

Well C1 image log (Figure 33) displays features with variations in acoustic impedance contrast. The dark semi-vertical structures indicate natural fractures, inconsistent with other features and structures of the entire well. The dark colours are due to poor reflectivity of structures. The natural enhanced fractures are observed at depths (277-281.5m) with steeply dipping character. The enhanced natural fracture structures in this well are $\sim<90^0$ apart. They appear to occur in different fields between 0^0 and 90^0. Note also that above the enhanced fractures, the sine wave indicate a well-developed natural fracture with to a sine-wave geometry (in pink in Figure 33). The enhanced fractures are formed as a result of drilling and often times are referred to as drilling-induced natural fractures, these ones have also been observed on core photographs (Figure *34*).

Well C1 (277-283m)

Top
277.9 m
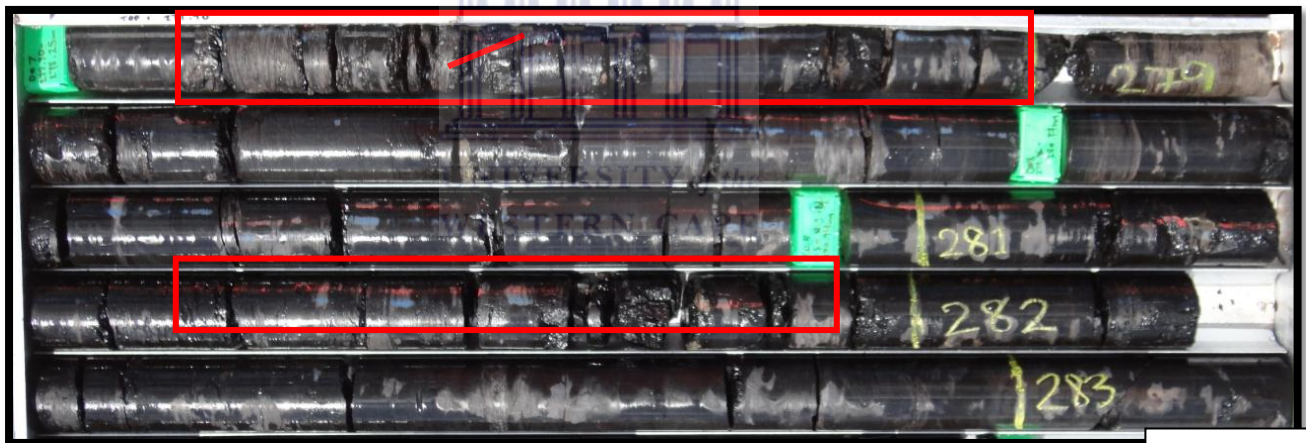
Base 283.2 m

Figure 34 Core photograph from well C1 depth interval (277-283m), in red boxes shows drill-induced natural fractures, the red line inside upper red box indicates the orientation of the fracture.

However Figure *35* indicates a zone within the coal interval with breakout features shown by the etched orange features on the image, the caliper log shows an observable bulge along the same interval where the breakouts are indicated. One can say with high confidence that these are breakouts and below there is a natural fracture shown by the fully developed sine-wave.
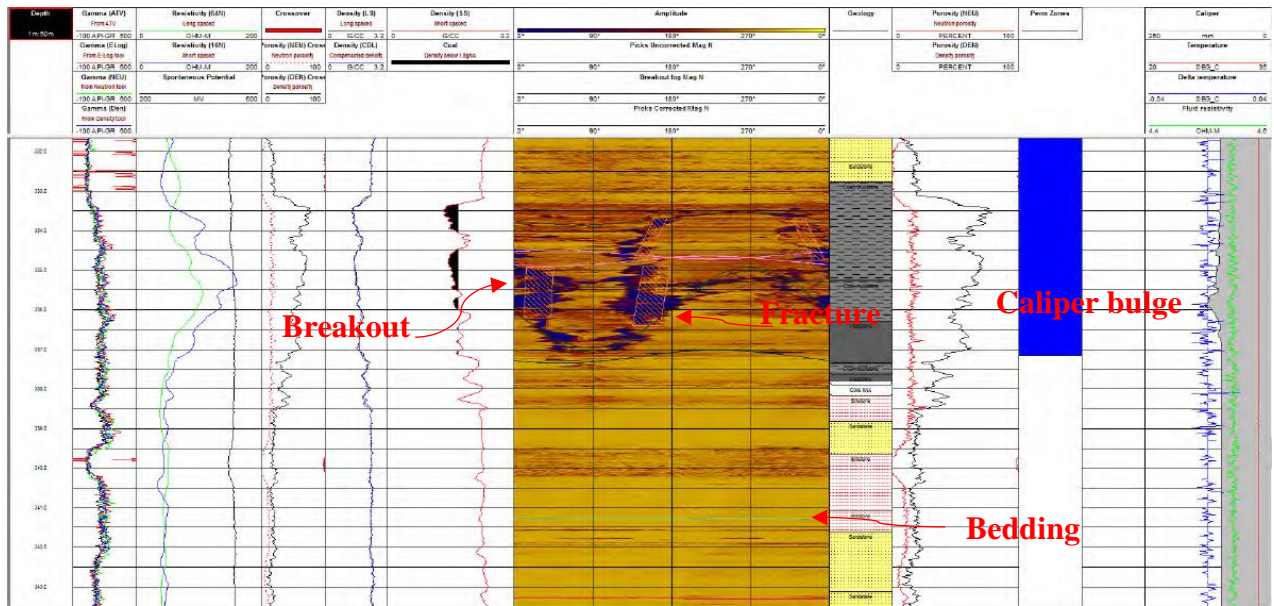
Figure *35 High confidence sinusoidal fracture at depth 335-336m on the ATV amplitude image. Note the bulge on the caliper log in grey that may indicate drilling induced fractures.*

Structural interpretation of features
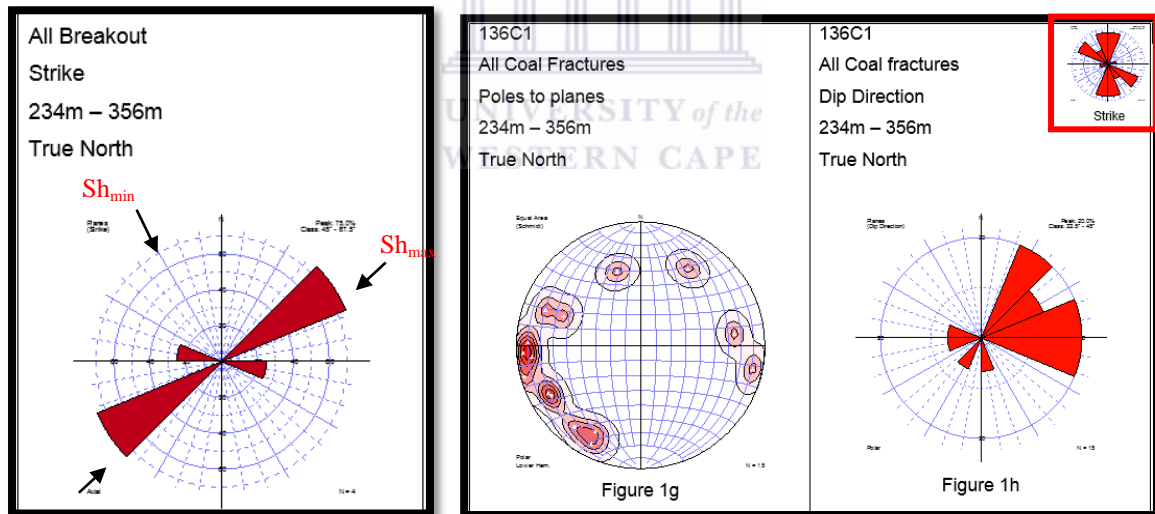
Figure 36 *Orientation of fractures (***Figure 32***), coal seam interval Z1 on well C3. Note the trend of fractures E-W. Note strike rose plot on top right corner delineated by red box*

The (Figure 36) is a display on the left all breakouts observed in well C1on the left. On the right diagram there is a stereographic plot, showing poles to planes, some data plotted are scattered while the majority plot along the west and east. Finally the azimuth rose plot on the right displays the dominant dip directions of all fractures in coals within the outlined interval. The coal fractures dip to the E and W, being E the dominant direction. The top right corner rose plot shows the strike of all coal fractures and seem to have a dominant N-S and have a

62

very important NW-SE strike orientation. Fractures in sedimentary rocks reflect the stress system they formed under through time.

From the breakout plot (Figure 36), the breakouts have a NE-SW dominant orientation. Breakouts always orientate themselves parallel to the minimum horizontal stress (Sh_{min}) which in this case is in an easterly direction of dip. The maximum horizontal stress (Sh_{max}), is always at right angles to (Sh_{min}) and at the same time parallel to the strike of breakouts. (Sh_{max}) is oriented NE-SW in these breakouts.

However coal fractures maintain a N-S strike orientation slightly similar to the (Sh_{max}), where N-S orientation is also the direction of the maximum horizontal stress (Sh_{max}), off by 30^0. If such case exists then the coal fractures sub-parallel to the (Sh_{max}) may optimally be open and may enhance methane gas flow. In this case coal fractures which have the NNE-SSE strike orientation will aid better flow and appear open.

Well C4 (334-345m)
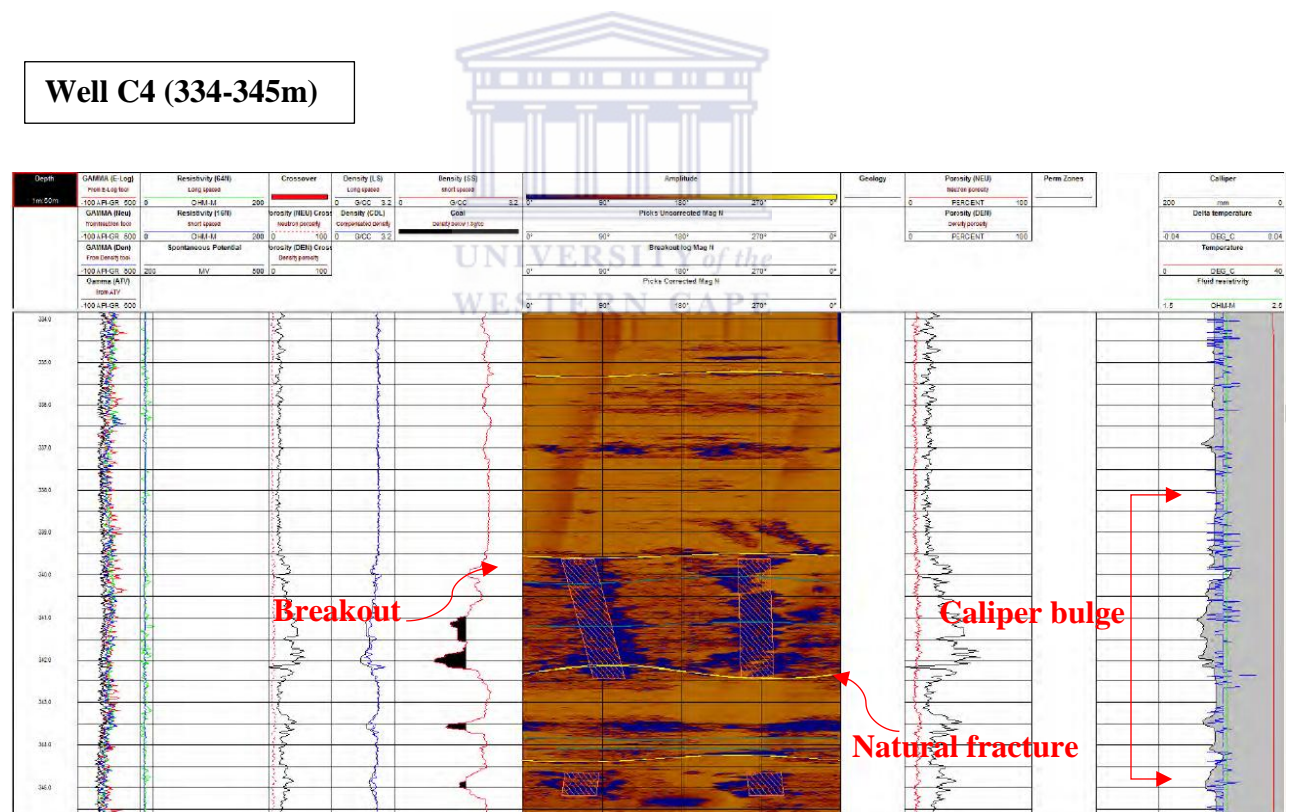
Figure 37 *Well C4 showing abundant borehole breakouts on interval 340-345.5m. Notice how the caliper log bulges in and out along the intervals.*

Structural features Well C4 & C3

Well C4 depicts well developed breakouts on the image log (Figure 37) with a structural orientation E-W and are observed 90^0 from each other, these are labelled by the etched polygons on image log. The presence of breakouts is also seen on the caliper log, notice the bulges on the caliper log. The breakouts on this well are consistent in orientation, maintaining an E-W dip direction at depth 340-342m and 344-345m respectively.

Natural fractures are also detected on this well and are shown as yellow sine waves, the fractures in well C4 are not too steeply dipping.

Well C3 (Figure 38) appears to have breakouts orientated in the same direction as well C4 which is in a dominant E-W dip direction. These two wells are adjacent to one another in the field, however they do not occur within the same structural block (Figure 21). Well C3 also depicts inclined fractures (indicated in the image log as green lines) that are not fully developed and appear to be discontinuous, not fitting to a sinusoid.

Well C3 (417-428m)
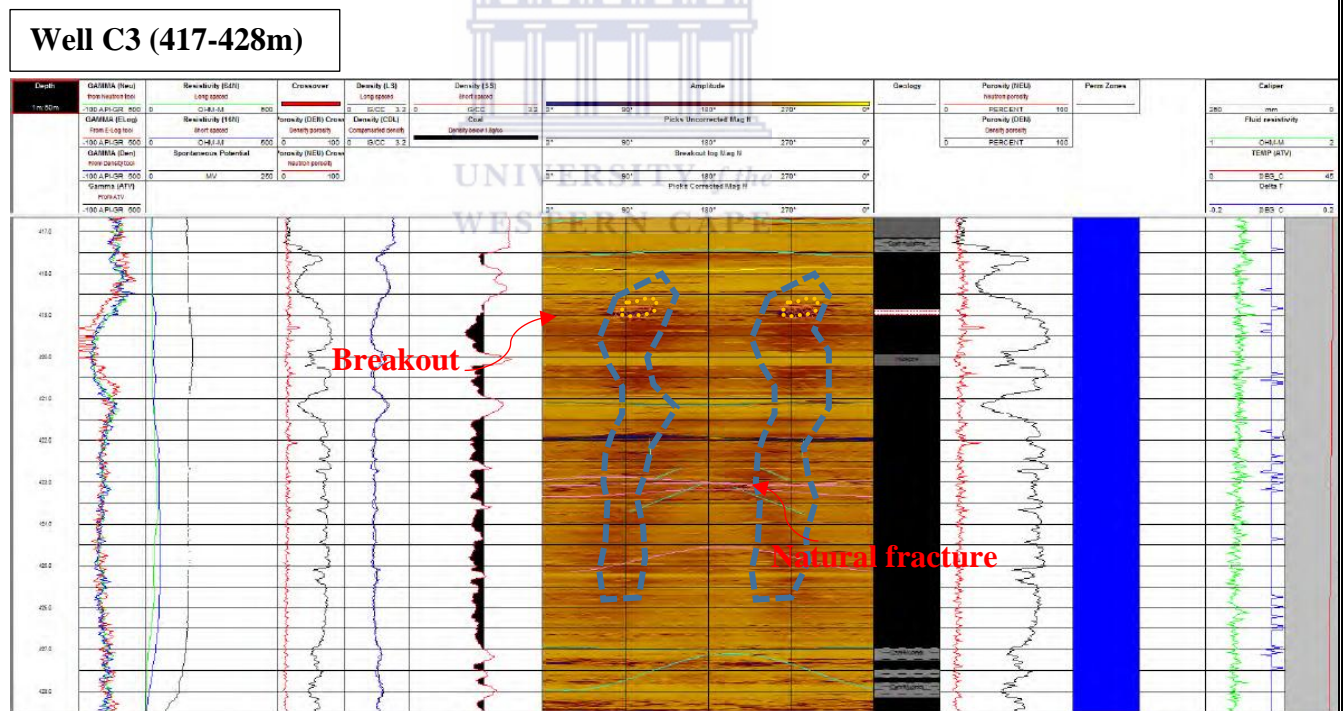
Figure 38 *Well C3 indicating breakouts at depth 418m. Note the well-developed breakouts shown by the etched orange polygons, also the light shade of the continuous breakout in the form of a background shadow (dotted blue polygons) is not as better developed throughout the well. Also notice the inclined fractures (green lines).*

Structural interpretation of features

However well C4 breakouts are orientated in an E-W dip direction similar to those observed on well C3 (Figure 37& Figure 38). If the breakouts on these wells are in the same direction then the directions of maximum horizontal stress (Sh_{max}) and minimum horizontal stress (Sh_{min}) can be extrapolated from well C3 breakout structural interpretation. The breakout strikes for well C3 are oriented in a N-S direction like Sh_{max} while Sh_{min} is orientated along the E-W dip direction. The cleats in this well are sub-parallel to Sh_{max}, therefore the cleats with the NE-SW orientation will have optimal flow and increased permeability.

The coal fractures however in well C3 will not have optimal flow as some dominant fractures on the strike plot (on the top right corner) plot in the direction of Sh_{min} and the fractures with the dominant E-W orientation will be healed, some orientated N-S will provide enhanced flow in this well. However the NW-SE trend of the fractures on the strike plot are very important as well and may yield a flow of gas as they do not plot in the Sh_{min} direction.

We can now infer that the orientation breakouts on well C4 would be similar to those of well C3. Thus looking at the fracture orientation of well C4 plotted as strike rose (Figure 39) one can conclude that if $sh_{max,}$ is N-S as in well C3 (Figure 32), then the $sh_{max,,}$ in well C4 (Figure 39; all fractures $> 50^0$) is in the same direction, therefore all fractures detected in well C4 will yield enhanced permeability as they are orientated parallel to the maximum horizontal stress. The fractures will then open up under the least compressive stress sh_{min}, and in this case in an E-W direction as seen on the dip direction rose plot (Figure 39).

C3 all coal fractures
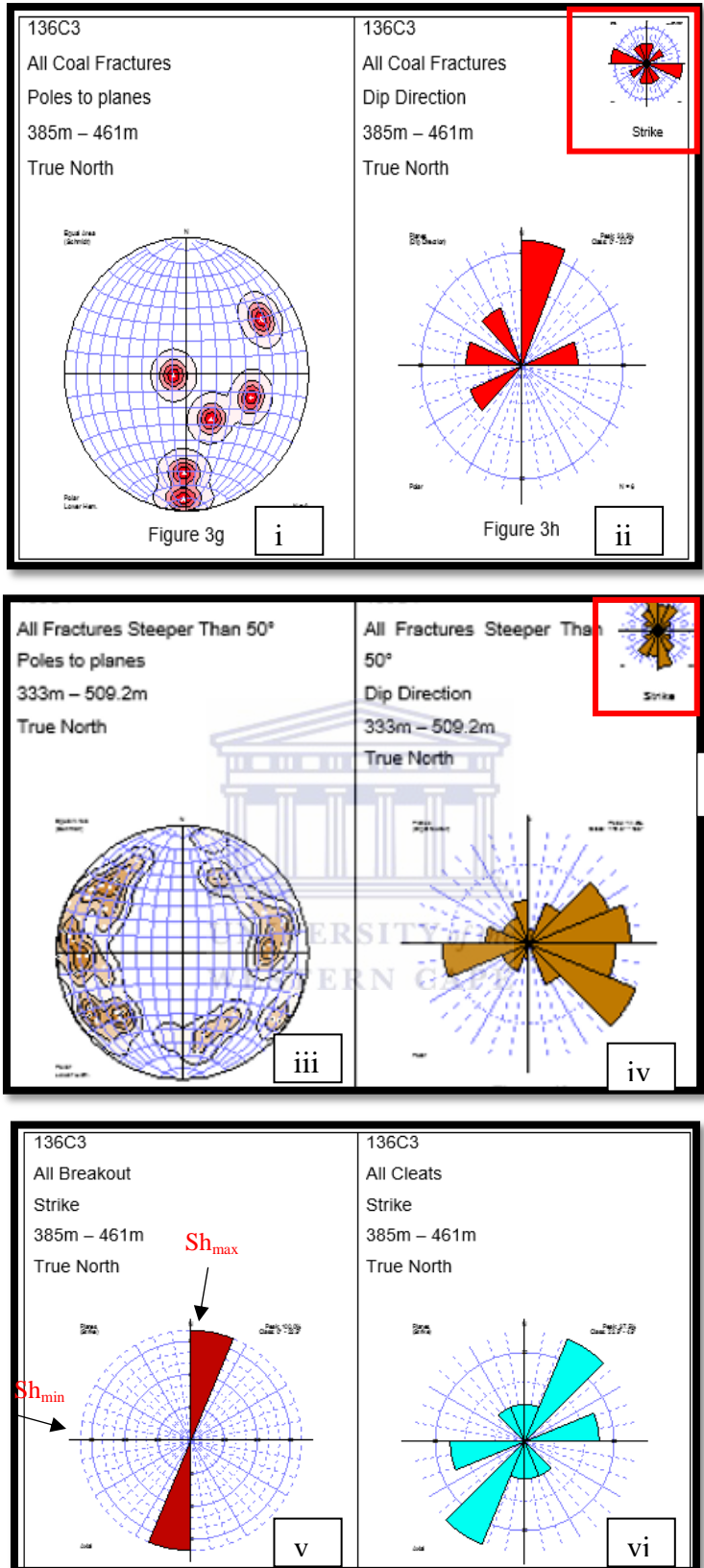
C4 all fractures > 50^0

C3 all breakouts & Cleats

Figure 39 *Orientation of fractures on (figures i & iii) plotted on the stereographic polar plot fractures plotted as poles to planes and on (figure ii) an azimuth rose plot depicting the true orientation of fractures which gives the dominant direction of dip on both side-side diagrams. Strike rose plots are indicated by the red boxed on the top right corner on (figures ii & iv). The bottom figure (v & vi) shows fracture data steeper than 50^0 (high angled fractures and the right fracture data dipping lower than 50^0 (low angled fracture).*

Well C5
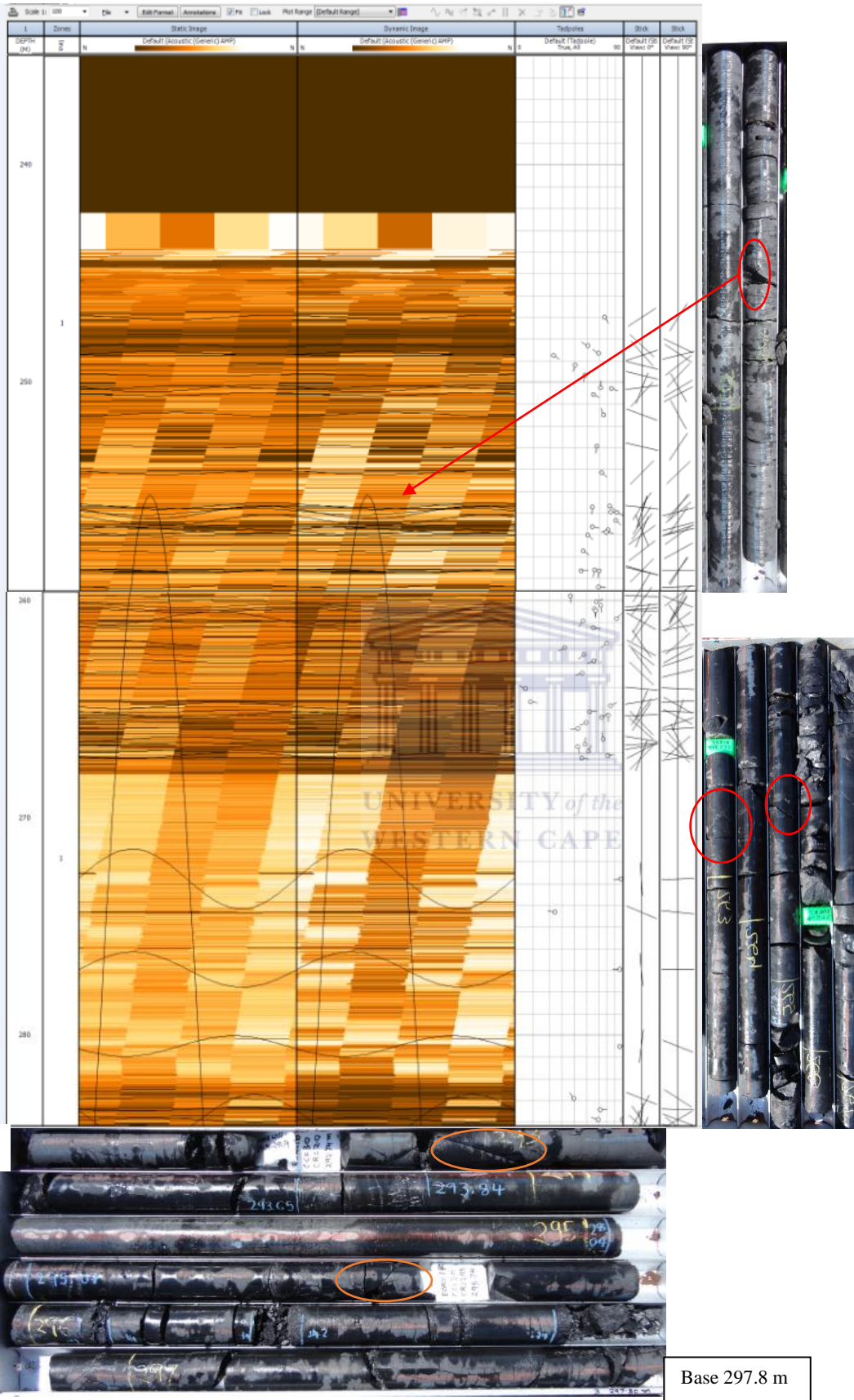
Top 292 m

Base 297.8 m

Figure 40 *An Acoustic Televiewer image log depicting amplitudes within the sub-surface, the interpretation show the sinusoids representing structural features, high angled sinusoids show fractures and low angled sinusoids interpreted as bedding plane, this is associated with core photographs depicting fractures along the same intervals, marked by the red (inclined fractures) and orange (vertical fractures) circles.*

Structural interpretation of fractures

The azimuth rose plot is a better tool to interpret the stress field orientation, it may be seen on the ATV well log plot of well C5 (Figure 40 & Figure 41). This well has numerous dolerite intrusions separating the main coal interval. Fractures are very abundant in both sedimentary and volcanic (dolerite) exhibit fractures. The fractures on these lithologies is indicated by the azimuth rose plots on track 6 (Figure 41)of the well log, tadpole plots on track 7 and dips plotted as sticks on tracks 8 and 9. A number of low angled fractures are observed and follow the sine wave in most parts of well C5, and a few steep angled fractures both within coal intervals and dolerites, these are indicated by the blue lines on the image log (Figure 41). Fractures presented along the sedimentary structures by the azimuth rose plot indicate the dominant dip direction of fractures and appear to be more organized than fractures observed on rose plots of dolerite zones. The dolerites show a disorganized pattern which encompass the rose diagram such that this cannot be used as a good indicator of the dominant in-situ stress field. The tadpole plots indicating low dip are fractures in the dolerites and higher dip fractures in coals and related sedimentary strata. The stick plots here displays the dips of the high angled and low angled fractures and two trends can be seen in Figure 40. The high angled almost vertical fractures, inclined fractures and more almost horizontal fractures which could be bedding planes due to nature of dip angle.

Figure 41 displays the expected structural orientation of all fractures detected by the ATV image log on well C5. Plot 1 show all the fractures detected in the interval across the entire well, notice how the rose plot scattered. The fractures include those in both sedimentary rocks and in dolerites thus the dolerite fractures contaminate the fracture stress field distribution. Dolerite fractures are distinguished from the fractures lower than 50^0 on plot 3. Fractures in dolerites form due to thermal relaxation as the dolerite cools, and as can be noted from plot 1 of (Figure 42), the fractures still pick up the N-S strike trend, indicating the stress field depicted by wells above. The fractures in coal and in surrounding rocks in well C5 all follow the N-S strike trend as see previously in wells C1 and C3.

Due to lack of breakouts on this well one cannot interpret the stress orientation of the fractures with confidence, but we can however extrapolate this from well C6 (Figure 43) which is located within the same structural block as well C5 and will provide even better confidence than extrapolation done between wells C3 and C4 falling in different blocks (Figure 43).
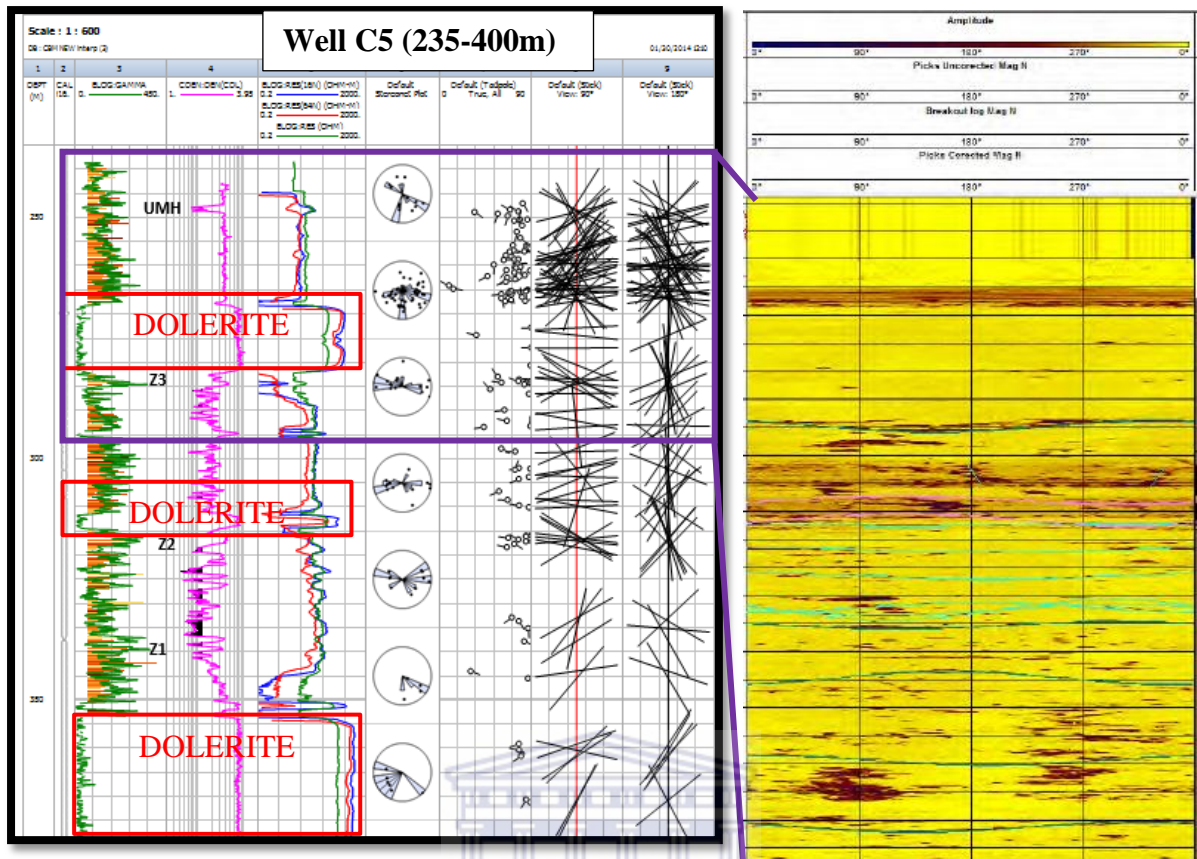
Figure *41 Well C5 displaying Caliper log on track one, density log showing the main coal intervals and the three resistivity curves, the last three tracks indicate the feature orientations through azimuth rose plots, tadpole plots and two different angled stick plot. The main coal seams are shown by Z3, Z2 & Z3, and a series of dolerite intrusions are observed and outlined by red boxes in this well. Note the image log plot at depth 243-255m indicating the features marked by tadpoles and stick plots.*
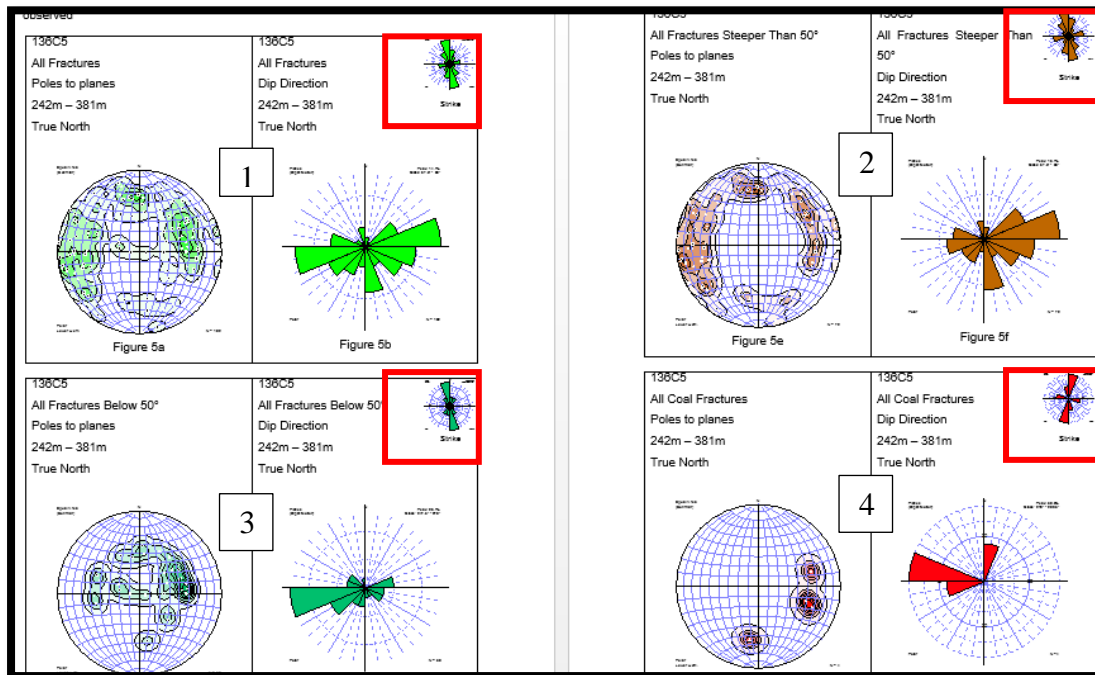
Figure *42 Structural orientation of fractures in well C5, notice the strike rose plot marked by the red box in all intervals (242-381m) has a general N-S orientation.*
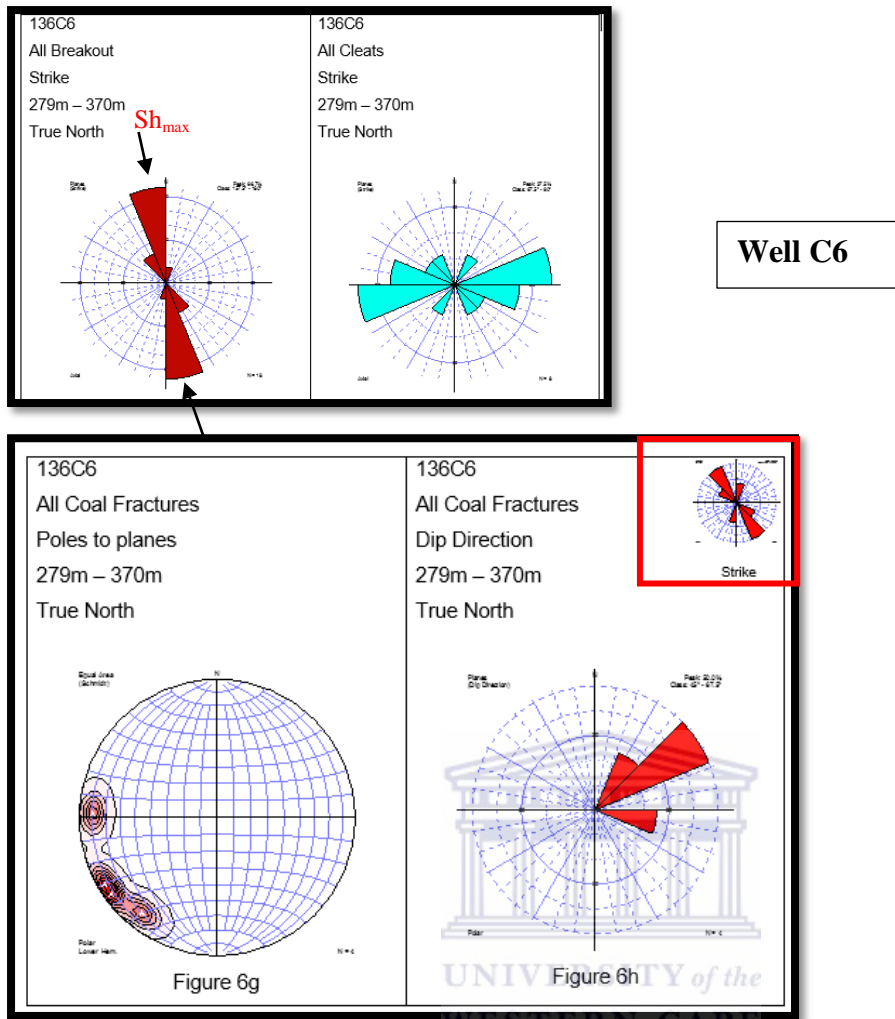
Figure *43 structural features from well C6. Note the breakout strike rose plot of this well gives the stress indication for well C5.*

Well C6 displays a N-S rose plot orientation which is an indication of in-situ stress field, with maximum horizontal stress orientated N-S trend, this when extrapolated with fractures observed in well C5 suggests that the fractures as observed along the strike rose plots at the top right corners of all four plots in figure 41 will yield better productivity in that well as the fractures on the plots are orientated more or less parallel to sh_{max} stress field. Therefore the fractures are opening relative to the minimum horizontal stress *(sh_{max})* orientated E-W.

Although this may be a good indication for all fractures observed in well C5, well C6 fractures especially the cleat system are not ideally orientated parallel to sh_{max} thus these fractures will be closed or healed as they will be sealed by the maximum horizontal compressive stress. The coal fractures of this well will however be open as the fracture stress field is orientated along the same orientation as the maximum stress. The natural fractures in coal within this well will be the only flow system to enhance permeability.

5.3.3   MID & M-N Cross plots

MID plot and M-N plot properties are derived from a series of porosity logs such as density, neutron and sonic, traditionally these are used as mineral identifiers but can be used for numerous applications such as in this case of fracture identification.

We will follow a methodical workflow on how these were derived and what information can be extracted from these correlation cross-plots.

5.3.3.1   MID CROSSPLOTS

For the MID cross-plots, the plot gives a relationship of the apparent-matrix density (g/cm^3) with its apparent-matrix transit time (µs/m). This relationship is extracted from the sonic and density logs through a computation which involves calculating apparent-matrix density and apparent-matrix transit time from the conventional logs. The computation encompass the following equation

Equation 1

$$\rho maa = \frac{(\rho b - \varphi t * \rho f)}{1 - \varphi t}$$

Where;

$\rho b = Bulk\ Density$

$\varphi t = Sonic\ porosity$

Taken from well logs curves

$\rho f = Fluid\ density, water = 1$ g/cc considering water

Equation 2

$$tmaa = \frac{(DT - \varphi t * tf)}{1 - \varphi f}$$

Where;

$DT = Sonic\ log$

Taken from well logs curves

$\varphi t = Sonic\ Porosity$

$tf = Fluid\ Transit\ time\ @189(µs/m)$

Fluid transit time is high as expected in coal intervals than in other clastic lithologies

Equation 1 and 2 will produce *ρmaa* and *tmaa* for each well evaluated. If therefore a well's data points when plotted appear to plot to the left of the plot area then that can be an indication of fracture presence. Figure 44 shows an MID cross-plot evidencing fractures at 240-340 m depth.

Figure 44 *MID cross-plot for well C1 depicting fracture zones where data points plot to the left of the plot area*

For well C1 (Figure 44), the target interval is within depths 240-350m and this depth includes all the coal zones/intervals. The plot only focuses on fractures present in coal seam intervals even though this can be done for the entire well, some points are however indicative of those zones unplotted. Using both equations one and two mentioned above the X and Y axis were populated with *tmaa* and *ρmaa* values respectively. A third variable displayed is a gamma ray lithology identifier, shown as colour scheme was added to increase the reliability of the plot. The colour of each point represents its gamma ray log reading according to a colour scheme where GR = 0-15 API is a very clean/ pure coal, GR = 30 API Coal, GR = 45 Coaly mudstone and GR > 45 would be clastic such as mudstone, siltstone, carbonaceous mudstone, etc. This colour scheme can also highlight the location of shales and mudstones mainly seen as the green points of high gamma ray count. The apparent matrix density and apparent matrix transit times for the shale/ mudstones can be read off the plot and have positive correlation, in this case the values of these lithologies fall between *ρmaa* of 1.6-3.4 and *tmaa* ranging from 220-600

The density of coals is always expected to be approximately 1.75 g/cm^3 or lower, therefore a cut-off of 1.75 g/cm^3 will be used in this study. However the transit time in coals 240µs/m is much longer than most formations.

So the data points in well C1 marked by the blue polygon on the left (Figure 44) indicate fracture presence. Now in order to validate in which lithology the fractures are, the apparent matrix density and GR values must be considered. The apparent matrix density is between 1.6 and 2.4 g/cm^3 at a *tmaa* between 220-340 µs/m, and evidence a coal interval while the GR values point to a few coaly mudstones, coal and a few pure coal zones within the fractured intervals. Even though most of the fractures may fall within the interbeds of carbonaceous mudstones, silts and mudstones also occur as the high density and high GR values and varying transit times point to.

Even though the aim is to confirm the presence of fractures in pure coal zones which can enhance permeability and flow of adsorbed methane gas, the presence of fractures on the surrounding lithologies can also be a positive effect. Respect to the nature of the fractures, we can hypothesize that fractures in non-coal intervals maybe of tectonic origin and those in the coal the result from tectonics or from coal maturation. This hypothesis can be proved by the fractures identified on core and of course literature on the tectonics of the region.
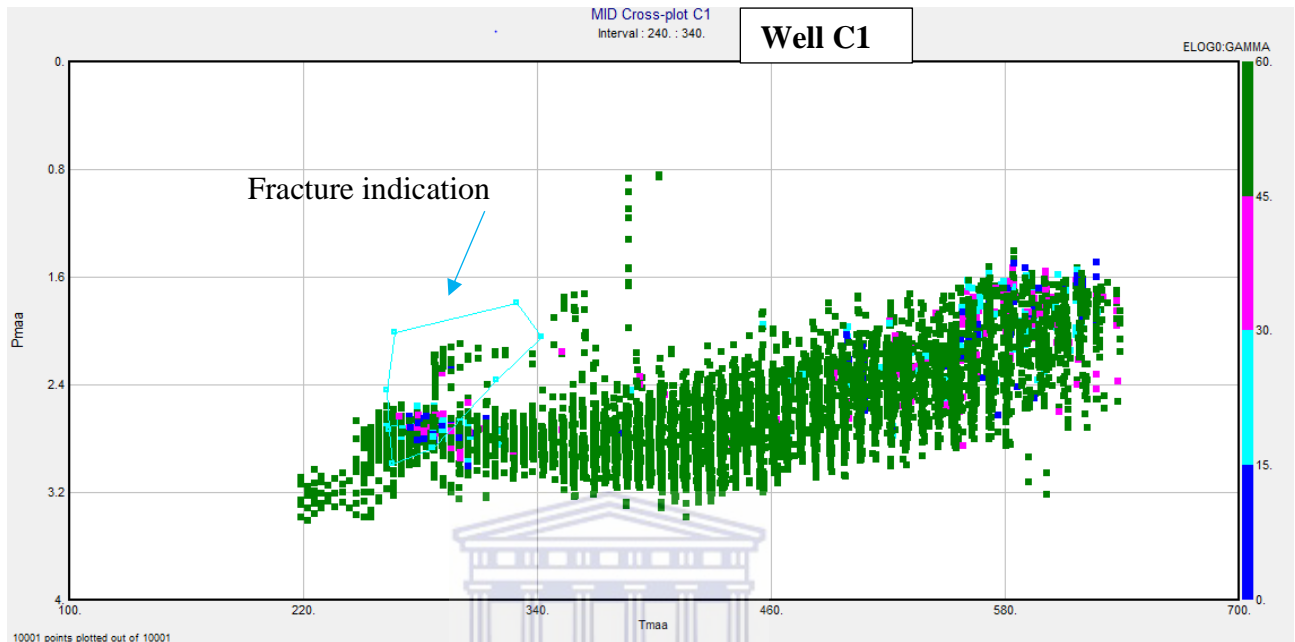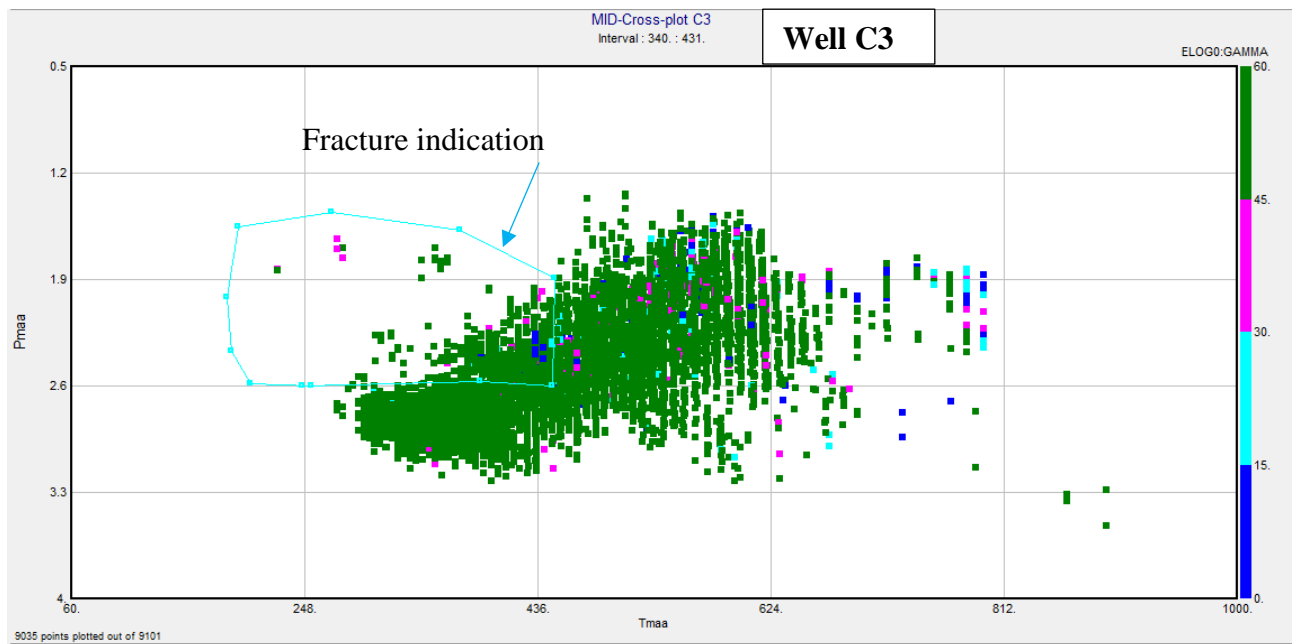

Figure 45 *MID cross-plot for well C3 depicting fracture zones where data points plot to the left of the plot area, better representation of coal intervals than in well C1.*

Well C3 (Figure 45), has even better results where even more low density data points fall within the fracture detection polygon with GR counts indicating coal with high transit times. For this reason there is a high level of confidence that the methane bearing coal seams in those intervals are fractured and this may in this case be an indication of coal maturity.

Though most of the wells have fracture indications with the use of this methodology some did not respond in the similar manner as in well C7 (Figure 46). The fractured intervals fell in the other lithology category, this could be due to the fact that the mudstone laminations tend to have some coal stringers and thus the overall density of the rock maybe slightly higher than that of a clean coal, these zones cannot be disregarded on that account as they form part of a larger coal seam interval and do tend to contribute to flow (Figure 46).

Another assumption would be that there might be fractures with higher apparent-matrix densities along those zones. These lithologies may be affected by a large degree of cementation such as calcite cement as it was observed on the core and therefore the detected fractures may be closed or healed.
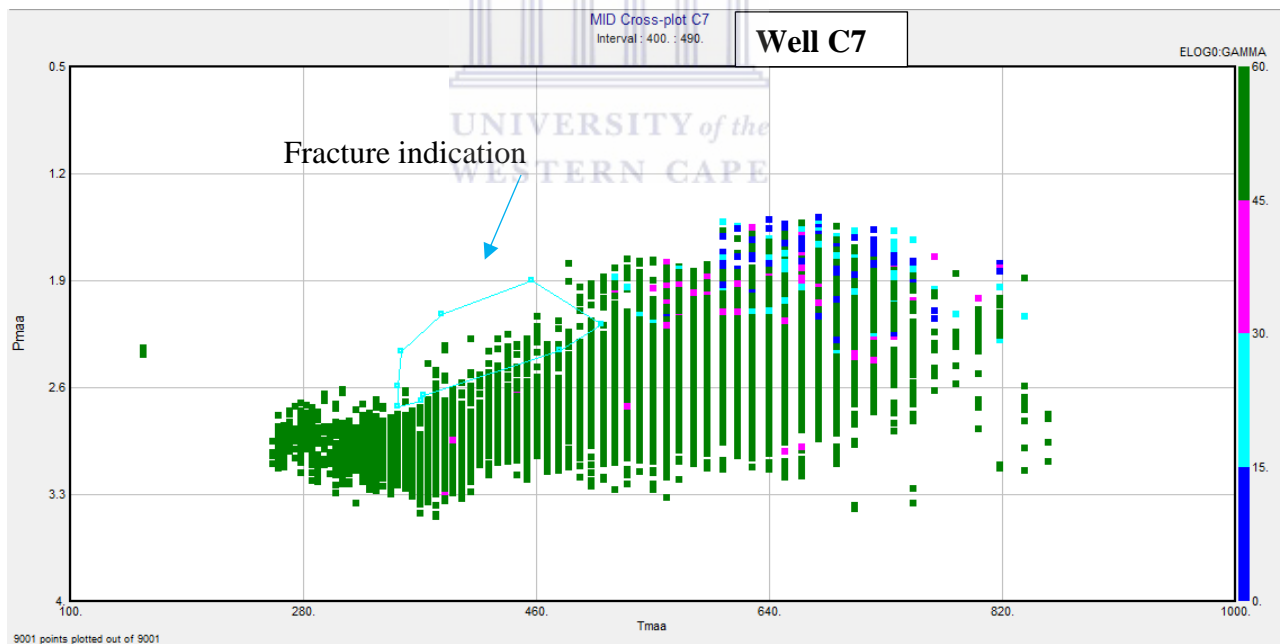
Figure 46 *MID plot for well C7 fractures detected in non-coal/non-pure coal intervals.*

5.3.3.2 Resistivity-Porosity Cross-plot

When dealing with fractures cementation becomes a critical aspect in fracture analysis and its degree greatly affects those fractures if any are present in the formation. Therefore it becomes crucial to evaluate the cementation factor in the lithologies of interest as this may reduce permeability and hamper flow.
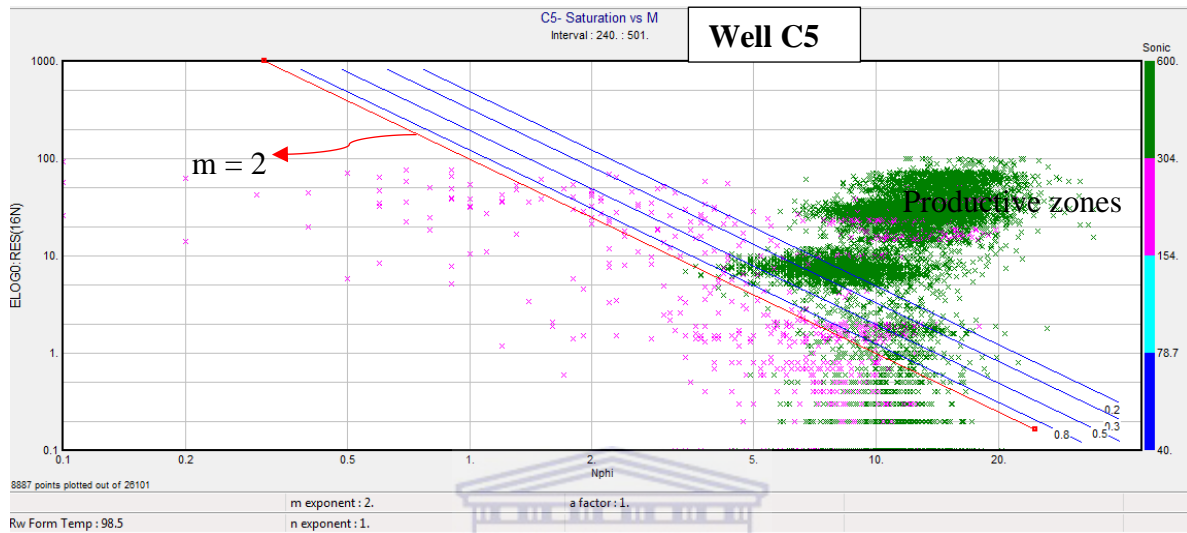
Figure 47 *Resistivity-Neutron porosity relationship and the subsequent Saturations and cementation factors, high m exponent indicates lack of fractures but high HC indication.*

Figure 47Figure 48 depicts the relationship between the cementation factor ('m') and the water saturation in matrix pores or fracture porosity, these are generally cross-plots of short spaced resistivity (Res) against neutron porosity (Nphi). This relationship was assessed in two scenarios a) where M is equal to 2 (Figure 47), and b) where M is equal to 1 (Figure 48). In a) the red line is the M = 2 gradient and is in an un-fractured interval with slow sonic transit times thus not in the main coal zones. Below this gradient the data points are in a 100% water saturated zone thus we see a downwards increase in water saturation from the Sw = 0.2 line. The high M value could also be an indication of hydrocarbon presence. If we pay attention to the Sw = 0.8 line this means that along line 80% of the pores are water filled with a 20% margin that could be either water and hydrocarbon filled.
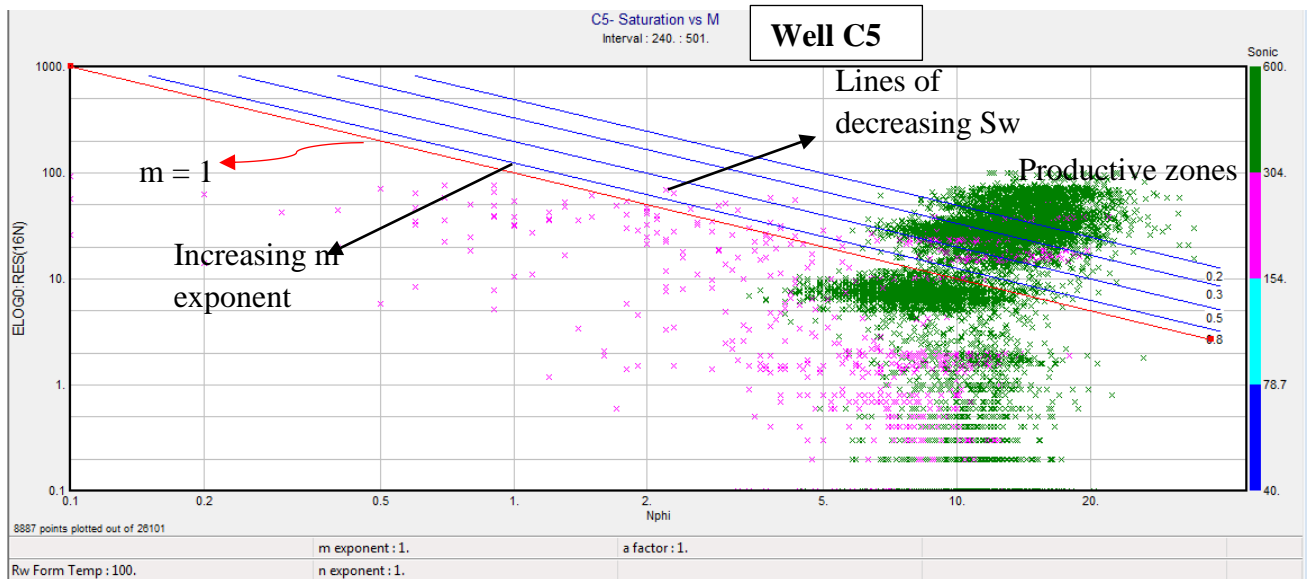
Figure 48 *Resistivity-Porosity plot indicating fractured zones as a function of cementation and potential HC yield as a result of Water saturation.*

In b) for M=1 (Figure 48) the blue lines depict lines of decreasing water saturation thus low cementation factor and an indication of fractures along these intervals. Following the arrow showing line m =1, the data points falling below that line are in a highly water saturated zone which is also characterized by high degree of cementation. No fractures are expected to be detected in this region

The data points above Sw = 0.2 fall within the productive zones of low water saturation and low cementation. This zone should yield more flow.

5.3.3.3 M-N Plots

For the computation of M-N parameters for the cross-plot generation one needs to define properties for both M and N. So through Interactive Petrophysics (IP) using the calculations we were able to define a user formula which gives the relationship of M and N parameters used to indicate fracture presence in lithologies. This is done by using for M sonic-density relationship and for N neutron-density data which yields a porosity relationship and aids for identification of fractures. M and N variables are calculated by the following equations (Asquith & Gibson, 2004)

Equation 3

$$M = \frac{\Delta tf - \Delta t}{\rho b - \rho f} * 0.01$$

Where
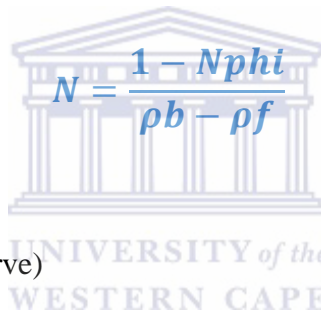
Δtf = Sonic transit time (fluids) @189μs/m

Δt = Sonic transit time (log curve)

ρb = Bulk Density (log curve)

ρf = Fluid density @ 1g/cc

Equation 4

$$N = \frac{1 - Nphi}{\rho b - \rho f}$$

Where

$Nphi$ = Neutron porosity (log curve)

ρb = Bulk Density (log curve)

ρf = Fluid density @ 1g/cc

When these two parameters are cross-plotted against each other fractures are identified by the data set plotting the top right corner (Figure 49). For confidence and to aid knowledge of the zones along which fractures are identified, a third dimension is added. In this case a Gamma Ray colour code was used, the same was as in the MID crossplots
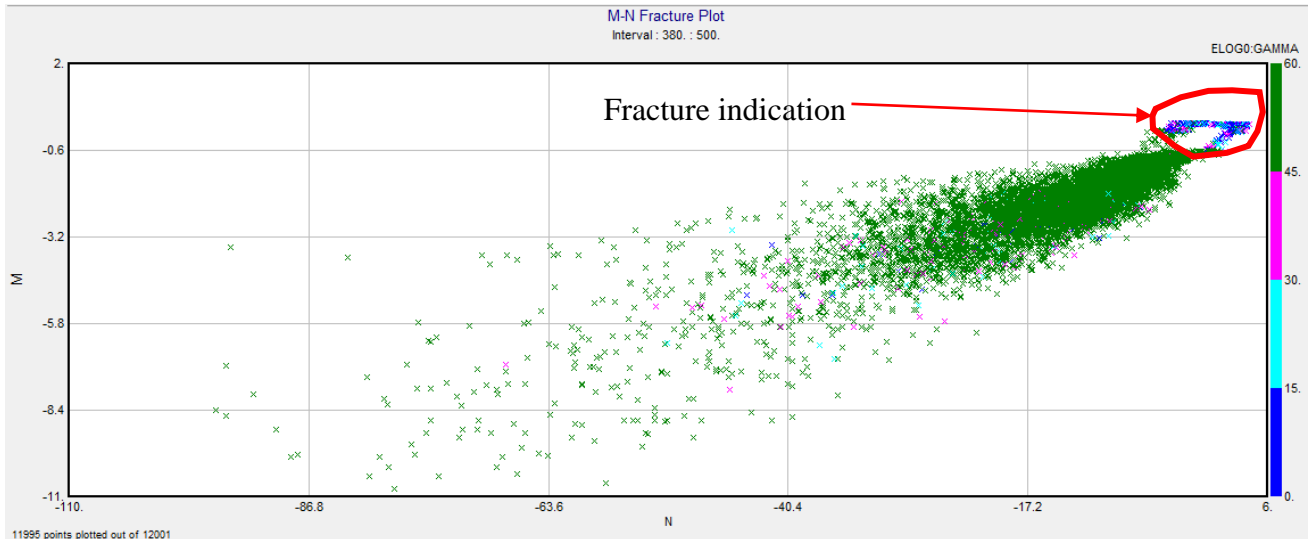
Figure 49 *M-N fracture plot for well C4, note the data points plotting to the top right corner indicate fracture presence and paired with the GR log mainly the low GR count data points plot furthest up*

The data points within the red polygon with high M and N values indicate fractured intervals with secondary porosity. The secondary porosity is attributed from vugs and fractures within the formation and provides a good indication of a high permeability zone in well C4 (Figure 49).

Although wells C4, C3 & C5 have a similar trend in M-N plot, with the coal intervals plotting on the top right corner, wells C6 and C7 do not show fractures at that interval but within the high gamma ray reading zones. The coal zones are tailing behind in that trend and thus this plot for the wells C6 and C7 is not a good indication of fracture presence (Figure 50 and 43). Even though the fractures are not contained within the expected coal zones in well C6, fractures do exist in the non-coal strata (Figure 43).
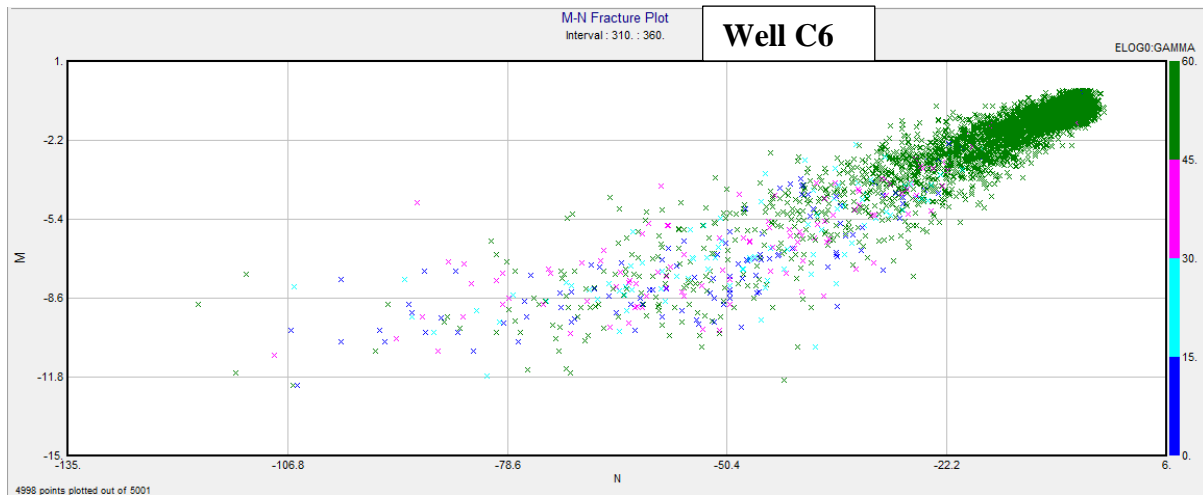
Figure 50 *Plot shows the lack of fractures within the coal intervals within this well, fractures however are present as the data points plot to the top right corner of the graph, but these fractures are contained in non-coal intervals intercalated within the coal seams.*

An indication of fracture presence on well C6 denoted by structures interpreted from image logs (Figure 43). Note however as discussed in the topics above, the breakout orientation tells whether the fractures or cleats are open or closed if they are parallel to the breakout maximum horizontal stress. On Figure 43 the cleat strike is in the orientation of the minimum horizontal stress and thus the cleats are sealed in the direction of the maximum horizontal stress. This could be the reason why the M-N cross-plot of well C6 could not indicate fractures in the coal zones.

5.4 QUANTITATIVE ANALYSIS OF FRACTURES

This topic involves the calculation of fracture properties quantitatively and involves three properties being;

5.4.1 Porosity Fracture Index (φf_{index})

Porosity fracture index involves the estimation of the inter-granular porosity calculated from sonic log data and fracture porosity from neutron-density log data. The following equation was used in IP to calculate the porosity fracture index for the entire well for all the wells evaluated (Yan et al., 2009)

Equation 5

$$\varphi f_{index} = \frac{|\varphi ND - \varphi S|}{\varphi ND}$$

Where

φf_{index} = Porosity fracture index

φND = Neutron-Density porosity

φS = Sonic porosity

Equation 6
$$\varphi f = \varphi ND - \varphi S$$

Where

$\boldsymbol{\varphi f}$ = Fracture Porosity

φND = Neutron-Density porosity

$\boldsymbol{\varphi S}$ = Sonic porosity

The result of this equation is a distinction whether the fractured formation is indeed a dual porosity system, where the effective porosity consists of both matrix porosity and a secondary fracture porosity. The result of the two curves generated by these two equations can be evaluated to understand the main porosity system. The fracture porosity index gives information about the degree of fracture to be expected at an interval.

5.4.2 Resistivity Fracture Index

This computation helps to predict the fracture information quantitatively based on mud filtrate invasion principles. By studying the mud filtrate invasion behavior of shallow and deep resistivity we can determine the degree of fractures, based on work done on fracture corridors where deep invasion through fractured intervals in oil or gas zones causes deep resistivity drop to levels of shallow resistivity indicating extremely high permeability (Ozkaya et al., 2007). Deep and shallow resistivity logs are generally used to calculate this resistivity fracture index for fractured intervals. This computation however wasn't only done for known or coal intervals as there may be other fractures in the formation than coal cleats, and these tend to be in other coal related lithologies due to tectonic stresses and may or may not contribute to flow. For this evaluation the choice of resistivity fracture index of the water zone has be used. This equation allows to calculate this parameter in intervals in the water lag as we know we are not dealing with conventional reservoirs (coal matrix tends to have water), it is that water that is pumped initially to lower the pressure to aid gas flow to wellbore. It is as a result of this the following equation was used (Yan et al., 2009).

Equation 7

$$R\varphi_{index} = \left\{\left(\frac{1}{Rd} - \frac{1}{Rs}\right) \Big/ \left(\frac{1}{Rw} - \frac{1}{Rmf}\right)\right\}^{\wedge}\frac{1}{m}$$

Where:

$R\varphi_{index}$ = Resistivity fracture index

Rmf = Mud filtrate resistivity

Rs = Shallow resistivity laterolog

Rd = Deep resistivity laterolog

Rw = Water resistivity

M = Cementation factor = 1 for this data

5.4.3   Fracture Aperture (ε)

Fracture aperture is calculated from shallow and deep dual resistivity logs and both vertical fracture aperture and horizontal fracture aperture are evaluated from this relationship. This applies the following equation (Yan et al., 2009).

Equation 8

$$\varepsilon(v) = \left(\frac{1}{Rlls} - \frac{1}{Rlld}\right) * (10^4 / (\frac{0.4}{Rmf}))$$

Where

$\varepsilon(v)$ = Vertical fracture aperture

$Rlls$ = Shallow resistivity laterolog

$Rlld$ = Deep resistivity laterolog Rmf = Mud filtrate resistivity

Equation 9

$$\varepsilon(h) = \frac{\left(\frac{1}{Rlld} - \frac{1}{Rlls}\right) * 10^4}{1.2 \frac{1}{Rmf}}$$

Where

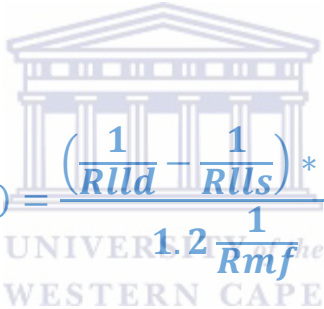$\varepsilon(h)$ = Horizontal fracture aperture

$Rlls$ = Shallow resistivity laterolog

$Rlld$ = Deep resistivity laterolog Rmf = Mud filtrate resistivity

5.4.4 Quantitative analysis Results

Based on C1 Well log (Figure 51) the PhiF_index is the porosity fracture index and gives information about the intensity of the fractures that could be expected from a certain interval and it has to be compared with the fracture porosity. This method is traditionally used for breakouts and induced fracture analysis by pairing the porosity index with caliper log. But for this study there are some induced fractures seen on core photographs.

Note in (Figure 51) (above the green line depth 270 m) how the porosity index is high, fracture porosity is also high and the horizontal fracture aperture is also high (or positive) and the cementation m factor is low. This is a good indication that the fracture porosity is increased due to the higher horizontal fracture aperture compared to the negative vertical aperture. Thus one can conclude and say there are fractures indicated and they are not fully cemented and may contribute to flow.

At depth of ~265m above the orange marker line, the shaley lithology with high density shows a medium porosity fracture index (PhieF_index) with low PhiF. The horizontal aperture is very low and the vertical aperture is slightly higher, m is high in this interval which means the little indicated fractures are cemented. The entire vertical section seems to have a low and high trend of the parameters described in previous topics, but the horizontal aperture seems to improve with depth though the cementation factor (m) also appears to be larger in those zones at depths 305-340m in this well

The resistivity fracture index is the result of shallow, deep resistivity laterologs, water resistivity and mud filtrate resistivity for water zone. This curve shows the resistivity of fractures in the form of an index. Note how the resistivity fracture index behaves similarly to the aperture (horizontal) indicating fluid presence and the m factor is low at those intervals pointing to a local permeability enhancement.
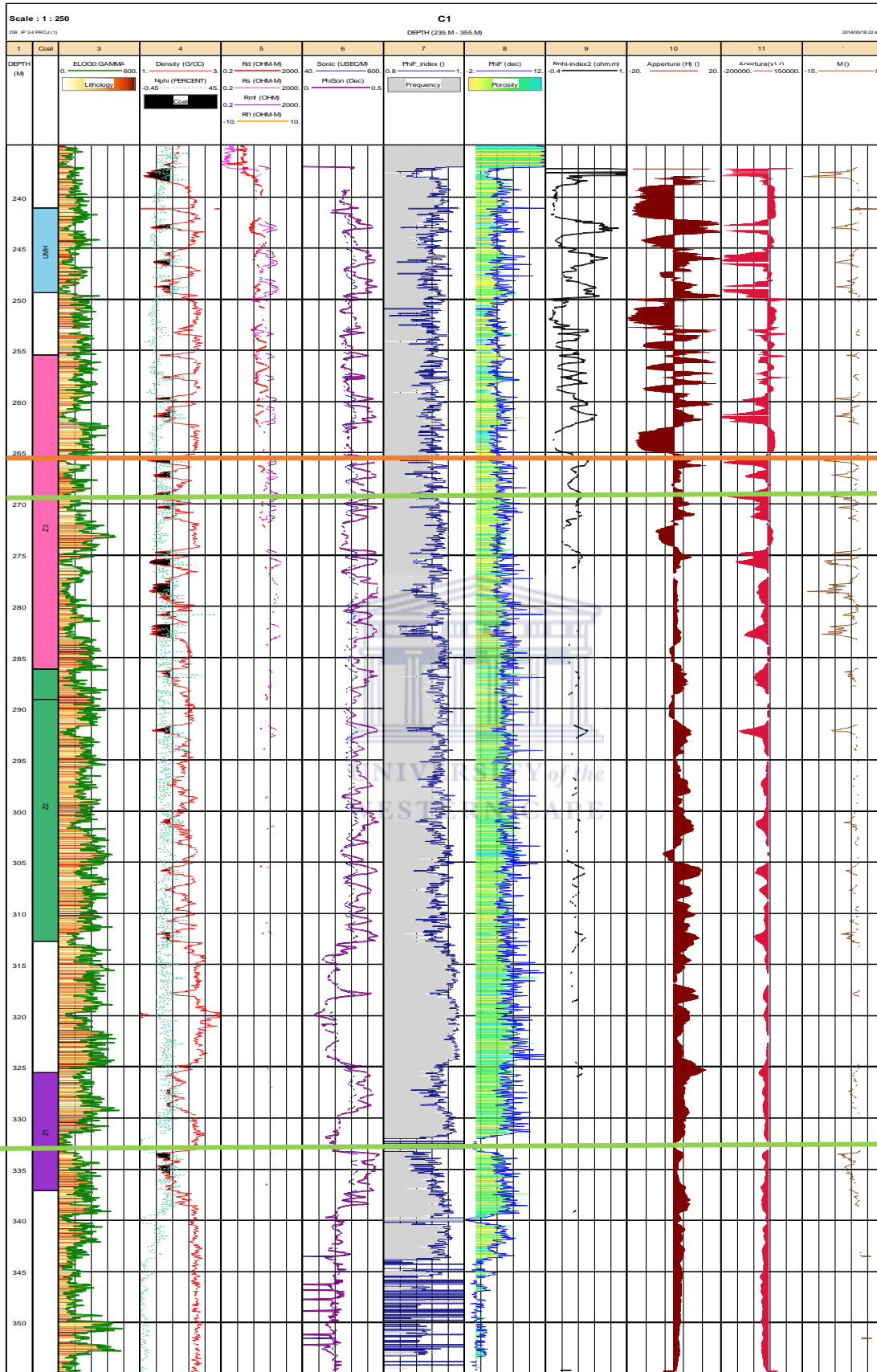
Figure 51 *Fracture parameters for well C1 (PhiF, PhiF_index, Rphi_index, Aperture (H&V) and cementation factor m are represented from track 7-12. Fractures discussed in the text.*
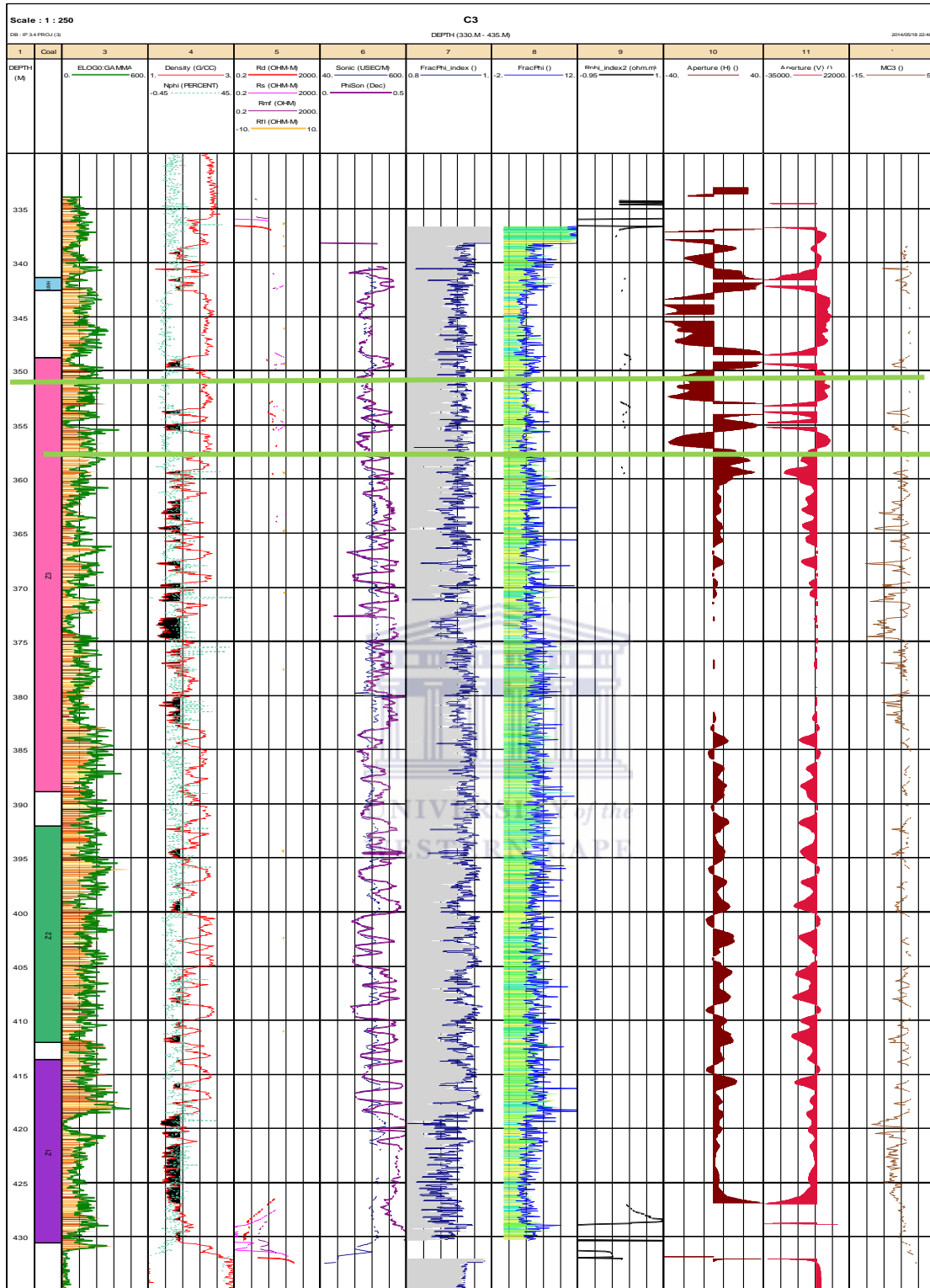
Figure 52 *Well logs indicating derived fracture parameters for well C3 in track 7 through 12.*

Note when the horizontal aperture is high, the vertical aperture is low and the cementation is low thus the horizontal flow may be the dominant one and this is seen across many of the evaluated wells. The frequency of the fracture porosity index well C3 correlates better with the fracture porosity and also with the horizontal fracture aperture. The cementation along the

high horizontal fracture aperture is generally low (indicated by the green lines). This indicates permeable zones. Notice the resistivity fracture index is a function of aperture (horizontal) and porosity, the resistivity fracture index is positive with a high fracture porosity kick, see above the green line 350 m depth; and it is observed low when fracture porosity and resistivity fracture index are low due to an increased cementation factor (m) (Figure 52).
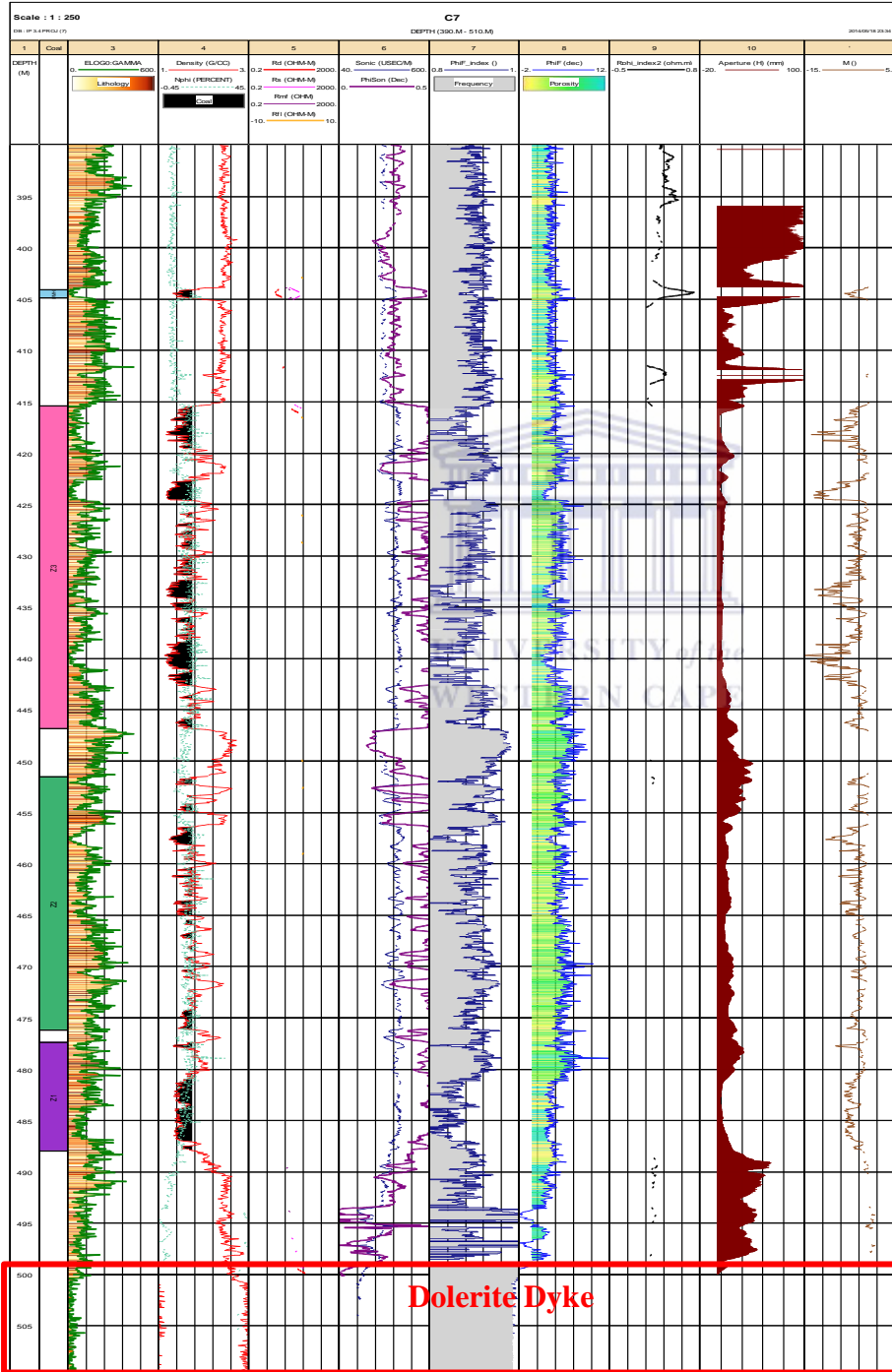
Figure 53 Well log with fracture parameters for well C7. Note the presence of dolerite dyke at the base of the coal sequences.

Well C7 appears to have a higher cementation factor (Figure *53*). The horizontal fracture aperture on this well is high as well as the m factor; the fractures within this well may be healed as a result of the high cementation. Due to presence of dolerites above and below the coal seam intervals one can assume that the heat liberated during the dolerite intrusion may have mineralized the fractures and filled them in the process, closing the detected horizontal fracture aperture (Figure *53*). The other factor may be that the original fractures (in situ/tectonic) are the ones sealed and the high frequency fractures with high porosity may have formed as a result of the process of doming of the magma causing hydrothermal fractures detected at ~415-500m in this well.
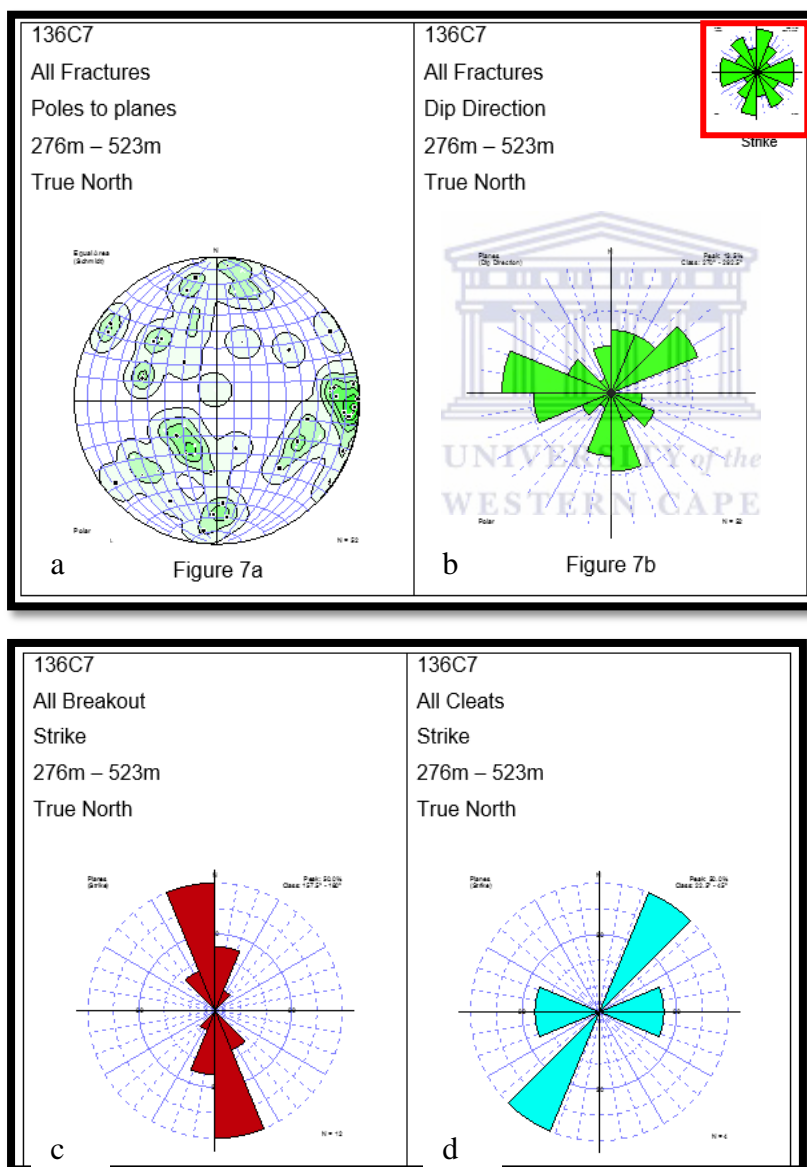
Figure 54 *Stereo and rose plots for well C7 structural interpretation.*

The presence of the dolerite in well C7 can also have an impact in hydrothermal fractures as a result of cooling. The fractures in all strata are represented by (Figure 54a) and thus dolerite fractures tend to be disorganized and appear throughout the stereo plot and on the rose plot encompass multiple directions (Figure 54b). Note the strike rose plot (Figure 54b) is multimodal even though the N-S can be interpreted as the dominant orientation. If pay attention to Figure 54c, the breakout orientation shows the N-S striking trend which is also the orientation of the maximum compressive stress. The majority of cleats may yield better flow as they are open in the somewhat direction of the inferred in-situ stress field (Figure 54d). However the E-W striking cleats in this well will be tightly healed as they oppose the maximum stress, this is also seen on the inset of Figure 54b where the majority of fractures along the E-W direction will be closed. This could be the effect of the dolerite leading to cleat-fracture mineralization and this is also confirmed by the high cementation factor (Figure *53*).

6   CONCLUSION

Coal has become one of the most primary used natural resource across the globe as it is the most reliable and abundant of mineral resources. Coal exploration in Botswana has taken a great turn, yielding large reserves and resources of the Kalahari Karoo basin which straddles most of the country. The Permian coals with targets in the Morupule and Serowe formation have been discussed and analyzed for fractures.

Fracture networks can be accurately described from image log data and may be paired with other aspects such as core description, fracture property calculations and conventional log identification. Fractures present in coal successions may be basin and tectonically induced, coal cleats, shear fractures and those associated with drilling activity.

Most coals possess fractures and along which large amounts of gas are adsorbed, thus a qualitative and quantitative description of the fracture system and its petrophysical evaluation are fundamental to gas production. The core photographs analyzed indicate fracture of different origin, including tectonically induced fractures, drilling induced petal-centerline fractures & breakouts, cleats (in brittle zones) and natural enhanced fracture systems. These sets of fractures are also observable in ATV image logs. A structural analysis of the fractures indicates two major stress regimes. The tectonic natural fractures indicate in-situ stress orientation and the breakouts indicate present day stress orientation.

Stereographic plots of studied wells show fractures occur in almost every orientation and multidirectional when the dolerite fractures are included in the dataset. The rose plots shows a dominant N-S strike and a less dominant E-W strike trend in most of the studied wells. The low angled fractures have a dominant strike of NNW-SSE and these fractures may be interpreted as shear or minor thrust fractures. High angled fractures maintain a N-S strike and may indicate a high angled joint system.

Coal cleat development may influence permeability depending on whether they are open or closed (or healed), this is observed on wells C3, C4, C5 and C9 as open cleats, yet closed on wells C1, C6, partially closed on wells C7 and C8. It is however difficult to analyze cleats on image logs as they are in most instances below image log resolution. The fractures may be closed due to natural calcite cementation present in shale layers or due to thermally induced mineralization as a result of dolerite intrusion.

The MID cross-plot indicated fracture in all the wells evaluated and mostly on lithologies different from coal indicated by the blue, pink or light blue colours on the GR log colour code (Figure 45 and Figure 46). The plot may have not indicated fractures in coals due to the cleat system being closed such as in well C6, where also the M-N fracture plot did not detect fractures in coal intervals (Figure 50).

Thus a combination of image logs, structural interpretation of fractures evaluated and location, of fractures may yield more confident result when dealing with fractures in tight matrix strata.

Once the fractures have been studied and their orientation and also location is understood the fracture parameters may be evaluated to understand their possible contribution to gas production. This also pertains to the degree the fractures will enhance permeability and flow to the wellbore should the fracture study be promising for production. Fracture parameters do include the fracture porosity and its index, resistivity fracture index and the most important parameter the aperture index (both vertical and horizontal). These parameters aid in understanding whether the fractures evaluated will increase pore permeability or will they be sealed hindering the flow of methane gas. Parameters like fracture porosity index can provide a frequency of any changes in fracture porosity (figures 51, 52 and 53). This is the secondary porosity within the formation, when combined with the resistivity fracture index it evidences the behavior of fluids in different zones of invasion. The fracture porosity index is somewhat proportional to the aperture index (horizontal) where the cementation factor is low. This further proves that fractures may be open and could be healed within the same formation depending on calcite presence, dolerite intrusion or mainly due to the orientation of fractures in respect to the maximum or minimum compressive stresses. Where fractures are parallel to the maximum horizontal compressive stress (Sh_{max} paleo-stress regime), the fractures are open parallel to the minimum horizontal stress direction (Sh_{min}) which is also an indication of current stress.

However when the breakout stress orientation is evaluated we observed that the direction of Sh_{max} and Sh_{min} changes from block to one fault-bounded block to the next one along the field. This may have caused rotations in the stress fields due to tectonic emplacement of dolerites due to regional changes in the stress system.

90

7 RECOMMENDATIONS

The methodology followed in this study has been derived for tight hydrocarbon reservoirs, where it is usually applied. Coal Bed Methane study is unconventional and thus the ability to characterize fractures in coals using this approach shows great connection of the two reservoirs. This thesis provides a way to evaluate coal seam fractures, as coals themselves are tight matrix units. The following are technical recommendations to this study:

➢ Core photographs used in this study have not been slabbed and splashed with water, this process may cause reflections and depict a lustrous nature of coals which may not be the case.

➢ Interpretation in successions should always differentiate fractures in the dolerite from fractures in the sedimentary successions for a better comparison of stress orientation. These can have different origins or respond to different local stresses. These may be miss-matched if put together such as in figure 53.

➢ Permeability tests are required to fully evaluate and to characterize with confidence which wells will have better flow.

➢ Determination of fracture thickness and width and also fractures probability from image log data.
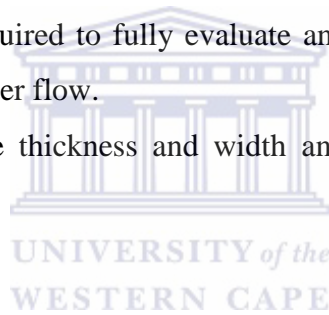
8 REFERENCES

Advanced Resources International, Inc, 2003. *Results of the Central Kalahari Karoo Basin Coalbed Methane Feasibility Study,* Arlington, VA USA : s.n.

Asquith, G. & Gibson, R., 2004. *Basic well log analysis for Geologists,* Tulsa Oklohoma: AAPG.

Bennet, J., 1989. *Review of Lower Karoo coal basins and coal resource development in parts of central and southern Africa with particular reference to northern Malawi,* Nottingham: British Geological Survey.

Bordy, E., Segwabe, T. & Makuke, B., 2010. Sedimentology of the Upper Triassic-Lower Jurassic Mosolotsane Formation (Karoo Supergroup), Kalahari Karoo Basin, Botswana. *Journal of Earth Sciences,* pp. 1-14.

Callaghan, C., 2013. *Mineral Resource based Growth Pole-Industrialisation.,* s.l.: s.n.

Catuneanu, O. et al., 2005. The Karoo BAsins of south-central Africa. *African Earth Science,* pp. 1-43.

Crain, E., 2013. *Crain's Petrophysics Pocket Pal.* s.l.:s.n.

Geology, C., 2013. *Coal Geolology.* [Online]
Available at: http://coalgeology.com
[Accessed 19 May 2014].

Halliburton, 2008. *Coalbed Methane: Principles Practices.* s.l.:s.n.

Harpalani, S. & Liu, S., 2013. *Coalbed Methane: Important Source of Natural Gas Resource,* San Francisco: American Rock Mechanics Association.

Kampunzu, A., Armstrong, R., Modisi, M. & Mapeo, R., 2000. Ion microprobe U-Pb ages on detrital zircon grains form the Ghanzi Group, Implication for the identification of a Kibaran-age crust in northwest Botswana. *Journal of Africa Earth Scince,* pp. 579-587.

Kingston, J., 1988. *The undiscovered Recoverable Pteroleum Resources of Southern Africa,* s.l.: U.S Geological Survey.

Lacazette, A., 2000. *NAtural Fracture Nomenclature: Distinguishing natural from induced fractures in image logs,* Tulsa: s.n.

Laubach, S., Marrett, R., Olson, J. & Scott, A., 1998. Characteristics and origins of coal cleat: A review. *International Journal of Coal Geology,* pp. 1-33.

Levine, J., 1993. Coalification: The evolution of coal as source rock and reservoir rock for oil and gas. *AAPG Studies in Geology,* Volume 38, pp. 39-78.

Mandal, D., Tewari, D. & Rautela, M., 2004. *Aalysis of Micro-Fracturesnin Coal for Coal Bed Methane Exploitation in Jharia Coal Fiels,* s.l.: 5th Conference & Exposition on Petroleum Geophysics, Hyderabad.

Mclntire, C., 2010. Okavango Delta, Chobe, Northern Kalahari. *Bradt Botswana*.

Ministry, B., 2003. *Coal Bed Methane Study,* s.l.: Department of Geological Survey.

Modie, N., 2007. *The Paleozoic Palynostratigraphy of the Karoo Supergroupand Palynofacies insight into Paleoenvironmental Intepretations, Kalahari Karoo Basin, Botswan,* s.l.: Universite de Brentagne Occidentale.

Myers, J., 2010. *Energy II: Electricity: Powering the world (CBM).* [Online]
Available at:
http://www.gg.uwyo.edu/content/lecture/energy/fossil_fuels/cbm/formation/retention/cleats
[Accessed 10 May 2014].

Outburst, 2013. *Underground Coal.* [Online]
Available at: http://www.undergroundcoal.com.au/outburst/rank.aspx
[Accessed 19 May 2014].

Ozkaya, S., GeoScience, B. A. & Kloos, J., 2007. *Detection of Fracture Corridors from Openhole Logs in Horizontal Wells,* Mumbai: Society of Petrophysicists and Well Log Analysis.

Potgieter, J., 2013. *Botswana Exploration Corehole Project, Detailed Operating Plan,* s.l.: Unpublished Work.

Potgieter, J. & Andersen, N., 2012. *An Evaluation of the Coalbed Methane Potential of the Central Kalahari Area of Botswana from a Geological Perspective,* s.l.: Unpublished work.

Project, N. E. E. D., 2014. *SmugMug.* [Online]
Available at: http://need-media.smugmug.com/Graphics/Graphics/17024036_Bdmf8C/1295824178_2JgX3xW#!i=1295823840&k=FfhkrZH
[Accessed 19 May 2014].

Rider, M. & Kennedy, M., 2011. *The Geological Interpretation of Well Logs.* 3rd ed. Scotland: Rider--French Consulting Ltd.

Segwabe, T., 2008. *The Geological Framework and Depositional Environments of the Coal-bearing Karoo Strata in the Central Kalahari Karoo basin, Botswana,* s.l.: Rhodes University.

Smith, R., 1984. The Lithostratigraphy of the Karoo Supergroup in Botswana. *Bulletin Series, Bulletine 24,* pp. 1-200.

Survey, D. o. G., 2004. *CoalBed Methane Study,* s.l.: s.n.

Thomas, L., 2002. *Coal Geology.* 1st ed. Chichester: John Wiley & Sons Ltd.

Wireline-Workshop, 2008. *Wire Line Logging; Televiewer.* s.l.

Wood, G., Kehn, T., Carter, D. & Culbertson, W., 1980. *USGS: Geological Survey Circular 891.* [Online]
Available at: http://pubs.usgs.gov/circ/c891/geophysical.htm
[Accessed 13 February 2014].

Yan, J., Lubbe, R. & Payne, S., 2009. *Petrophysical fracture identification for rock physics studies,* Teddigton, London: Ikon Science Ltd.

UNIVERSITY *of the*

WESTERN CAPE

MAP OF WELLS WITH STRIKE ROSE PLOTS OF BREAKOUTS & COAL FRACTURE ORIENTATION & STRESS FIELDS